NASA CONTRACTOR REPORT

NASA CR-2670

NASA CR-2670

TECH LIBRARY KAFB, NM
0061462

INFLUENCE OF SURFACE ROUGHNESS AND WAVINESS ON FILM THICKNESS AND PRESSURE DISTRIBUTION IN ELASTOHYDRODYNAMIC CONTACTS

LOAN COPY: RETURN TO
AFWL TECHNICAL LIBRARY
KIRTLAND AFB, N. M.

Lorac S. H. Chow and Herbert S. Cheng

Prepared by
NORTHWESTERN UNIVERSITY
Evanston, Ill. 60201
for Lewis Research Center

NATIONAL AERONAUTICS AND SPACE ADMINISTRATION • WASHINGTON, D. C. • APRIL 1976

TECH LIBRARY KAFB, NM
0061462

1. Report No. NASA CR-2670	2. Government Accession No.	3. Recipient's Catalog No.
4. Title and Subtitle INFLUENCE OF SURFACE ROUGHNESS AND WAVINESS ON FILM THICKNESS AND PRESSURE DISTRIBUTION IN ELASTOHYDRODYNAMIC CONTACTS		5. Report Date April 1976
		6. Performing Organization Code
7. Author(s) Lorac S. H. Chow and Herbert S. Cheng		8. Performing Organization Report No. None
		10. Work Unit No.
9. Performing Organization Name and Address Northwestern University Evanston, Illinois 60201		11. Contract or Grant No. NGR-14-007-084
		13. Type of Report and Period Covered Contractor Report
12. Sponsoring Agency Name and Address National Aeronautics and Space Administration Washington, D.C. 20546		14. Sponsoring Agency Code

15. Supplementary Notes

Final report. Project Manager, Erwin V. Zaretsky, Fluid System Components Division, NASA Lewis Research Center, Cleveland, Ohio

16. Abstract

The Christensen theory of a stochastic model for hydrodynamic lubrication of rough surfaces was extended to elastohydrodynamic lubrication between two rollers. The Grubin-type equation including asperity effects in the inlet region was derived. Solutions for the reduced pressure at the entrance as a function of the ratio of the average nominal film thickness to the rms surface roughness (in terms of standard deviation σ) were obtained numerically. Results were obtained for purely transverse as well as purely longitudinal surface roughness for cases with or without slip. The reduced pressure was shown to decrease slightly by considering longitudinal surface roughness. The transverse surface roughness, on the other hand, had a slight beneficial effect on the average film thickness at the inlet. The same approach was used to study the effect of surface roughness on lubrication between rigid rollers and lubrication of an infinitely wide slider bearing. Results of these two cases showed that the effects of surface roughness have the same trend as those found in elastohydrodynamic contacts. A comparison was made between the results using the stochastic approach and the results using the conventional deterministic method for the inlet pressure in a Hertzian contact assuming a sinusoidal roughness. It was found that the validity of the stochastic approach depends upon the number of wave cycles n within the Hertzian contact. Using the flow balance concept, the perturbed Reynolds equation, which includes a single three-dimensional rigid asperity in one of the lubricating surfaces, was derived and solved for the perturbed pressure distribution. In addition, Cheng's numerical scheme, for EHD contacts, was modified to incorporate a single two-dimensional elastic asperity, or a waviness profile, on the stationary surface. The perturbed pressures obtained by these three different models were compared.

17. Key Words (Suggested by Author(s)) Transient viscosity; Elastohydrodynamic; Pressure viscosity; Lubricant film thickness	18. Distribution Statement Unclassified - unlimited STAR Category 37 (rev.)

19. Security Classif. (of this report)	20. Security Classif. (of this page)	21. No. of Pages	22. Price*
Unclassified	Unclassified	157	$6.25

* For sale by the National Technical Information Service, Springfield, Virginia 22161

TABLE OF CONTENTS

LIST OF FIGURES

LIST OF SYMBOLS

a' = semi-major axis of the ellipsoidal asperity

b = half width of Hertzian contact

b' = semi-minor axis of the ellipsoidal asperity

$\bar{b}$ = b'/b

c = integration constant

c_1 = maximum asperity height

$\bar{c}_1$ = c_1/h_o

C_{UD} = $48(U_D/H_o^2)(\bar{b})$

$1/E'$ = $1/2\left(\frac{1-\nu_1^2}{E_1} + \frac{1-\nu_2^2}{E_2}\right)$

E_1, E_2 = Young's modulus for rollers 1 and 2

$f(\gamma)$ = probability density function of random variable γ

$g(\delta^*)$ = probability density function of surface roughness distribution

$$= \begin{cases} 35/96\ (1-\delta^{*2}/9)^3 & -3 < \delta^* < 3 \\ 0 & \text{elsewhere} \end{cases} \quad \text{for polynomial distribution function}$$

$$= \begin{cases} 1/(\pi\sqrt{1-\delta^{*2}/9}) & -3 < \delta^* < 3 \\ 0 & \text{elsewhere} \end{cases} \quad \text{for sinusoidal distribution function}$$

G = $\alpha E'$

$$G_2 = \int_{-\infty}^{\infty} \frac{g(\delta^*)}{\left(1 + \frac{\bar{\sigma}}{H}\delta^*\right)^3}\, d\delta^*$$

$$G_4 = \int_{-\infty}^{\infty} \frac{\delta^* g(\delta^*)}{\left(1 + \frac{\bar{\sigma}}{H}\delta^*\right)^3}\, d\delta^*$$

h = average film thickness

h_1 = smooth-film thickness of an EHD contact

h_c = average center film thickness of rigid rollers

h_g = smooth-film thickness between two rigid rollers

h_o = center film thickness at $x = 0$ for EHD contacts as well as for rigid roller; also used as the minimum film thickness for the slider bearing

h_T = local film thickness

h^* = average reference film thickness at $p = dp/dx = 0$

h_{min} = nominal film thickness at the exit of the slider bearing (for the slider bearing analysis, $h_{min} = h_o$)

H = h/h_o

H_1 = h_1/h_o

H_o = h_o/R

H_T = h_T/h_o

K_D = $(Q_W^* - Q_R^*)/Q_R^*$

K_E = Q_R^*/Q_s^*

K_R = w_R^*/w_s^*

i = a dummy index

j = a dummy index

ℓ = overall characteristic length of a slider bearing

m = slope of the inclined surface of a slider

m_1, m_2, m_3, m_4

= mass of lubricants flowing into or out of the grid

M = the number of grids in the Y-direction such that $y/a' = \pm 5$ at M

$M(x)$ = see Eq. (2.10)

n = number of wave cycles within the Hertzian contact

N = the number of grids in the X-direction such that $x/b' = \pm 5$ at N

p = local pressure

p_1 = smooth film pressure

p_{Hz} = maximum Hertzian pressure

$\bar{p}$ = the expected or mean value of p

P = p/p_{Hz}

P		$= p/p_{Hz}$ for EHD analyses
P		$= h_o^2\bar{p}/(6\mu\ (u_1+u_2)\ R)$ for the analysis of rigid rollers
P		$= h_o^2\bar{p}/(6\mu u_1 \ell)$ for the analysis of a slider bearing
P_1		$= p_1/p_{Hz}$
P_{Hz}		$= p_{Hz}/E'$
q		$= \dfrac{1-e^{-\alpha p}}{\alpha}$
$\bar{q}$		= the expected or mean value of q
Q		$= \dfrac{R^2}{6\mu_o(u_1+u_2)b}\cdot q = 48\sqrt{\dfrac{W}{2\pi}}\ U\left(\dfrac{\bar{\delta}}{E'}\right)$
Q_R		$= Q^*$ calculated by the stochastic theory for roughness model
Q_W		$= Q^*$ calculated by the waviness model
Q_S^*		$= Q^*$ for the smooth film analysis
R		$= R_1\ R_2/(\ R_1+R_2\ )$
R_1, R_2		= radii of rollers 1 and 2
S		$= 2(u_1-u_2)/(u_1+u_2)$
t		= time
u_1, u_2		= velocities of surfaces 1 and 2
u		$= (u_1+u_2)/2$
U		$= \mu_s(u_1+u_2)/(2E'R)$
U_D		$= \mu_s(u_1-u_2)/(2E'R)$
w		= load per unit width
W		$= w/E'R$
W_R^*		$= W^*$ calculated by stochastic theory for rigid rollers
W_s^*		$= W^*$ calculated by smooth film theory for rigid rollers
W^*		$= h_o^2\ w/(\ 6\mu(u_1+u_2)R^2)$ for the analysis of rigid rollers
W^*		$= h_o^2\ w/(\ 6\mu u_1 \ell^2\ )$ for the analysis of a slider bearing

x	= coordinate along the sliding direction
x_3	= distance between the asperity center and the contact center
x^*	= reference coordinate at $p = dp/dx = 0$
X_3	= x_3/b
X	= x/b for EHD analyses
X	= x/R for the analysis of rigid rollers
X	= x/ℓ for the analysis of a slider bearing
Δt	= grid size in x-direction
ΔX	= $\Delta x/b$
y	= coordinate perpendicular to the sliding direction
Y	= y/R'
Δy	= grid size in Y-direction
ΔY	= $\Delta y/a'$
μ	= viscosity
μ_s	= ambient viscosity
$\bar{\mu}$	= μ/μ_s
σ	= $\sqrt{\sigma_1^2 + \sigma_2^2}$
σ_1, σ_2	= standard deviation of roughness amplitudes of surfaces 1 and 2
δ	= $\delta_1 + \delta_2$
δ_1, δ_2	= roughness amplitude measured from the mean level of surfaces 1 and 2
δ_{max}	= the maximum asperity amplitude
δ^*	= δ/σ
δ^*_{max}	= 3
ξ	= dummy variable
$\bar{\xi}$	= ξ/b
ν_1, ν_2	= Poison's ratio of rollers 1 and 2
α	= pressure viscosity coefficient

$\bar{\alpha}$ = αp_{Hz}

γ = random variable, also used as ellipticity ratio a'/b'

$\epsilon\{\ \}$ = the expected value of { }

θ = the phase angle of the waviness surface profile measured from X = 0

θ_1, θ_2 = θ of surfaces 1 and 2

ϕ = perturbed pressure

Φ = ϕ/p_{Hz}

Φ_{max}, Φ_{min} = the maximum and the minimum perturbed pressure measured from the average pressure profile

Δ_s = $\Phi_{max} - \Phi_{min}$

ρ = lubricant density

$\bar{\delta}$ = δ/h_o

$\bar{\delta}_1$ = δ_1/h_o

$\bar{\delta}_2$ = δ_2/h_o

$\bar{\delta}_{max}$ = δ_{max}/h_o

$\bar{\sigma}$ = σ/h_o

SUMMARY

The Christensen Theory of a stochastic model for hydrodynamic lubrication of rough surfaces is extended to elastohydrodynamic lubrication between two rollers. The Grubin-type equation including asperity effects in the inlet region is derived. Solutions for the reduced pressure at the entrance as a function of the ratio of the average nominal film thickness to the r.m.s. surface roughness (in terms of standard deviation σ), have been obtained numerically. Results were obtained for purely transverse as well as purely longitudinal surface roughness for cases with or without slip. The reduced pressure is shown to decrease slightly by considering longitudinal surface roughness. The transverse surface roughness, on the other hand, has a slight beneficial effect on the average film thickness at the inlet.

The same approach was used to study the effect of surface roughness on lubrication between rigid rollers and lubrication of an infinitely-wide slider bearing. Results of these two cases show that the effects of surface roughness have the same trend as those found in elastohydrodynamic contacts.

A comparison is made between the results using the stochastic approach and the results using the conventional deterministic method for the inlet pressure in a Hertzian contact assuming a sinusoidal roughness. It was found that the validity of the stochastic approach depends upon the number of wave cycles n within the Hertzian contact. For n larger than a critical number, which depends upon the ratio of asperity height to the nominal film thickness, δ_{max}/h_o, the stochastic theory yields the same results as that obtained by the deterministic approach.

Using the flow balance concept, the perturbed Reynolds equation, which includes a single three-dimensional rigid asperity in one of the lubricating surfaces, is derived and solved for the perturbed pressure distribution. In addition, the Cheng's numerical scheme , for EHD contacts, is modified to incorporate a single two-dimensional elastic asperity, or a waviness profile, on the stationary surface. The perturbed pressures obtained by these three different models are compared. Qualitatively, the results for the single 2D elastic asperity and the waviness profile model by using Cheng's scheme, are mostly the same. However, some results obtained for the single 3D rigid asperity exhibit different trends when compared with the single 2D elastic asperity or the waviness profile. In the case of the waviness profile in which the local elastic deformation is allowed, the magnitude of the pressure fluctuation Δ_s, is found to increase when the pressure viscosity parameter G, or the ratio of the asperity amplitude to the nominal film thickness, δ_{max}/h_o, increases. On the other hand, Δ_s is found to decrease as the magnitude of the Hertzian pressure P_{Hz}, or the ratio of the nominal film thickness to the radius of the equivalent cylinder, h_o/R increases.

CHAPTER I

INTRODUCTION

In conventional sliding bearings, there usually exists a high degree of conformity between bearing surfaces, and this enables a substantial load to be generated by the thin oil film. The performance of these bearings can be satisfactorily predicted by solving the Reynolds equation for the pressure distribution within the lubricant film. However, for highly loaded concentrated contacts, such as gears, cams and rolling contact elements, the lubrication phenomenon cannot be predicted by Reynolds equation alone. Local elastic deformation of the solid under high pressure becomes influencial in determining the load capacity and film thickness of these contacts. The study of lubrication processes including the elastic effects is presently known as elastohydrodynamic lubrication (EHL).

To date, the theories for hydrodynamic and elastohydrodynamic lubrication have reached a very advanced stage. However, these theories are mostly based on the assumption that the lubricating surfaces can be described by smooth mathematical functions. In reality, surfaces are never perfectly smooth in a microscopic scale. In the hydrodynamic lubrication regime, the asperity heights of the rough surfaces are much smaller than the average lubricant film. Thus, the effect of surface roughness on hydrodynamic lubrication, in most cases, can be neglected. Hence, the smooth film hydrodynamic lubrication theories provides a very satisfactory prediction of lubrication performance. In elastohydrodynamic lubrication of concentrated contacts,there exist two distinctively different regimes, the full film and the partial film EHL. In the full film regime, the average nominal film thickness is usually much greater than the asperity heights, and, in this regime, the behavior of the contact can be predicted quite satisfactorily by smooth-film EHL theories. In the partial film regime, the asperity heights are of the same order as the average nominal lubricant film. Thus, the effect of surface roughness in the regime must be considered.

EHD film thickness has been well accepted as an important bearing design parameter. The degree of asperity interactions, and the surface distress in the forms of wear, pitting and scuffing are associated with the ratio of the average nominal film thickness to the r.m.s. surface roughness (in terms of standard deviation σ), in EHD contacts. In many cases, bearing failures can be attributed to insufficient film thickness which leads to asperity contacts. Thus, there is a need to determine the surface on the film forming capability in EHD contacts. Therefore, the second chapter of this dissertation is focused on the effect of surface roughness on the average film thickness between lubricated rollers. The stochastic theory developed by Christensen [7] is extended to determine the surface roughness influence on the inlet film thickness of EHD contacts. In addition, the roughness effect on the load capacity in rigid rollers and infinitely-wide slider bearing is also studied.

The third chapter compares the difference between the roughness effect and waviness effect on the average film thickness in EHD contacts. It also provides some criteria to determine the applicability of the stochastic theory.

The pressure profile enables one to predict the stress distribution of the lubricated contact. In the fourth and fifth chapters, the effect of surface roughness on the pressure distribution are discussed. In

Chapter IV, comparisons are made between the effect on the perturbed pressure due to a single three-dimensional rigid asperity and due to a single two-dimensional elastic asperity within an EHD contact. In Chapter V, the surface profile before elastic deformation is assumed to be in the form of sinusoidal waviness. The effects of the following non-dimensional variables: the Hertzian pressure P_{Hz}, the nominal center film thickness h_o/R, the pressure viscosity parameter G, the number of wave cycles within the Hertzian contact, n, and the asperity height h_o/R, on the magnitude of the pressure fluctuation as well as the perturbed pressure profile are studied.

CHAPTER II

THE EFFECT OF SURFACE ROUGHNESS ON THE AVERAGE FILM THICKNESS BETWEEN LUBRICATED ROLLERS

2.1 INTRODUCTION

The inclusion of surface irregularities in lubrication analysis can be traced back to [1-3], in which the roughness is modelled as sinusoidal or saw-tooth waviness. Subsequently, Tseng and Saibel [6] introduced the stochastic concept based on random surface roughness analysis on lubrication. Their method deals with surfaces with one dimensional transverse roughness only. The stochastic model has been revived by Christensen and his colleagues [7,8,9,16,17] in studying the lubrication process between rigid surfaces containing surface roughness modelled as ridges oriented transversely or longitudinally. Recently, the effects striated roughness on both bearing surfaces have been obtained by Rhow and Elrod [18].

The effect of surface roughness on film thickness in EHD contact has not been fully explored. However, there have been some related work. For instance, Fowles [4] studied the EHD lubrication between identical sliding asperities. Lee and Cheng [5] have studied the effect of a single asperity on the film and pressure distribution during its entrance into an elastohydrodynamic contact. The load sharing between fluid film and asperity contacts as well as the traction in partial EHD contacts have been studied by Tallian [10], and Thompson and Bocci [12]. Johnson, Greenwood and Poon [11] have used an approximate analysis to ascertain the effect of roughness on the EHD film thickness. They concluded that, to a first approximation, the separation between two rough surfaces is very close to that calculated by the smooth film theory. Recently, pressure and traction rippling inEHD contact of rough surfaces have been calculated by Tallian [19], by using Christensen's stochastic model of hydrodynamic lubrication.

In the present analysis, Christensen's approach [7] is extended to determine the surface roughness influence on the inlet film thickness of EHD contacts. The Grubin-type hydrodynamic equation in the inlet region for the rough surfaces is derived and solved numerically. Results are compared with smooth-film theories. In addition, the load capacity in rigid rollers and in an infinitely-wide bearing is also presented for comparison.

2.2 GOVERNING EQUATION

Assuming that the lubricant is isothermal and incompressible and the side-leakage is negligible, the one-dimensional Reynolds equation governing the pressure in an EHD contact is

$$\frac{\partial}{\partial x}\left(\frac{h_T^3}{12\mu}\frac{\partial p}{\partial x}\right) = \left(\frac{u_1 + u_2}{2}\right)\frac{\partial h_T}{\partial x} + \frac{\partial h_T}{\partial t} \tag{2.1}$$

where h_T is the local total film thickness consisting of the following three parts

$$h_T = h + \delta_1 + \delta_2 \tag{2.2}$$

In the above, h is the local average film thickness, and δ_1, δ_2, the roughness profile measured from the mean level of surface profiles 1 and 2 (Fig. 2.1).

2.2.1 Transverse Surface Roughness

In this case the asperities on both lubricating surfaces are straight ridges perpendicular to the direction of rolling. Equation (2.2) becomes

$$h_T = h + \delta_1(x - u_1 t) + \delta_2(x - u_2 t) \tag{2.3}$$

With the relations,

$$\frac{\partial}{\partial t}\delta_1(x - u_1 t) = -u_1\frac{\partial \delta_1}{\partial x} \tag{2.4}$$

$$\frac{\partial}{\partial t}\delta_2(x - u_2 t) = -u_2\frac{\partial \delta_2}{\partial x} \tag{2.5}$$

Eq. (2.1) is simplified to

$$\frac{\partial}{\partial x}\left[\frac{h_T^3}{12\mu}\frac{\partial p}{\partial x} - \frac{u_1 + u_2}{2}\,h + \frac{u_1 - u_2}{2}(\delta_1 - \delta_2)\right] = \frac{\partial h}{\partial t} \tag{2.6}$$

It is assumed here that there are enough numbers of asperities within the Hertzian zone such that h can be considered as a constant of time. Let the bracketed term in the left-hand side of Eq. (2.6) be denoted by

$$M = \frac{h_T^3}{12\mu}\frac{\partial p}{\partial x} - \frac{u_1 + u_2}{2} h + \frac{u_1 - u_2}{2} (\delta_1 - \delta_2) \tag{2.7}$$

For infinitely-wide slider bearing and rigid roller bearing, M is expressed as above. In elastohydrodynamic contact, the reduced pressure, q , and viscosity, μ, which are respectively

$$q = \frac{1 - e^{-dp}}{\alpha} \tag{2.8}$$

$$\mu = \mu_s e^{\alpha p} \tag{2.9}$$

are introduced. Then, M in an EHD contact is

$$M = \frac{h_T^3}{12\mu_s}\frac{\partial q}{\partial x} - \frac{u_1 + u_2}{2} h + \frac{u_1 - u_2}{2} (\delta_1 - \delta_2) \tag{2.10}$$

It is shown in appendix A that M in the case of EHD contact, rigid roller bearing, or infinitely-wide slider bearing is a stochastic quantity with a negligible variance comparing to the variance of the terms on the right hand side.

Re-arranging Eq. (2.7) and taking expected values on both sides, one obtains

$$\epsilon\left\{\frac{M}{h_T^3}\right\} = \frac{1}{12\mu}\,\epsilon\left\{\frac{dp}{dx}\right\} - \frac{u_1 + u_2}{2} h\,\epsilon\left\{\frac{1}{h_T^3}\right\} + \frac{u_1 - u_2}{2}\left[\epsilon\left\{\frac{\delta_1}{h_T^3}\right\} - \epsilon\left\{\frac{\delta_2}{h_T^3}\right\}\right] \tag{2.11}$$

where

$$\epsilon\left\{\;\right\} = \int_{-\infty}^{+\infty}\left\{\;\right\} f(r)\delta\gamma \tag{2.12}$$

and f(r) is the probability density distribution of the random variable γ.

Since M is a stochastic quantity with zero (or negligible) variance, M and $\frac{1}{h_T^3}$ can be considered to be (approximately) stochastically independent quantities. Hence

$$\epsilon\left\{\frac{M}{h_T^3}\right\} = M\,\epsilon\left\{\frac{1}{h_T^3}\right\} \tag{2.13}$$

Then Eq. (2.11) can be re-written as

$$M = \frac{1}{12\mu}\frac{d\bar{p}}{dx}\frac{1}{\epsilon\left\{\frac{1}{h_T^3}\right\}} - \frac{u_1 + u_2}{2}\,h + \frac{u_1 - u_2}{2}\,\frac{\epsilon\left\{\frac{\delta_1}{h_T^3}\right\} - \epsilon\left\{\frac{\delta_2}{h_T^3}\right\}}{\epsilon\left\{\frac{1}{h_T^3}\right\}} \tag{2.14}$$

where $\bar{p}$ is now the expected or mean value of p. Substituting Eq. (2.14) into Eq. (2.6) and re-arranging, one obtains the stochastic Reynolds equation for rigid rollers bearing and infinitely-wide slider bearing.

$$\frac{d}{dx}\left[\frac{1}{12\mu}\frac{d\bar{p}}{dx}\frac{1}{\epsilon\left\{\frac{1}{h_T^3}\right\}}\right] = \frac{u_1 + u_2}{2}\frac{dh}{dx} - \frac{u_1 - u_2}{2}\frac{d}{dx}\left[\frac{\epsilon\left\{\frac{\delta_1}{h_T^3}\right\} - \epsilon\left\{\frac{\delta_2}{h_T^3}\right\}}{\epsilon\left\{\frac{1}{h_T^3}\right\}}\right] \tag{2.15}$$

Similarly, the stochastic Reynolds equation for EHD contact can be expressed as

$$\frac{d}{dx}\left[\frac{1}{12\mu_a}\frac{d\bar{q}}{dx}\frac{1}{\epsilon\left\{\frac{1}{h_T^3}\right\}}\right] = \frac{u_1 + u_2}{2}\frac{dh}{dx} - \frac{u_1 - u_2}{2}\frac{d}{dx}\left[\frac{\epsilon\left\{\frac{\delta_1}{h_T^3}\right\} - \epsilon\left\{\frac{\delta_2}{h_T^3}\right\}}{\epsilon\left\{\frac{1}{h_T^3}\right\}}\right] \tag{2.16}$$

2.2.2 Longitudinal Surface Roughness

When the asperity ridges are parallel to the direction of rolling, δ_1 and δ_2 are independent upon x, u_1, u_2 and t. Again, assuming $\frac{\partial h}{\partial t} = 0$, then Eq. (2.1) can be simplified to

$$\frac{d}{dx}\left(\frac{h_T^3}{12\mu}\frac{dp}{dx}\right) = \frac{u_1 + u_2}{2}\frac{dh}{dx} \tag{2.17}$$

For the cases of rigid rollers and infinitely-wide slider bearings, with longitudinal surface roughness, it is shown in [7] that the stochastic Reynolds equation is of the form

$$\frac{d}{dx}\left[\frac{1}{12\mu}\frac{d\bar{p}}{dx}\,\epsilon\left\{h_T^3\right\}\right] = \frac{u_1 + u_2}{2}\,\frac{dh}{dx} \tag{2.18}$$

Similarly, the stochastic Reynolds equation of an EHD contact can be shown to be

$$\frac{d}{dx}\left[\frac{1}{12\mu_s}\frac{d\bar{q}}{dx}\,\epsilon\left\{h_T^3\right\}\right] = \frac{u_1 + u_2}{2}\,\frac{dh}{dx} \tag{2.19}$$

If the roughness distribution is symmetric to zero mean

$$\epsilon\left\{h_T^3\right\} = h^3\left(1 + 3\,\frac{\sigma^2}{h^2}\right) \quad . \tag{2.19a}$$

2.3 METHOD OF SOLUTION

2.3.1 Elastohydrodynamic Contacts

Using Grubin's approach, it is assumed that the average surface profile, h, in the inlet region is governed by the deformation produced by a Hertzian elliptical pressure distribution in the contacting region. From [14], this profile is given by

$$H - 1 = \frac{h - h_o}{h_o} = \frac{4W}{\pi H_o}\left[\,|X|\cdot\sqrt{X^2 - 1} - \ln\left(|X| + \sqrt{X^2 - 1}\right)\right] \tag{2.20}$$

Introducing dimensionless variables Q, X, H, H_T, $\bar{\sigma}$, U, $\bar{\delta}_1$, $\bar{\delta}_2$, $\bar{\delta}$ and S as defined in the Nomenclature, Eq. (2.16), for the transverse roughness becomes,

$$\frac{d}{dX}\left[\frac{dQ}{dX}\,\frac{H_o^2}{\epsilon\left\{\frac{1}{H_T^3}\right\}}\right] = \frac{dH}{dX} - \frac{S}{2}\,\frac{d}{dX}\left[\frac{\epsilon\left\{\frac{\bar{\delta}_1}{H_T^3}\right\} - \epsilon\left\{\frac{\bar{\delta}_1}{H_T^3}\right\}}{\epsilon\left\{\frac{1}{H_T^3}\right\}}\right] \tag{2.21}$$

The boundary conditions are:

$$\frac{dQ}{dX} = 0 \qquad \text{at} \qquad X = -1 \qquad (\text{at } H = 1) \tag{2.22}$$

$$Q = 0 \qquad \text{at} \qquad X = -\infty \tag{2.23}$$

2.3.1.a Pure Rolling Case

In this case, S = 0, and Eq. (2.21) becomes

$$\frac{d}{dX}\left[\frac{dQ}{dX}\,\frac{H_o^2}{\epsilon\left\{\frac{1}{H_T^3}\right\}}\right] = \frac{dH}{dX} \tag{2.24}$$

Integrating Eq. (2.24) twice with the two boundary conditions, one obtains

$$Q^* = Q\big|_{X=-1} = \int_{-\infty}^{-1} \frac{H-1}{H^3 H_o^2} \cdot G_2 \, dX \tag{2.25}$$

where $G_2 = H^3\,\epsilon\left\{\frac{1}{H_T^3}\right\}$

$$= H^3 \int_{-\infty}^{\infty} \frac{g(\delta^*)}{\frac{h^3}{h_o^3}\left(1 + \frac{\delta}{h}\right)^3}\, d\delta^*$$

$$= \int_{-\infty}^{\infty} \frac{g(\delta^*)}{\left[1 + \delta^*\left(\frac{\bar{\sigma}}{H}\right)\right]^3}\, d\delta^* \tag{2.26}$$

and $\delta^* = \bar{\delta}/\bar{\sigma}$

$\bar{\delta} = \bar{\delta}_1 + \bar{\delta}_2$

$\bar{\sigma}$ is the composite standard deviation and is defined as $\bar{\sigma}^2 = \bar{\sigma}_1^{\,2} + \bar{\sigma}_2^{\,2}$, $g(\delta^*)$ is the roughness height distribution function.

Once $\bar{\sigma}$ and $g(\delta^*)$ are given, Eq. (2.25) can be evaluated numerically for Q^*.

2.3.1.b Rolling and Sliding

If there is relative sliding between surfaces, S will not be zero, and the last term in the stochastic Reynolds equation, Eq. (2.21), will not necessarily vanish. However, if the roughness distribution function of both surface profiles are the same, then

$$\epsilon\left\{\frac{\bar{\delta}_1}{H_T^3}\right\} = \epsilon\left\{\frac{\bar{\delta}_2}{H_T^3}\right\} \tag{2.27}$$

Using this relation, Eq. (2.21) becomes

$$\frac{d}{dX}\left[\frac{dQ}{dX}\,\frac{H_o^2}{\epsilon\left\{\frac{1}{H_T^3}\right\}}\right] = \frac{dH}{dX} \tag{2.28}$$

which is the same as Eq. (2.24) of the pure rolling case. Q^* will accordingly be the same as that expressed in Eq. (2.25).

If, on the other hand, one of the contacting surfaces is considered rough while the other one smooth, then Eq. (2.21) becomes

$$\frac{d}{dX}\left[\frac{dQ}{dX}\,\frac{H_o^2}{\epsilon\left\{\frac{1}{H_T^3}\right\}}\right] = \frac{dH}{dX} \pm \frac{S}{2}\,\frac{d}{dX}\left[\frac{\epsilon\left\{\frac{\bar{\delta}}{H_T^3}\right\}}{\epsilon\left\{\frac{1}{H_T^3}\right\}}\right] \tag{2.29}$$

where the plus sign is for $\bar{\delta}_1 = 0$, and minus sign for $\bar{\delta}_2 = 0$.

(See Appendix B for the Fortran IV listing of the numerical analysis.)

Defining
$$G_4 = \frac{H^3}{\bar{\sigma}} \; \epsilon \left\{\frac{\delta}{H_T^3}\right\}$$

$$= \frac{H^3}{\bar{\sigma}} \int_{-\infty}^{\infty} \frac{\bar{\sigma}\,\delta^* g(\delta^*)\, d\delta^*}{H^3\left[1 + (\frac{\bar{\sigma}}{H})\delta^*\right]^3}$$

$$= \int_{-\infty}^{\infty} \frac{\delta^* g(\delta^*)}{\left[1 + (\frac{\bar{\sigma}}{H})\delta^*\right]^3} \tag{2.30}$$

Eq. (2.29), expressed in G_2 and G_4, becomes

$$\frac{d}{dX}\left[\frac{H_o^2\, H^3}{G_2}\frac{dQ}{dX} - H \mp \frac{S\bar{\sigma}}{2}\frac{G_4}{G_2}\right] = 0 \tag{2.31}$$

Using boundary condition (2.22), one obtains

$$H_o^2 \frac{H^3}{G_2}\frac{dQ}{dX} - H \mp \frac{S\bar{\sigma}}{2}\frac{G_4}{G_2} = -\,1 \mp \frac{S\bar{\sigma}}{2}\left(\frac{G_4}{G_2}\right)_{X=-1} \tag{2.32}$$

Integrating Eq. (2.32) between $-\infty$ and -1, one obtains the expression for Q^*

$$Q^* = \frac{1}{H_o^2}\left\{\int_{-\infty}^{-1}\left(\frac{H - 1}{H^3}\right) G_2 dX \pm \frac{S\bar{\sigma}}{2}\int_{-\infty}^{-1}\frac{1}{H^3}\left[G_4 - G_2\left(\frac{G_4}{G_2}\right)_{X=-1}\right] dX\right\} \tag{2.33}$$

Eq. (2.33) can be integrated numerically for Q^* for various slide to roll ratios from the pure rolling case, $S = 0$, to the simple sliding case for which $u_1 = u$, $u_2 = 0$, and $S = 2$.

For EHD contacts with longitudinal surface roughness, the stochastic Reynolds equation following Eq. (2.19) becomes

$$\frac{d}{dX}\left\{H_o^2 H^3\left[1 + 3\left(\frac{\bar{\sigma}}{H}\right)^2\right]\frac{dQ}{dX}\right\} = \frac{dH}{dX} \tag{2.34}$$

The above equation is valid for any rolling and sliding EHD contacts. Using boundary conditions, Eqs. (2.22) and (2.23), the reduced pressure Q^* at X = -1 can be integrated as

$$Q^* = \int_{-\infty}^{-1} \frac{H - 1}{H_o^2 H^3 \left[1 + 3 \left(\frac{\bar{\sigma}}{H}\right)^2\right]} dX \tag{2.35}$$

2.3.2 Rigid Rollers

If the elastic deformation of the rollers is neglected, the smooth, average surface profile can be approximated by a parabolic profile

$$H = \frac{h}{h_o} = 1 + \frac{X^2}{2\left(\frac{h_o}{R}\right)} \tag{2.36}$$

where

$X = x/R$

h_o = the average center film thickness

Using the same approach as developed in EHD contacts, but with different dimensionless variables for P, X, X^*, H, H_T, H^*, $\bar{\sigma}$, $\bar{\delta}_2$ and $\bar{\delta}$ as defined in the Nomenclature, the stochastic Reynolds equation for rigid rollers with transverse surface roughness can be expressed as

$$\frac{d}{dX}\left[\frac{dP}{dX} \frac{1}{\epsilon\left\{\frac{1}{H_T^3}\right\}}\right] = \frac{dH}{dX} - \frac{S}{2}\frac{d}{dX}\left[\frac{\epsilon\left\{\frac{\bar{\delta}_1}{H_T^3}\right\} - \epsilon\left\{\frac{\bar{\delta}_2}{H_T^3}\right\}}{\epsilon\left\{\frac{1}{H_T^3}\right\}}\right] \tag{2.37}$$

This equation has the same form as Eq. (2.21) of the EHD contacts. However, the boundary conditions for the case of rigid rollers will be different from Eqs. (2.22) and (2.23). They are given by

$$\frac{dP}{dX} = 0 \ , \qquad P = 0 \qquad \text{at} \quad X = X^*$$
$$P = 0 \qquad\qquad\qquad \text{at} \quad X = -\infty \tag{2.38}$$

Using these boundary conditions, Eq. (2.37) can be readily integrated to yield

$$P(X) = \int_{-\infty}^{X} \left(\frac{H - H^*}{H^3}\right) G_2 \, d\xi \pm \frac{S\bar{\sigma}}{2} \int_{-\infty}^{X} \frac{1}{H^3} \left[G_4 - \left(\frac{G_4}{G_2}\right)_{X=X^*} \cdot G_2\right] d\xi \tag{2.39}$$

when ξ is a dummy variable for X, and X^* and H^* are determined by imposing $P(X^*) = 0$. Eq. (2.39) can be integrated numerically to yield P for the pure rolling case (S = 0), simple sliding case (S = 2), as well as rolling and sliding case (any S). Once P(X) is found, the dimensionless load W^*, can be determined by

$$W^* = \left[\frac{h_o^2}{6\mu \left(u_1 + u_2\right) R^2}\right] W = \int_{-\infty}^{X^*} P(X)\, dX \tag{2.40}$$

For rigid rollers with longitudinal surface roughness, the stochastic Reynolds equation is

$$\frac{d}{dX} \left\{H^3 \left[1 + 3 \left(\frac{\bar{\sigma}}{H}\right)^2\right] \frac{dP}{dX}\right\} = \frac{dH}{dX} \tag{2.41}$$

Using boundary conditions, Eq. (2.38), one obtains

$$P = \int_{-\infty}^{X} \frac{H - H^*}{H^3 \left[1 + 3 \left(\frac{\bar{\sigma}}{H}\right)^2\right]} \, d\xi \tag{2.42}$$

where X^* and H^* are determined by the condition $P(X^*) = 0$. The dimensionless pressure and load can be determined in the same manner as that for rigid rollers with transverse surface roughness.

2.3.3 Infinitely-Wide Slider

For an infinitely-wide slider, the smooth, average surface profile can be represented by

$$H(X) = \frac{h(x)}{h_o} = 1 + \frac{m\ell}{h_o}(1 - X) \tag{2.43}$$

where

$h_o = h_{min}$ = minimum film thickness at the exit of the slider
m = slope of the slider

ℓ = length of the slider

Introducing dimensionless variables P, H_T, X, H and $\bar{\delta}$ as defined in the Nomenclature, one obtains the stochastic Reynolds equation for an infinitely-wide slider with transverse surface roughness,

$$\frac{d}{dX}\left[\frac{dP}{dX}\,\frac{1}{\epsilon\left\{\frac{1}{H_T^3}\right\}}\right] = \frac{dH}{dX} - \frac{d}{dX}\left[\frac{\epsilon\left\{\frac{\bar{\delta}_1}{H_T^3}\right\} - \epsilon\left\{\frac{\bar{\delta}_2}{H_T^3}\right\}}{\epsilon\left\{\frac{1}{H_T^3}\right\}}\right] \tag{2.44}$$

The boundary conditions for Eq. (2.44) are

$$P(0) = P(1) = 0 \tag{2.45}$$

For both surfaces having the same roughness characteristics,

$$\epsilon\left\{\frac{\bar{\delta}_1}{H_T^3}\right\} = \epsilon\left\{\frac{\bar{\delta}_2}{H_T^3}\right\} \tag{2.46}$$

Eq. (2.44) becomes

$$\frac{d}{dX}\left[\frac{dp}{dX}\frac{H^3}{G_2}\right] = \frac{dH}{dX} \tag{2.47}$$

Integrating twice, one obtains

$$P(X) = \int_o^X \frac{G_2}{H^2}\, d\xi - C\int_o^X \frac{G_2}{H^3}\, d\xi \tag{2.48}$$

where C is evaluated by the boundary condition P(1) = 0. For one surface rough, and the opposing surface smooth, Eq. (2.44) takes the form

$$\frac{d}{dX}\left[\frac{dP}{dX}\frac{1}{\epsilon\left\{\frac{1}{H_T^3}\right\}}\right] = \frac{dH}{dX} \pm \frac{d}{dX}\left[\frac{\epsilon\left\{\frac{\bar{\delta}}{H_T^3}\right\}}{\epsilon\left\{\frac{1}{H_T^3}\right\}}\right] \tag{2.49}$$

where the plus sign represents the case of a smooth surface sliding against a stationary rough surface, and the negative sign implies the rough sliding against smooth surface. Eq. (2.49), expressed in terms of G_2 and G_4, becomes

$$\frac{d}{dX}\left[\frac{dP}{dX}\frac{H^3}{G_2}\right] = \frac{dH}{dX} \pm \bar{\sigma}\frac{d}{dX}\left(\frac{G_4}{G_2}\right) \tag{2.50}$$

Integration of the above equation yields

$$P(X) = \int_o^X \frac{G_2}{H^2}\, d\xi \pm \bar{\sigma}\int_o^X \frac{G_4}{H^3}\, d\xi - C\int_o^X \frac{G_2}{H^3}\, d\xi \tag{2.51}$$

where C is determined by the boundary condition, P(1) = 0.

For the infinitely-wide slider with longitudinal surface roughness, the stochastic Reynolds equation is

$$\frac{d}{dX}\left\{H^3\left[1 + 3\left(\frac{\bar{\sigma}}{H}\right)^2\right]\frac{dP}{dX}\right\} = \frac{dH}{dX} \tag{2.52}$$

which, after integrating twice, yields

$$P(X) = \int_{-\infty}^{X} \frac{d\xi}{H^2\left[1 + 3\left(\frac{\bar{\sigma}}{H}\right)^2\right]} - C\int_{o}^{X} \frac{d\xi}{H^3\left[1 + 3\left(\frac{\bar{\sigma}}{H}\right)^2\right]} \tag{2.53}$$

with C determined by $P(1) = 0$. In all the above cases, the load can be evaluated by

$$W^* = \int_{o}^{1} P(X)dX \tag{2.54}$$

2.3.4 <u>Roughness Distribution Function</u>

The roughness distribution function employed in this paper is the same as that used by Christensen [7], namely,

$$g(\delta^*) = \begin{cases} \frac{35}{96}\left(1 - \frac{\delta^{*2}}{9}\right)^3 & -\delta^*_{max} < \delta^* < \delta^*_{max.} \\ 0 & \text{Elsewhere} \end{cases} \tag{2.55}$$

$$\delta^*_{max.} = 3 \tag{2.56}$$

This polynomial distribution function is an approximation to Gaussian distribution. The reason using this polynomial function is that the roughness height distribution function of many engineering surfaces is very close to Gaussian [20], and that a Gaussian distribution always implies a finite probability of having asperities of very large sizes which are very unlikely in practice.

2.4 DISCUSSION OF RESULTS

2.4.1 EHD Contacts

The effect of surface roughness on the pressure generation at the inlet of EHD contacts can be presented conveniently by using a quantity K_E, defined as the ratio of the inlet pressure calculated from the stochastic theory, Q_R^*, to that calculated from the Grubin's smooth-film theory, Q_S^*. Thus,

$$K_E = Q_R^*/Q_S^* \tag{2.57}$$

In Fig. (2.4), the ratio K_E is plotted against a surface roughness parameter, $\bar{\delta}_{max}$, for the following four cases

1) pure rolling with transverse surface roughness
2) pure rolling with longitudinal surface roughness
3) rolling and sliding with $S = 0.2$ and $\delta_1 = 0$ (smooth surface is faster)
4) rolling and sliding with $S = 0.2$ and $\delta_2 = 0$ (rough surface is faster)

The dimensionless load and film thickness for the above cases are $W = 3 \times 10^{-5}$ and $H_o = \frac{h_o}{R} = 10^{-5}$.

These curves are obtained by changing the magnitude of $\bar{\delta}_{max}$. It is seen that, for pure rolling with longitudinal surface roughness, K_E is reduced very slightly due to surface roughness effects. Even for $\bar{\delta}_{max}$ as high as 0.99, the reduction is only about 7.5%.

Contrast to the effect of longitudinal roughness, the transverse roughness has a much more pronounced effect on the integrated pressure. It tends to increase the dimensionless reduced pressure and hence also tends to increase the load capacity as $\bar{\delta}_{max}$ increases. For pure rolling, the transverse roughness causes an increase in Q^* from 7% to 30% as $\bar{\delta}_{max}$ is increased from 0.6 to 0.99. The effect of relative sliding between a smooth surface and a rough surface in EHD contacts is shown in the two curves for $S = 0.2$. Even for such a small slip, there is already noticeable departure from the pure rolling case. For the case where the smooth surface is faster, there is an additional pumping effect, compared to the pure rolling case. The reverse is true if the roughness surface is faster.

The effect of H_o is studied in Fig. (2.6). It is shown that the three curves for $H_o = 10^{-5}$, 5×10^{-5}, 9×10^{-5} almost coincide with one another. This indicates that the roughness effect on EHL is almost entirely independent upon H_o.

Fig. (2.6) shows the integrated value of Q^* against H_o for the condition of pure rolling with transverse roughness, for different ratio of $\bar{\delta}_{max}$ ranging from 0.0 (smooth film theory) to 0.99. It is interesting to note that the curves are parallel straight lines. Again it is readily seen that the magnitude of Q^* depends on the ratio of $\bar{\delta}_{max}$. For $\bar{\delta}_{max} = 0.99$, there is approximately a 20% gain in the mean film thickness over that based on smooth film theory. For $\bar{\delta}_{max} = 0.9$, and 0.6, the gain in mean film thickness is about 15% and 5% respectively.

In the case of simple sliding of an EHD contact, i.e. S = 2, elastic deformation of asperities begins to be significant at X = -1. At this position, the values of $\bar{\sigma}$, the r.m.s. roughness amplitude and $g(\delta^*)$ the asperity distribution function, will no longer be the same as those of the undeformed asperities. Therefore Eq.(2.33) cannot be applied under this situation. One should notice that Eq. (2.33) is valid for rolling and sliding case, only when the elastic deformation of asperities near X = -1 can be assumed to be negligibly small. This occurs only when S is small.

2.4.2 Rigid Rollers

The effect of surface roughness on the dimensionless load of rigid rollers is presented in terms of K_R which is a quantity defined as the ratio of the dimensionless load from the stochastic theory, W_R^*, to that of the smooth film theory, W_S^*. Thus

$$K_R = W_R^*/W_S^* \tag{2.58}$$

Results of K_R versus $\bar{\delta}_{max}$ for the following six cases are shown in Fig. (2.7):

1. simple sliding of a smooth roller against a stationary rough roller with transverse surface roughness, $S = 2$,
2. rolling and sliding with transverse roughness; $S = 0.2$, $\delta_1 = 0$ (smooth surface is faster),
3. pure rolling with transverse roughness,
4. rolling and sliding with transverse roughness; $S = 0.2$, $\delta_2 = 0$ (rough surface is faster),
5. simple sliding of a rough roller against a stationary smooth roller with transverse roughness; $S = 2$,
6. longitudinal surface roughness.

The center film thickness for the above cases is $h_o/R = 5 \times 10^{-4}$.

Similar to elastic rollers, the effect of surface roughness on rigid rollers with longitudinal roughness is quite small. For $\bar{\delta}_{max} = 0.99$, the reduction of K_R is only about 5%.

For pure rolling with transverse roughness, K_R is increased by about 16% when $\bar{\delta}_{max} = 0.99$. For rolling and sliding with $S = 0.2$ and smooth surface moving faster, there is an increase in load carrying capacity, compared to the pure rolling case. The reverse is true when the rough surface is faster in the rolling and sliding case. When a smooth roller is sliding against a stationary rough roller, there is a substantial increase in K_R. When $\bar{\delta}_{max} = 0.6$ and 0.99, the gain in K_R are 8.5% and 39% respectively. However, when a rough roller is sliding against a stationary smooth roller, K_R is almost unaffected. When $\bar{\delta}_{max}$ is greater than 0.66, K_R begins to decrease slightly after a steady increase.

This small dip in K_R is suspected to be caused by using the above mentioned polynominal function as the surface roughness distribution function. When a sinusoidal distribution function [17] which is defined as,

$$g(\delta^*) = \begin{cases} \dfrac{1}{\pi\sqrt{9-\delta^{*2}}} & -3 < \delta^* < 3 \\ 0 & \text{Elsewhere} \end{cases} \tag{2.59}$$

is employed, the results which are not plotted here show that the dip disappears and that K_R increases with the increase of $\bar{\delta}_{max}$.

2.4.3 Infinitely-Wide Slider Bearing

In Fig. (2.8), W^* is plotted against $\bar{\delta}_{max}$ for the following four cases:

1. simple sliding of a smooth surface against a rough surface with transverse roughness,
2. both surfaces having the same roughness distribution functions with transverse roughness,
3. simple sliding of a rough surface against a smooth one, with transverse roughness,
4. longitudinal surface roughness.

Qualitatively, the roughness effect on a slider checks very well with that on rollers. When the roughness direction is longitudinally oriented, the load carrying capacity of the oil film is reduced..

In the case of transverse roughness, the effect on load capacity is always beneficial. For both surfaces having the same kind of roughness distribution function, W^* is increased by 66% approximately, when $\bar{\delta}_{max}$ is 0.99. For a smooth surface sliding against a rough one, the gain in W^* is even larger. W^* is increased by about 129% when $\bar{\delta}_{max}$ is 0.99. For a rough surface sliding against a smooth one, W^* is only increased slightly.

The authors' results agree very well to those obtained by Rhow and Elrod [18], who have studied the effects of two-sided straited roughness on the load-carrying capacity of an infinitely wide slider bearing. The only exception is that the authors' results show a small dip in W^*, when $\overline{\delta}_{max}$ is larger than 0.9. This small dip in W^* is caused by employing the polynomial function as the surface roughness distribution. When the sinusoidal distribution is used, the dip in W^* disappears.

2.5 CONCLUSIONS

1. Based on Christensen's stochastic model of hydrodynamic lubrication, a Grubin type elastohydrodynamic analysis at the inlet of a Hertzian contact indicates that surface roughness can have a noticeable effect on the level of mean film thickness between EHD contacts.

2. For longitudinal surface roughness, ridges parallel to the direction of rolling, the present analysis predicts an inlet pressure or inlet film thickness smaller than that predicted by the smooth-film EHD theory.

3. For transverse surface roughness, ridges perpendicular to the direction of rolling, the inlet mean film thickness level is increased noticeably due to the additional pumping by transverse ridges. The level of increase is mainly a function of δ_{max}/h_o, the ratio of the maximum ridge height to the mean film thickness at the inlet and is not sensitive to other operating parameters. For δ_{max}/h_o approaching unity, which corresponds to $h_o/\sigma = 3$ for $\delta_{max} = 3\sigma$, one can expect an increase of 25% in mean film thickness compared to the smooth-film EHD film thickness for pure rolling. Results for small slide to roll ratios indicates that the case of smooth sliding over rough gives further enhancement in mean film thickness, whereas the case of rough sliding over smooth yields a slight reduction in mean film thickness comparing to pure rolling. For high slide to roll ratios, it was found that local elastohydrodynamic effect due to local pressure fluctuations will become significant, and the present analysis based on the Grubin approach will become invalid.

4. For rigid rollers and infinitely-wide slider bearings, load capacities calculated for rough surfaces show trends similar to those found in EHD contacts. However, the effects for infinitely-wide slider bearings are much stronger than that for rigid rollers.

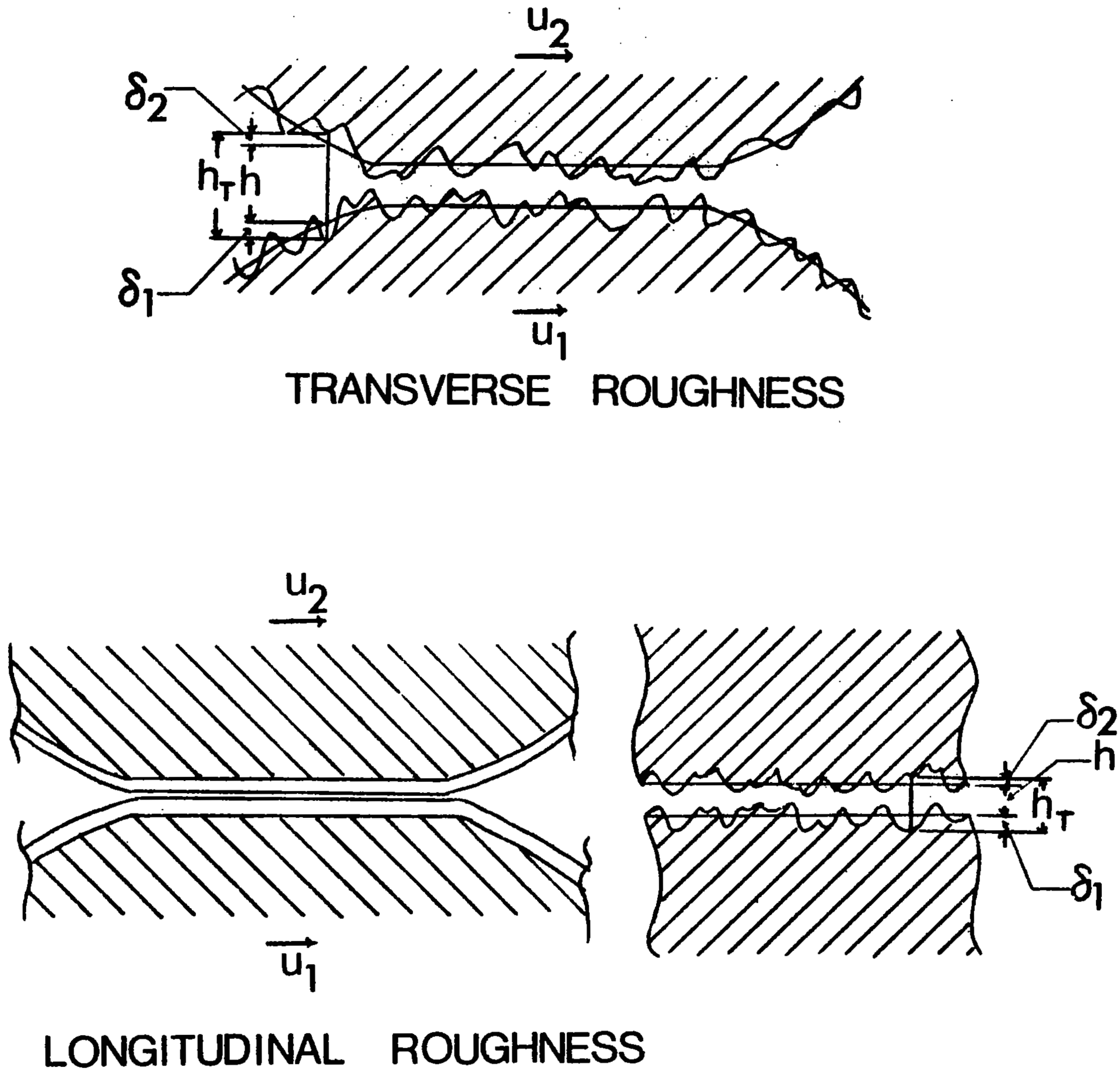

Figure 2-1 EHD Contacts Between Two Rough Surfaces

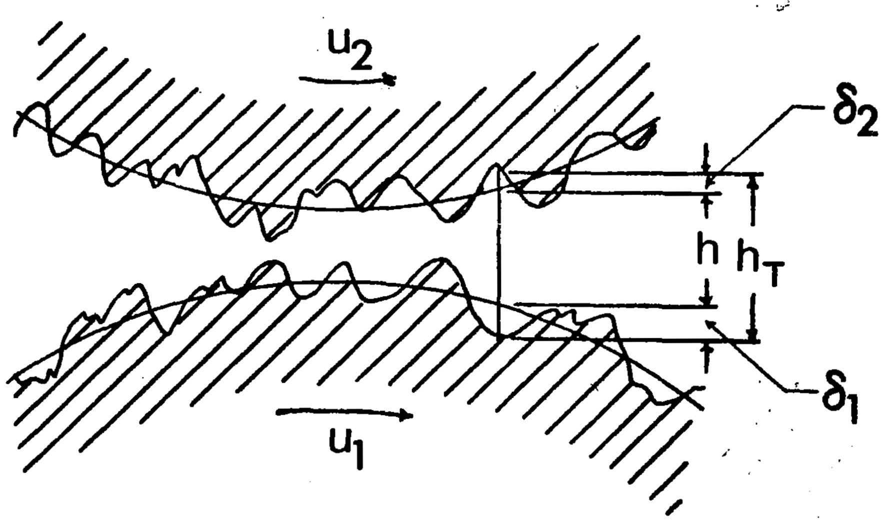

Figure 2-2 Rigid Rollers With Rough Surfaces

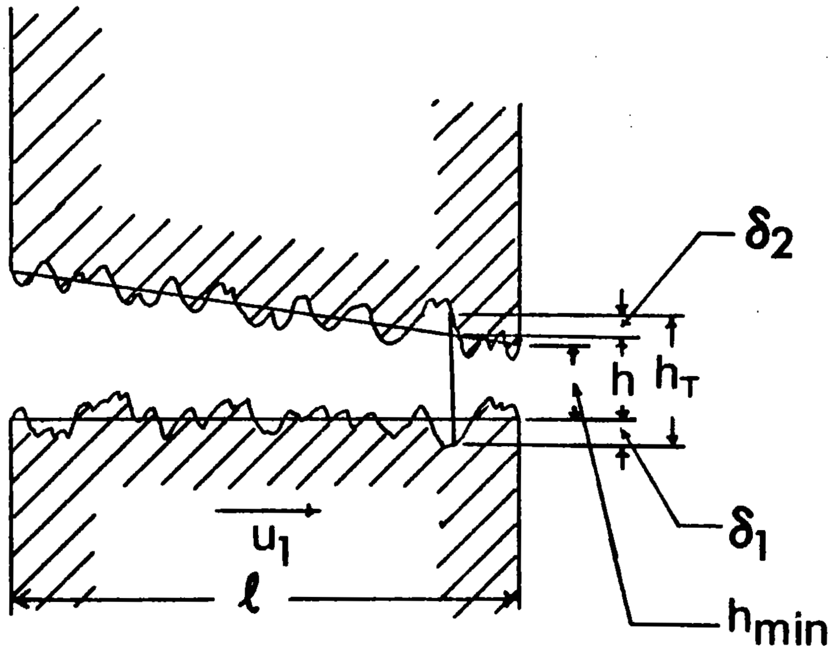

TRANSVERSE ROUGHNESS

Figure 2-3 An Infinitely-Wide Slider Bearing with Rough Surfaces

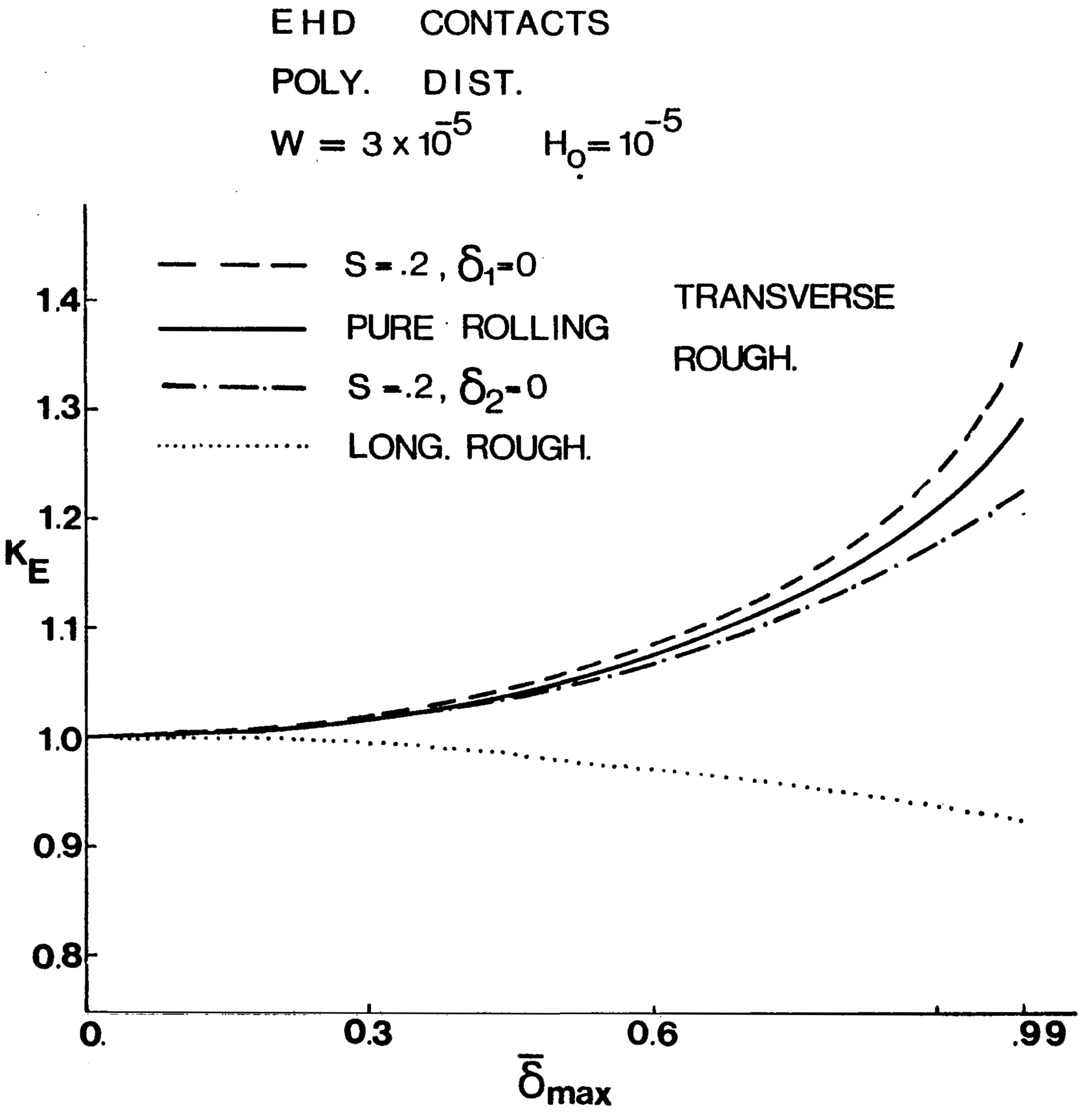

Fig. 2-4 The Effect of Transverse and Longitudinal Roughness on the Ratio of the Reduced Pressure for Rough Surfaces to that for Smooth Surfaces, $K_E = Q_R^*/Q_S^*$, of an EHD Contact

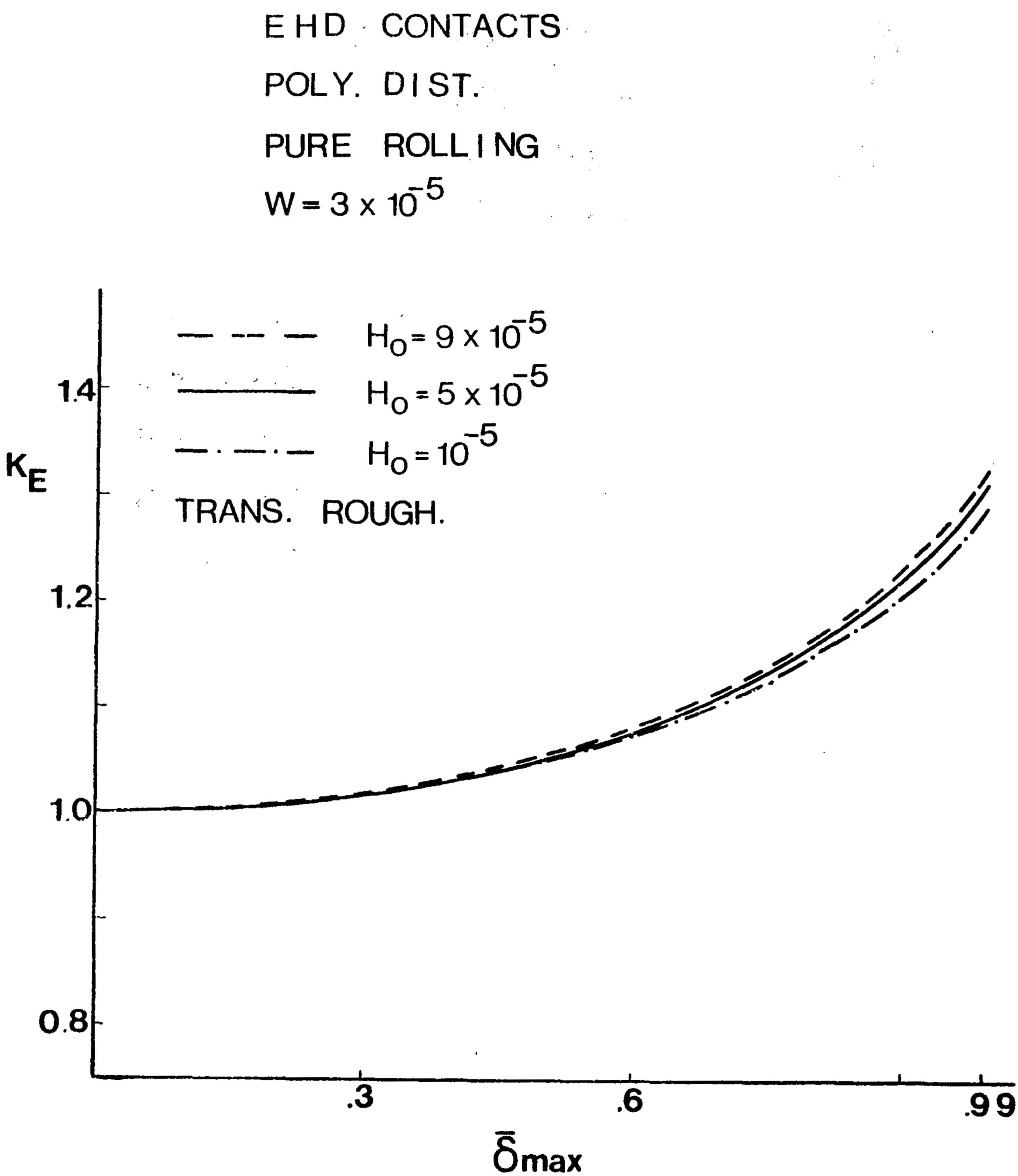

Fig. 2-5 The Effect of the Center Film Thickness, H_o, on the Ratio of the Reduced Pressure for Rough Surfaces to that for Smooth Surfaces, $K_E = Q_R^*/Q_S^*$, of an EHD Contact

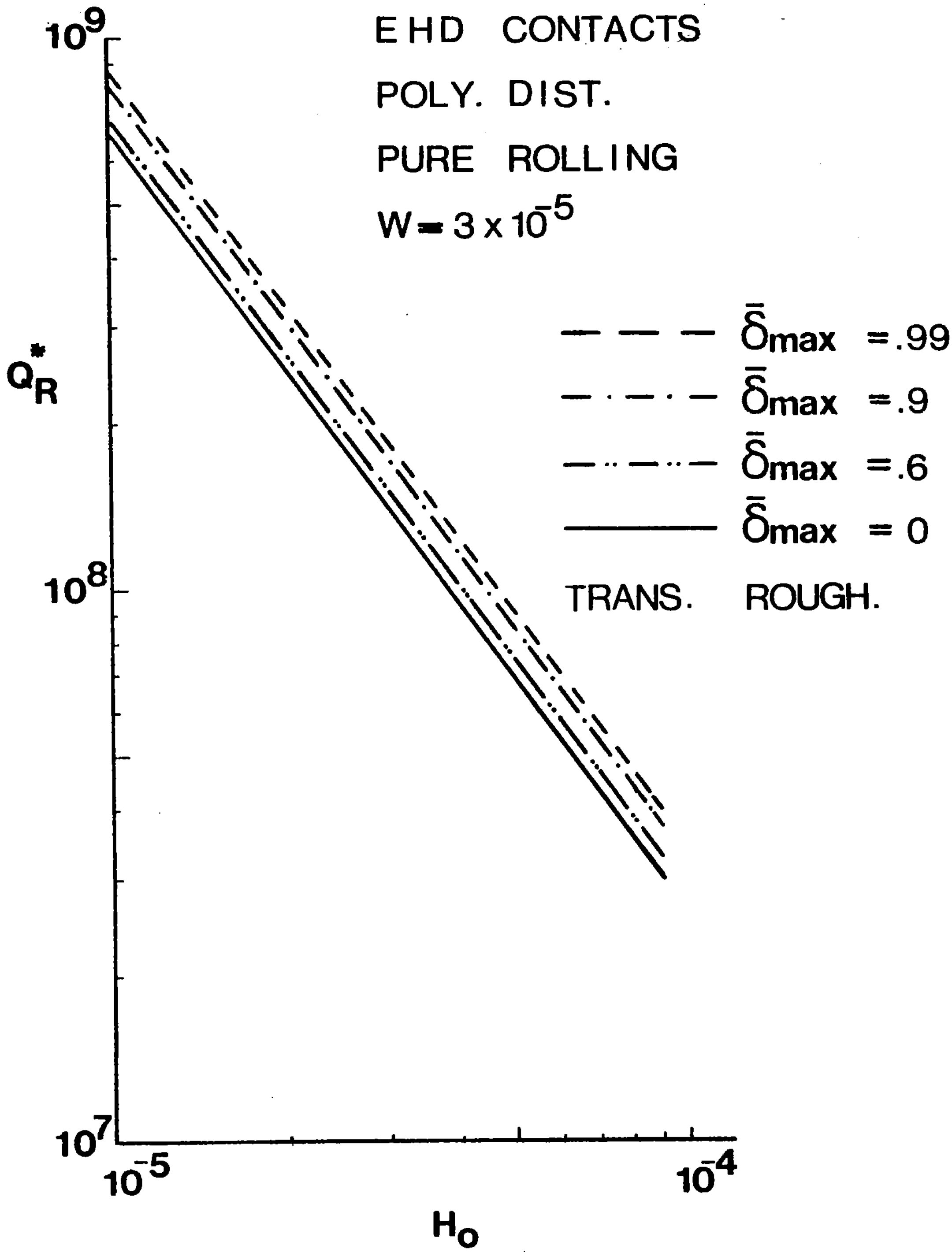

Fig. 2-6 The Effect of the Roughness Height to Center Film Thickness Ratio, $\bar{\delta}_{max}$, on the Normalized Reduced Pressure, Q_R^*, of an EHD Contact.

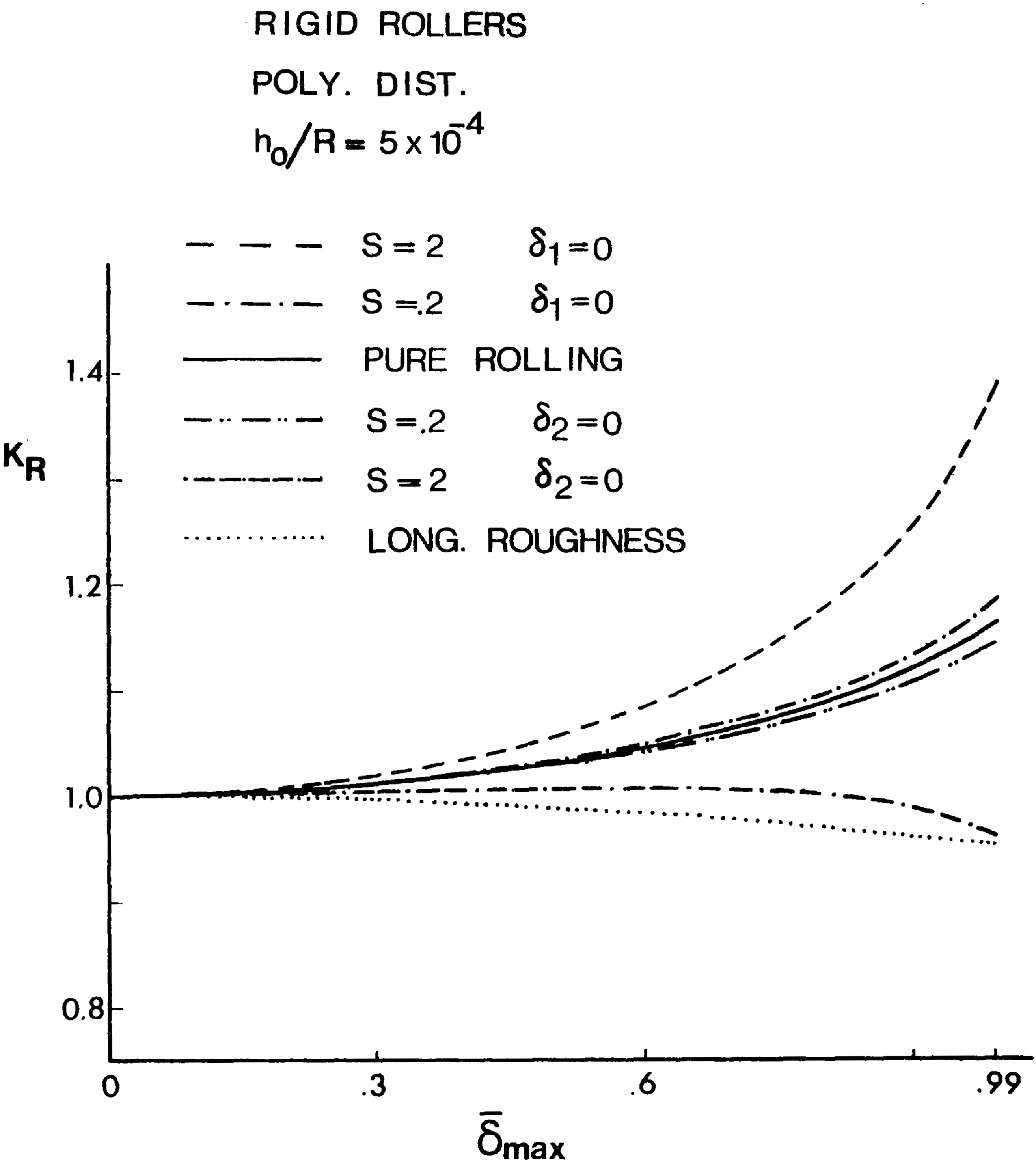

Fig. 2-7 The Variation of the Normalized Load Ratio, $K_R = W_R^*/W_S^*$, with the Roughness Height, $\bar{\delta}_{max} = \delta_{max}/h_o$, for Rigid Rollers

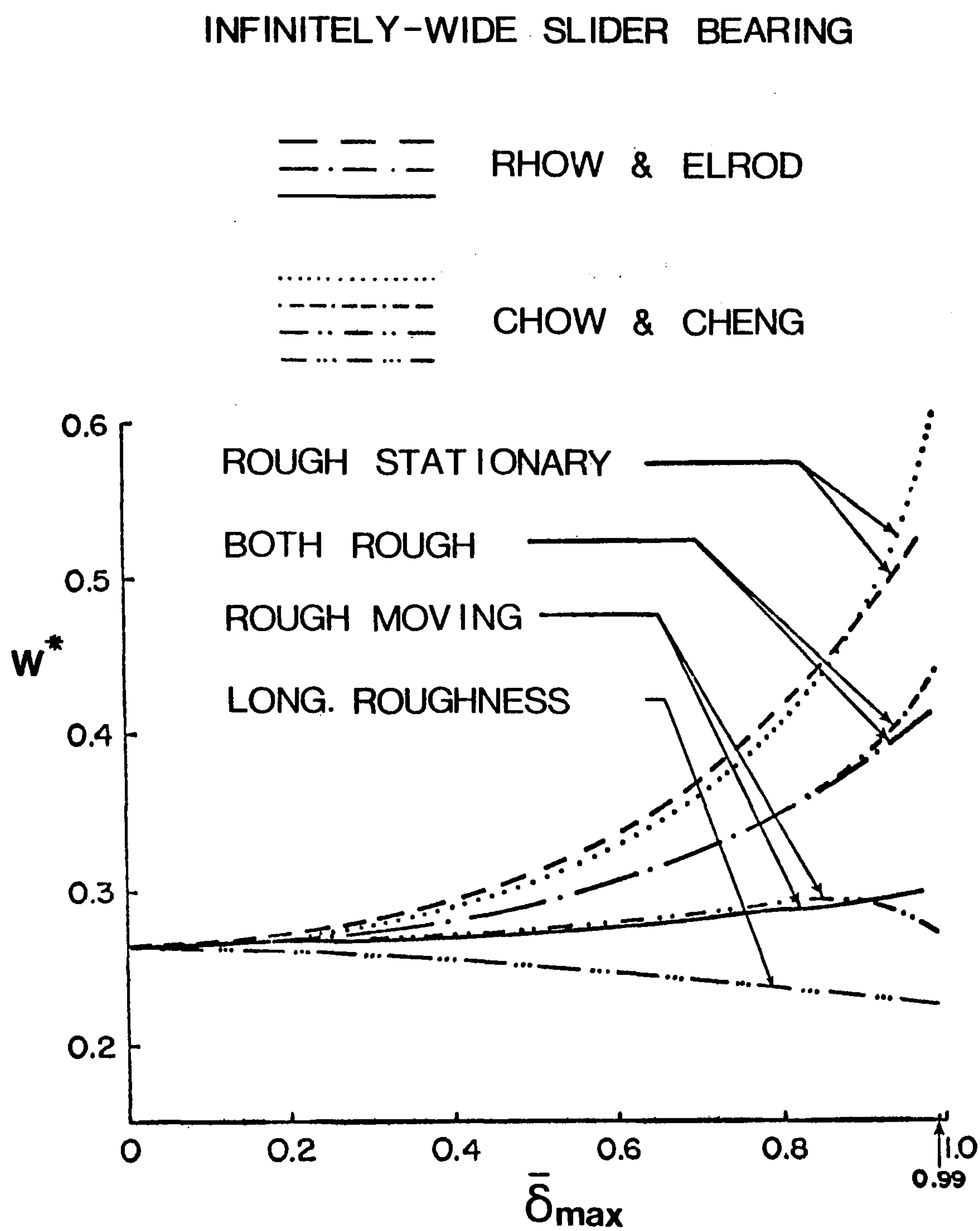

Fig. 2-8 The Variation of the Nor alized Load, $W^* = \frac{h_o^2}{6\mu u_1 \ell^2} w$, with the Roughness Height, $\bar{\delta}_{max}$, for an Infinitely-wide Slider Bearing

CHAPTER III

WAVINESS AND ROUGHNESS IN ELASTOHYDRODYNAMIC LUBRICATION

3.1 INTRODUCTION

A stochastic theory for elastohydrodynamic lubrication of contact with two-sided roughness has been developed in Chapter II. The basic requirement of this theory is that the roughness pattern must be very dense within the contact zone. In other words, the largest wavelength in the roughness spectrum must be small compared to the contact width. If the largest wavelength is of the same order of the contact width, surface roughness becomes surface waviness. The stochastic theory may be invalid in this region.

In order to ascertain the conditions under which the stochastic theory becomes valid the reduced pressure based on the deterministic approach using a sinusoidal profile and that calculated from the stochastic theory using a surface roughness distribution equivalent to the sinusoidal profile is compared. The comparison is only made for the transverse roughness since the effect of longitudinal roughness is usually negligibly small comparing to the effect of transverse roughness.

3.2 GOVERNING EQUATION

In comparing the effect of waviness and roughness on the reduced pressure, the surface profile is assumed to be in the form of sinusoidal waviness. The reduced pressure is then solved by the deterministic approach for the waviness case. At the same time, a density distribution function equivalent to the chosen sinusoidal wave is evaluated. Using this equivalent roughness distribution function, the reduced pressure for the roughness case is then solved by the stochastic approach as illustrated in Chapter II. Then, the effect of surface waviness and roughness will be compared for the pure rolling case.

3.2.1 The Waviness Case

In the waviness case, the one-dimensional Reynolds equation governing the pressure in an EHD contact of an isothermal and incompressible lubricant is

$$\frac{\partial}{\partial x}\left(\frac{h_T^3}{12\mu}\frac{\partial p}{\partial x}\right) = \frac{u_1 + u_2}{2}\frac{\partial h_T}{\partial x} + \frac{\partial h_T}{\partial t} \tag{3.1}$$

where h_T is the local total film thickness consisting of the following three parts h, δ_1, δ_2

where h = the nominal smooth part of the average film thickness

δ_1, δ_2 = roughness amplitude measured from the mean level of surfaces 1 and 2

$$\delta_1 = \delta_{max_1} \sin\left[(2n_1\pi)(x - u_1 t)\right] \tag{3.2}$$

$$\delta_2 = \delta_{max_2} \sin\left[(2n_2\pi)(x - u_2 t)\right] \tag{3.3}$$

$$\theta_1 = u_1 t$$

$$\theta_2 = u_2 t$$

It is assumed that the asperities on both surfaces are straight ridges perpendicular to the direction of rolling. With the relations

$$\frac{\partial \delta_1}{\partial t} = - u_1 \frac{\partial \delta_1}{\partial x} \tag{3.4}$$

$$\frac{\partial \delta_2}{\partial t} = - u_1 \frac{\partial \delta_2}{\partial x} \tag{3.5}$$

Eq. (3.1) is simplified as

$$\frac{d}{dx}\left(\frac{h_T^3}{12\mu}\frac{dp}{dx}\right) = \left(\frac{u_1 + u_2}{2}\right)\frac{dh}{dx} - \left(\frac{u_1 - u_2}{2}\right)\frac{d}{dx}\left(\delta_1 - \delta_2\right) + \frac{dh}{dt} \tag{3.6}$$

It is further assumed that there are enough number of asperities within the Hertzian contact zone such that h can be considered as a constant of time.

i.e. $$\frac{dh}{dt} = 0 \tag{3.7}$$

Hence, in the case of pure rolling, one obtains

$$\frac{d}{dx}\left(\frac{h_T^3}{12\mu}\frac{dp}{dx}\right) = u\,\frac{dh}{dx} \tag{3.8}$$

with dimensionless variables Q_w, X, H, H_T, $\bar{\sigma}$, U, $\bar{\delta}_1$, $\bar{\delta}_2$, and $\bar{\delta}$ as defined in the Nomenclature, Eq. (3.8) is transformed to

$$\frac{d}{dX}\left(H_T^3\frac{dQ_w}{dX}\right) = \frac{1}{H_o^2}\;\frac{dH}{dX} \tag{3.9}$$

where H, the average surface profile in the inlet region is governed by

$$H - 1 = \frac{h - h_o}{h_o} = \frac{4W}{\pi H_o}\left[\,|X|\sqrt{X^2 - 1} - \ell n\left(|X| + \sqrt{X^2 - 1}\right)\,\right] \tag{3.10}$$

The boundary conditions are:

$$\frac{dQ_w}{dX} = 0 \qquad \text{at} \qquad X = -1 \tag{3.11}$$

$$Q_w = 0 \qquad \text{at} \qquad X = -\infty \tag{3.12}$$

Integrating Eq. (3.10) twice with these two boundary conditions, one obtains

$$Q_w^* = Q_w\Big|_{X=-1} = \int_{-\infty}^{-1}\left(\frac{H - 1}{H_o^2\,H_T^3}\right) dX \tag{3.13}$$

In the pure rolling case

$$\theta_1 = \theta_2 = \theta = ut \tag{3.14}$$

In addition, it is assumed that

$$n_1 = n_2 = n \tag{3.15}$$

$$\delta_{max} = \delta_{1\ max} + \delta_{2\ max} \tag{3.16}$$

For given h_o/R, W, δ_{max}, n and θ, Eq. (3.13) is solved numerically by Simpson's integration routine.

3.2.2 The Roughness Case

The probability density function corresponding to a sinusoidal wave is [17]

$$f(\delta^*) = \begin{cases} \dfrac{1}{\dfrac{1}{\pi}\sqrt{1 - \frac{1}{9}\delta^{*2}}} & -3 < \delta^* < 3 \\ 0 & \text{elsewhere} \end{cases} \tag{3.17}$$

From Chapter II, the corresponding reduced pressure at the inlet is

$$Q_R^* = \int_{-\infty}^{-1} \left(\frac{H - 1}{H_o^2 H^3}\right) G_2 dX \tag{3.18}$$

where

$$G_2 = \frac{1}{\pi}\int_{-3}^{3} \frac{\dfrac{1}{\sqrt{1 - \frac{1}{9}\delta^{*2}}}}{\left[1 + \delta^*\left(\frac{\sigma}{H}\right)\right]^3} d\delta^* \tag{3.19}$$

$Q_R^* = Q^*$ calculated by stochastic theory.

Hence Q_R^* is evaluated for different values of δ_{max}.

3.3 DISCUSSION OF RESULTS

Though the following examples are only connected with the pressure generation at the inlet of elastohydrodynamic contacts, yet, qualitatively, the general trends of the results will be relevant to other types of bearing and surface irregularity.

The comparison between waviness and roughness can be presented conveniently by using a quantity K_D which is defined as

$$K_D = \frac{Q_W^* - Q_R^*}{Q_R^*} \tag{3.20}$$

where Q_W^* and Q_R^* stand for the inlet reduced pressure calculated from the waviness model and the roughness model respectively. Hence, by definition, K_D is the fractional deviation of the inlet reduced pressure of the waviness model from that of the corresponding roughness model. The results of such a comparison are shown in Fig. 3.1 to Fig. 3.3. The dimensionless load and film thickness for these examples are $W = 3 \times 10^{-5}$ and $H_o = h_o/R = 10^{-5}$, while the ratio δ_{max}/h_o in these three figures are 0.3, 0.45 and 0.6 respectively. The phase angles chosen are 0, $\pi/2$, π and $-\pi/2$ while the n-values are integers.

It is readily seen that K_D heavily depends upon the phase angle θ for small n. Particularly, for $\theta = \pi/2$ and $-\pi/2$, the magnitude of K_D even changes signs. However, the effect of phase angle on K_D decreases rapidly as n increases. Furthermore, for larger δ_{max} which means more pronounced asperity interaction, K_D is larger for the same n. For smaller δ_{max}, K_D is smaller. The approximate values of K_D at n = 5 and n = 10 for the extreme cases of $\theta = -\pi/2$ and $\pi/2$ are listed as follows

	n = 5			n = 10		
δ_{max}/h_o	0.3	0.45	0.6	0.3	0.45	0.6
K_D	±3.5%1	± 6%	±10%	±0.5%	± 1%	±1.5%

These results provide a better understanding to the statistical roughness theory. First, they show that the effect of phase angle vanishes with increasing n. Second, the effect of n becomes less important when n is greater than some critical value for a given δ_{max}. The discrepancy between the waviness model and the roughness model becomes poorer as δ_{max}/h_o increases. It is quite evident that n and δ_{max}/h_o are both important parameters that determine the validity of the statistical theory for roughness surfaces. For the particular numerical example used in these calculations, it is found that for $n > 10$, waviness is equivalent to roughness and that the stochastic theory holds. Even for $n = 5$, one can still apply the stochastic theory with reasonable accuracy.

3.4 CONCLUSIONS

For a given W and H_o

1. θ, n and δ_{max}/h_o are the parameters to determine the deviation of the stochastic, roughness made from the deterministic waviness model.

2. The effect of phase angle diminishes with increasing n.

3. The effect of n vanishes as n becomes large, and the stochastic theory for roughness surface is proved to be valid as n approaches a critical value depending on δ_{max}/h_o for a given W and H_o.

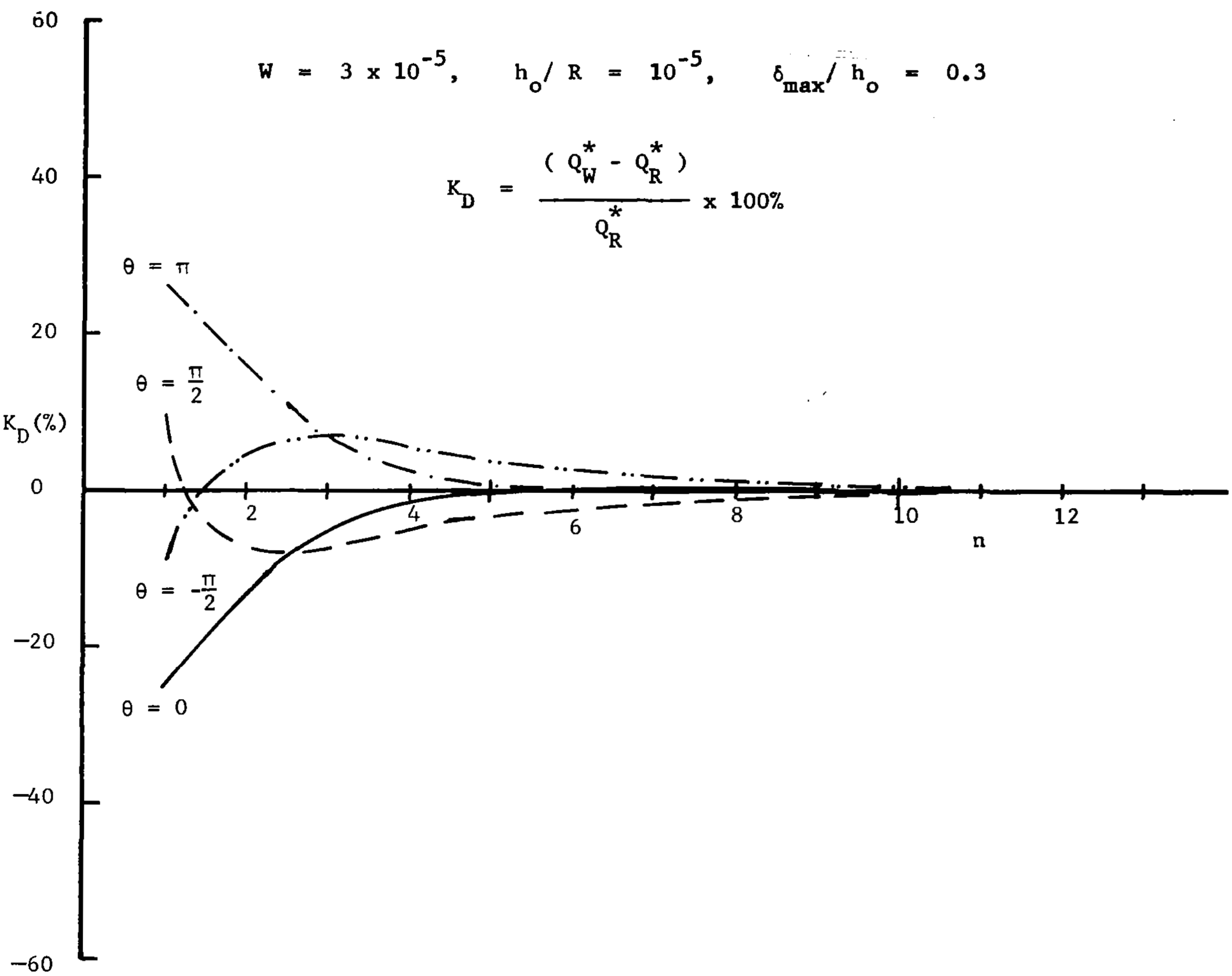

Fig. 3-1 The Effect of the Number of Wave Cycles, n, and the Phase Angle, θ, on the Percentage of Deviation of the Normalized Reduced Pressure, K_D, for Roughness to Thickness Ratio $\delta_{max}/h_o = 0.3$

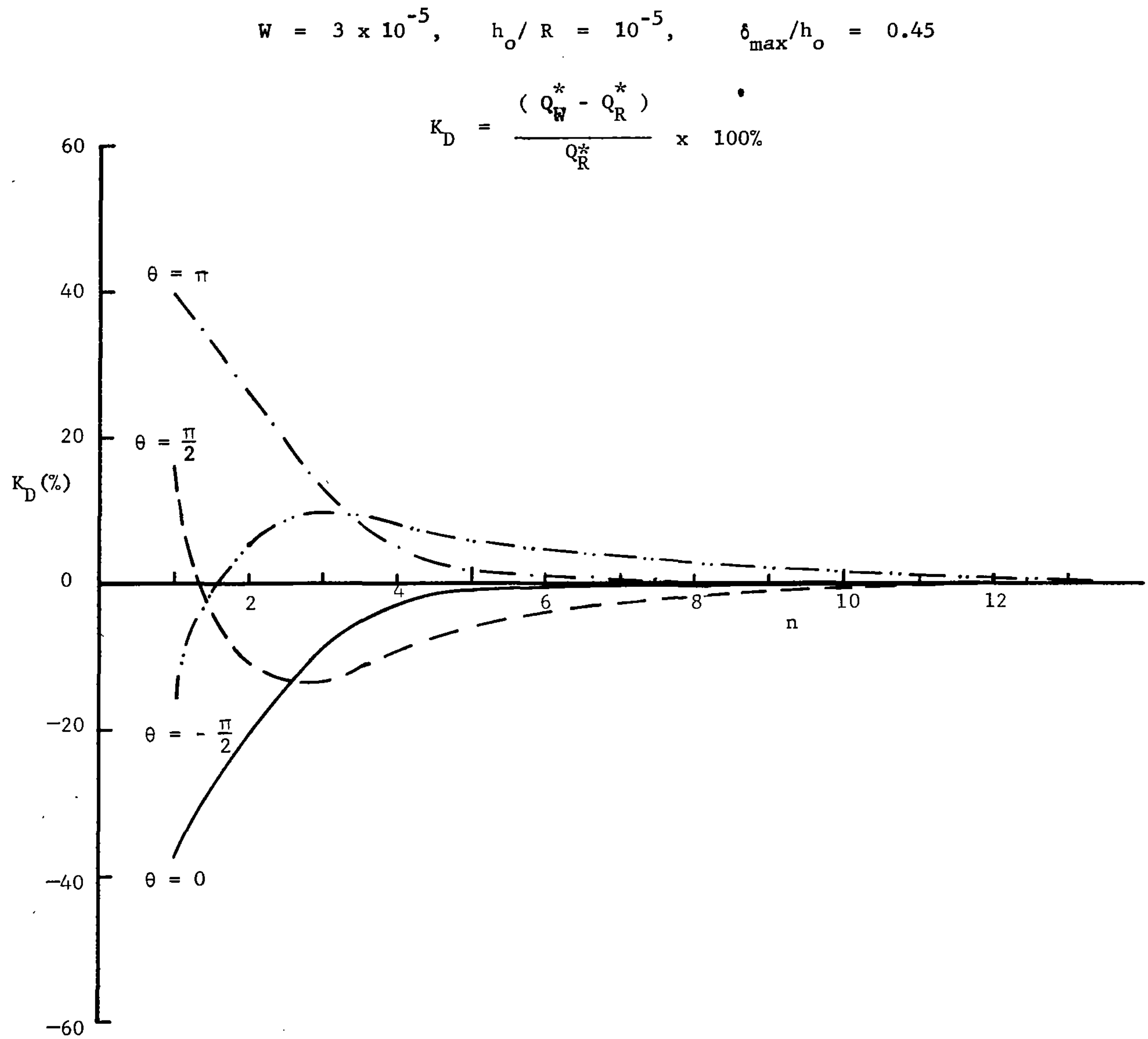

Fig. 3-2 The Effect of the Number of Wave Cycles, n, and the Phase Angle, θ, on the Percentage of Deviation of the Normalized Reduced Pressure, K_D, for Roughness to Thickness Ratio $\delta_{max}/h_o = 0.45$

$$W = 3 \times 10^{-5}, \quad h_o / R = 10^{-5}, \quad \delta_{max} / h_o = 0.6$$

$$K_D = \frac{(Q_W^* - Q_R^*)}{Q_R^*} \times 100\%$$

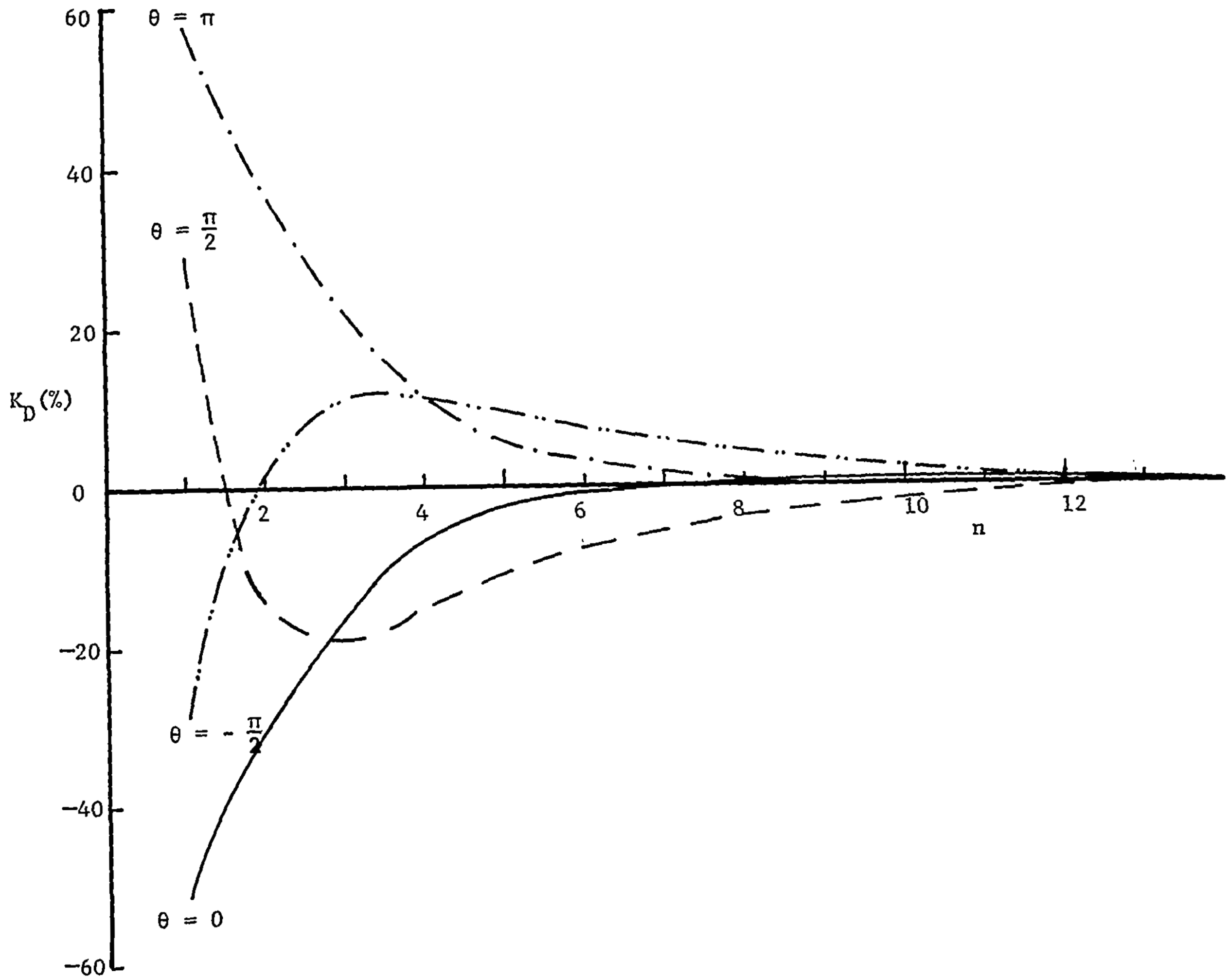

Fig. 3-3 The Effect of the Number of Wave Cycles, n, and the Phase Angle, θ, on the Percentage of Deviation of the Normalized Reduced Pressure, K_D, for Roughness to Thickness Ratio $\delta_{max}/h_o = 0.6$

CHAPTER IV

PRESSURE PERTURBATION IN EHD CONTACTS DUE TO AN ELLIPSOIDAL ASPERITY

4.1 INTRODUCTION

Recently, there has been a growing interest in the effect of surface roughness on the bearing performance in thin film lubrication. In Chapter II, the stochastic theory is used to study the effect of surface roughness on the average EHD film thickness and the integrated pressure at the inlet of the lubricated Hertzian contacts. However, the stochastic theory is incapable of predicting any detailed local perturbations in pressure or deformation caused by the asperities. It was recently pointed out by Tallian [19] that the pressure ripples can rise to a very high level in rolling and sliding EHD line contacts. These ripples are very likely one of the chief attributing factors to contact fatigue.

In the last few years, there has been considerable interest in the basic event involving a single asperity entering an EHD contact [5] or the encounter between two identical asperities [4]. The work in this chapter is aimed towards gaining further understanding of the effect of a single asperity on pressure distribution in a line EHD contact. Special attention is given to the three-dimensional aspect of the asperity which is assumed to be ellipsoidal at the tip. The effects of ellipticity (aspect ratio) on the double amplitude of pressure fluctuations under various rolling and sliding condition is examined in detail.

4.2 MATHEMATICAL ANALYSIS

The present analysis consists of two parts. The first part studies the pressure fluctuations due to a single three-dimensional ellipsoidal asperity at the inlet region of an EHD contact assuming that the asperity shape is unaffected by the perturbed pressures. These pressure fluctuations are determined by solving a perturbed Reynolds equation, in which the unperturbed pressure profile is obtained by using a line contact EHD analysis [22]. Results are presented as the perturbed pressure profile, Φ, as well as the amplitude of the pressure ripple, Δ_s, as a function of ellipticity ratio, γ, maximum Hertzian pressure, P_{Hz}, nominal EHD film thickness h_o/R, asperity size, $\bar{b}$, asperity height, c_1/h_o, pressure viscosity coefficient, G, slide to roll ratio, S, and the position of the asperity center X_3.

In the second part, the line contact EHD analysis [22] is modified to include a two dimensional asperity ridge on the stationary side of the lubricated contacts. In this approach, the elastic deformation of the asperity is included. Results which are presented as the double amplitude of the perturbed pressure as a function of P_{Hz}, h_o/R, $\bar{b}$, c_1/h_o, G, and X_3, are compared with those obtained for the three dimensional ellipsoidal asperity with large ellipticity ratio for the case of simple sliding between a smooth surface and a stationary asperity (S=2).

4.2.1 Geometrical Configuration

The contact between two cylinders as shown in Fig. (4.1a) can be described by an equivalent cylinder near a flat surface as shown in Fig. (4.1b). As the contact width is very small compared to the dimension of the cylinder, the film thickness for a rigid cylinder, h_g, without the asperity is

$$h_g \simeq h_o + \frac{x^2}{2R} \tag{4.1}$$

where x = coordinate along the film

$$R = \frac{R_1 R_2}{R_1 + R_2}$$

$R_1 R_2$ = radius of rollers 1 and 2,

h_o = undeformed center film thickness

With elastic deformation, the film thickness profile, still without the asperity [22] becomes

$$h_1 = h_o + \frac{x^2}{2R} - \frac{4}{\pi E'} \int_{-\infty}^{x_f} \ell n \frac{|\xi - x|}{|\xi|} p_1(\xi) d\xi \tag{4.2}$$

where h_1 = smooth-film thickness

h_o = center film thickness at x=0

$E' = \left[\frac{1}{2}\left(\frac{1-\nu_1^2}{E_1} + \frac{1-\nu_2^2}{E_2}\right)\right]^{-1}$

E_1, E_2 = Young's modulus for rollers 1 and 2

ν_1, ν_2 = Poisson's ratio of rollers 1 and 2

ξ = dummy variable for x

$p_1(\xi)$ = smooth-film pressure profile

Referring to Fig. (4.2) the height of a three-dimensional ellipsoidal asperity can be written as

$$\delta = \delta_1 \cos \eta \tag{4.3}$$

As the contact width is very small compared to the radius of the cylinder, η is very small and

$$\cos \eta \simeq 1 \tag{4.4}$$

Thus the asperity height function of a three-dimensional asperity can be approximately written as

$$\delta(x,y) \simeq \delta_1 = \begin{cases} c_1\left[\left(\frac{x - x_3}{b'}\right)^2 + \left(\frac{y}{a'}\right)^2 - 1\right] & \text{for } \left|\frac{x - x_3}{b'}\right| \le 1 \text{ and } \left|\frac{y}{a'}\right| \le 1 \\ 0 & \text{elsewhere} \end{cases} \tag{4.5}$$

Similarly, the asperity height function of a two dimensional asperity ridge can be expressed as

$$\delta(x) \simeq \begin{cases} c_1\left[\left(\frac{x - x_3}{b'}\right)^2 - 1\right] & \text{for } \left|\frac{x - x_3}{b'}\right| \le 1 \\ 0 & \text{elsewhere} \end{cases} \tag{4.6}$$

The total local film thickness, h_T, at any point under the surface asperity is

$$h_T = h_1 + \delta \tag{4.7}$$

4.2.2 Governing Equations

4.2.2.1 The Smooth-Film Case

Referring to [22], the two coupled equations governing the pressure and film distributions in an elastohydrodynamic line contact between two rollers with isothermal and incompressible lubricant are:

The Reynolds equation

$$\frac{dp_1}{dx} = 6\mu(u_1 + u_2)\left(\frac{h_1 - h}{h_1^3}\right) \tag{4.8}$$

where p_1, h_1, h and x are already defined

μ ≡ viscosity

u_1, u_2 ≡ velocity of rollers 1 and 2

and the film thickness profile as described in Eq. (4.2). In non-dimensional form, Eqs. (4.8) and (4.2) become

$$\frac{dP_1}{dX} = \left(\frac{48}{H_o^2}\right) U \bar{\mu} \left(\frac{H_1 - 1}{H_1^3}\right) \tag{4.9}$$

$$H_1 = 1 + \frac{16\, P_{Hz}^2}{H_o^2}\left(\frac{X^2}{2} - \frac{1}{\pi}\int_{-\infty}^{X_f} P_1(\xi)\, \ell n \frac{|\bar{\xi}-X|}{|\bar{\xi}|}\, d\bar{\xi}\right) \tag{4.10}$$

where $P_1 = p_1/p_{Hz}$, $X = x/b$, $H_1 = h_1/h_o$, $H_o = h_o/R$,

$U = \frac{\mu_s(u_1 + u_2)}{2E'R}$, $\bar{\mu} = \frac{\mu}{\mu_s}$, $b/R = 4\, P_{Hz}$, $P_{Hz} = p_{Hz}/E'$,

$\bar{\xi} = \xi/b$, $X_f = x_f/b$.

Using the same numerical scheme as developed in [22], these two equations are solved by the Newton-Ralphson method. $P_1(X)$, $H_1(X)$ and $\bar{U}$ are solved for a given set of h_o/R, P_{Hz}, and G. These smooth-film results are used as the inputs to the perturbed Reynolds equation described later.

4.2.2.2 The Discretized Reynolds Equation

It is assumed here that the viscosity is an exponential function of the pressure with a pressure viscosity coefficient α, i.e.

$$\mu = \mu_s\, e^{\alpha p} \tag{4.11}$$

In numerical form the steady Reynolds equation for an incompressible lubricant can be expressed by dividing the contact zone into small grids with irregular spacings. Referring to Fig. (4.3) and applying the principle of conservation of mass, one obtains for the ith grid

$$m_1 - m_2 = m_{restored} \tag{4.12}$$

where $m_1 = -\left(\frac{\rho h_1^3}{12\mu}\frac{\partial p_1}{6x}\right)_{i-1/2} + \frac{u_1 + u_2}{2}(\rho h_1)_{i-1/2}$

$$= -\frac{\rho}{12\mu_s}\left(h_1^3\, e^{-\alpha p_1}\, \frac{\partial p_1}{\partial x}\right)_{i-1/2} + \rho\,\frac{u_1 + u_2}{2}(h_1)_{i-1/2} \tag{4.13}$$

$$m_2 = -\frac{\rho}{12\mu_s}\left(h_1^3\, e^{-\alpha p_1}\,\frac{\partial p_1}{\partial x}\right)_{i+1/2} + \rho\,\frac{u_1+u_2}{2}\,(h_1)_{i+1/2} \tag{4.14}$$

$$m_{restored} = \frac{\partial}{\partial t}\left[\rho\,(h_1)_i \left\{\frac{(\Delta x)_{i-1} + (\Delta x)_i}{2}\right\}\right] = 0 \tag{4.15}$$

Combining Eqs. (4.12) to (4.15) and re-arranging, one obtains

$$\frac{1}{12\mu_s}\left[\left(h_1^3\, e^{-\alpha p_1}\,\frac{\partial p_1}{\partial x}\right)_{i+1/2} - \left(h_1^3\, e^{-\alpha p_1}\,\frac{\partial p_1}{\partial x}\right)_{i-1/2}\right]$$

$$= \frac{u_1+u_2}{2}\left[(h_1)_{i+1/2} - (h_1)_{i-1/2}\right] \tag{4.16}$$

Thus p_1, the smooth-film pressure profile and h_1, the smooth-film thickness are functions of x only.

4.2.2.3 The Perturbed Reynolds Equation

The pressure distribution can be considered as the sum of the smooth-film pressure, p_1 and the perturbed pressure, ϕ. Define

$$p = p_1 + \phi \tag{4.17}$$

Since p_1 is a function of x only, the derivatives of p are:

$$\frac{\partial p}{\partial x} = \frac{\partial p_1}{\partial x} + \frac{\partial \phi}{\partial x} \tag{4.18}$$

$$\frac{\partial p}{\partial y} = \frac{\partial \phi}{\partial y} \tag{4.19}$$

For a two-dimensional flow field, the principle of conservation of mass as applied to the (i,j)th grid as shown in Fig. (4.4) yields

$$\left[\frac{(\Delta y)_{j-1}+(\Delta y)_j}{2}\right](m_1-m_2)+\left[\frac{(\Delta x)_{i-1}+(\Delta x)_i}{2}\right](m_3-m_4)$$

$$=\frac{\partial}{\partial t}\left\{(\rho h_T)_{i-1/2,j}\left[\frac{(\Delta y)_{j-1}+(\Delta y)_j}{2}\right]\frac{(\Delta x)_{i-1}}{2}\right.$$

$$\left.+(\rho h_T)_{i+1/2,j}\left[\frac{(\Delta y)_{j-1}+(\Delta y)_j}{2}\right]\frac{(\Delta x)_i}{2}\right\} \tag{4.20}$$

where $$m_1=\left\{-\frac{\rho h_T^3}{12\mu}\frac{\partial p}{\partial x}+\rho\left(\frac{u_1+u_2}{2}\right)h_T\right\}_{i-1/2,j}$$

$$=\left\{-\frac{\rho h_T^3}{12\mu_s}e^{-\alpha(p_1+\phi)}\left(\frac{\partial p_1}{\partial x}+\frac{\partial\phi}{\partial x}\right)+\rho\left(\frac{u_1+u_2}{2}\right)(h_1+\delta)\right\}_{i-1/2,j} \tag{4.21}$$

It is assumed that the value of $\alpha\phi$ is much smaller than unity such that $e^{-\alpha\phi}$ can be linearized as

$$e^{-\alpha\phi}=(1-\alpha\phi) \tag{4.22}$$

by using Taylor's series expansion. Neglecting second order term, Eq. (4.21) can be re-written as

$$m_1=\left\{-\frac{\rho h_T^3}{12\mu_s}e^{-\alpha p_1}\left(\frac{\partial p_1}{\partial x}+\frac{\partial\phi}{\partial x}-\alpha\phi\frac{\partial p_1}{\partial x}\right)+\rho\left(\frac{u_1+u_2}{2}\right)(h_1+\delta)\right\}_{i-1/2,j} \tag{4.23}$$

Likewise, m_2, m_3, and m_4 can be shown to be

$$m_2=-\left\{\frac{\rho h_T^3}{12\mu_s}e^{-\alpha p_1}\left(\frac{\partial p_1}{\partial x}+\frac{\partial\phi}{\partial x}-\alpha\phi\frac{\partial p_1}{\partial x}\right)+\rho\left(\frac{u_1+u_2}{2}\right)(h_1+\delta)\right\}_{i+1/2,j} \tag{4.24}$$

$$m_3=-\left\{\frac{\rho h_T^3}{12\mu_s}e^{-\alpha p_1}\frac{\partial\phi}{\partial y}\right\}_{i,j-1/2} \tag{4.25}$$

$$m_4=-\left\{\frac{\rho h_T^3}{12\mu_s}e^{-\alpha p_1}\frac{\partial\phi}{\partial y}\right\}_{i,j+1/2} \tag{4.26}$$

Substituting Eqs. (4.23) to (4.26) into the left-hand side of Eq. (4.20), one obtains

$$\rho\left[\frac{(\Delta y)_{j-1}+(\Delta y)_j}{2}\right]\left\{\left(\frac{1}{12\mu_s}\right)\left[\left(h_T^3\, e^{-\alpha p_1}\,\frac{\partial\phi}{\partial x}\right)_{i+1/2,j}-\left(h_T^3\, e^{-\alpha p_1}\,\frac{\partial\phi}{\partial x}\right)_{i-1/2,j}\right]\right.$$

$$-\left(\frac{1}{12\mu_s}\right)\left[\left(h_T^3\, e^{-\alpha p_1}\,\alpha\phi\,\frac{\partial p_1}{\partial x}\right)_{i+1/2,j}-\left(h_T^3\, e^{-\alpha p_1}\,\alpha\phi\,\frac{\partial p_1}{\partial x}\right)_{i-1/2,j}\right]$$

$$-\left(\frac{1}{12\mu_s}\right)\left[\left(\left(h_1^3-h_T^3\right) e^{-\alpha p_1}\,\frac{\partial p_1}{\partial x}\right)_{i+1/2,j}-\left(\left(h_1^3-h_T^3\right) e^{-\alpha p_1}\,\frac{\partial p_1}{\partial x}\right)_{i-1/2,j}\right]$$

$$\left.-\left(\frac{u_1+u_2}{2}\right)\left[\frac{\delta_{i+1,j}-\delta_{i-1,j}}{2}\right]\right\}$$

$$+\rho\left[\frac{(\Delta x)_{i-1}+(\Delta x)_i}{2}\right]\left(\frac{1}{12\mu_s}\right)\left[\left(h_T^3\, e^{-\alpha p_1}\,\frac{\partial\phi}{\partial y}\right)_{i,j+1/2}\right.$$

$$\left.-\left(h_T^3\, e^{-\alpha p_1}\,\frac{\partial\phi}{\partial y}\right)_{i,j-1/2}\right] \tag{4.27}$$

With the relations

$$\frac{\partial h_1}{\partial t}=0 \tag{4.28}$$

and

$$\frac{\partial}{\partial t}\,\delta(x-u_2 t)=-\,u_2\,\frac{\partial\delta}{\partial x} \tag{4.29}$$

the right-hand side of Eq. (4.20) can be re-written as

$$\rho\left[\frac{(\Delta y)_{j-1}+(\Delta y)_j}{2}\right](-\,u_2)\left(\frac{\delta_{i+1,j}-\delta_{i-1,j}}{2}\right) \tag{4.30}$$

Equating Eqs. (4.27) and (4.30) and simplifying, one obtains

$$\left[(\Delta y)_{j-1}+(\Delta y)_j\right]\left\{\left[\left(h_T^3\, e^{-\alpha p_1}\frac{d\phi}{dx}\right)_{i+1/2,j}-\left(h_T^3\, e^{-\alpha p_1}\frac{d\phi}{dx}\right)_{i-1/2,j}\right]\right.$$

$$\left.-\left[\left(h_T^3\, e^{-\alpha p_1}\alpha\phi\frac{dp_1}{dx}\right)_{i+1/2,j}-\left(h_T^3\, e^{-\alpha p_1}\alpha\phi\frac{dp_1}{dx}\right)_{i-1/2,j}\right]\right\}$$

$$+\left[(\Delta x)_{i-1}+(\Delta x)_i\right]\left[\left(h_T^3\, e^{-\alpha p_1}\frac{d\phi}{dy}\right)_{i,j+1/2}-\left(h_T^3\, e^{-\alpha p_1}\frac{d\phi}{dy}\right)_{i,j-1/2}\right]$$

$$=\left[(\Delta y)_{j-1}+(\Delta y)_j\right]\left\{\left[\left(h_1^3-h_T^3\right)e^{-\alpha p_1}\frac{dp_1}{dx}\right]_{i+1/2,j}\right.$$

$$\left.-\left[\left(h_1^3-h_T^3\right)e^{-\alpha p_1}\frac{dp_1}{dx}\right]_{i-1/2,j}+6\mu_s(u_1-u_2)\left[\frac{\delta_{i+1,j}-\delta_{i-1,j}}{2}\right]\right\} \quad (4.31)$$

Using the central difference approximation for the pressure gradients, Eq. (4.31) is discretized to

$$\left[(\Delta y)_{j-1}+(\Delta y)_j\right]\left\{\left[\frac{\left(h_T^3\, e^{-\alpha p_1}\right)_{i+1,j}+\left(h_T^3\, e^{-\alpha p_1}\right)_{i,j}}{2}\right]\left(\frac{\phi_{i+1,j}-\phi_{i,j}}{(\Delta x)_i}\right)\right.$$

$$-\left[\frac{\left(h_T^3\, e^{-\alpha p_1}\right)_{i,j}+\left(h_T^3\, e^{-\alpha p_1}\right)_{i-1,j}}{2}\right]\frac{\left(\phi_{i,j}-\phi_{i-1,j}\right)}{(\Delta x)_{i-1}}$$

$$-\left[\frac{\left(h_T^3\, e^{-\alpha p_1}\alpha\phi\right)_{i+1,j}+\left(h_T^3\, e^{-\alpha p_1}\alpha\phi\right)_{i,j}}{2}\right]\left[\frac{(p_1)_{i+1}-(p_1)_i}{(\Delta x)_i}\right]$$

$$\left.+\left[\frac{\left(h_T^3\, e^{-\alpha p_1}\alpha\phi\right)_{i,j}+\left(h_T^3\, e^{-\alpha p_1}\alpha\phi\right)_{i-1,j}}{2}\right]\left[\frac{(p_1)_i-(p_1)_{i-1}}{(\Delta x)_{i-1}}\right]\right\} \quad (4.32)$$

$$+\left[(\Delta x)_{i-1}+(\Delta x)_i\right]\left\{\left[\frac{\left(h_T^3\, e^{-\alpha p_1}\right)_{i,j+1}+\left(h_T^3\, e^{-\alpha p_1}\right)_{i,j}}{2}\right]\frac{\left(\phi_{i,j+1}-\phi_{i,j}\right)}{(\Delta y)_j}\right.$$

$$\left.-\left[\frac{\left(h_T^3\, e^{-\alpha p_1}\right)_{i,j}+\left(h_T^3\, e^{-\alpha p_1}\right)_{i,j-1}}{2}\right]\frac{\left(\phi_{i,j}-\phi_{i,j-1}\right)}{(\Delta y)_{j-1}}\right\}$$

$$=\left[(\Delta y)_{j-1}+(\Delta y)_j\right]\left\{\frac{\left[\left(h_1^3-h_T^3\right)e^{-\alpha p_1}\right]_{i+1,j}+\left[\left(h_1^3-h_T^3\right)e^{-\alpha p_1}\right]_{i,j}}{2}\frac{\left[(p_1)_{i+1}-(p_1)_i\right]}{(\Delta x)_i}\right.$$

$$-\frac{\left[\left(h_1^3-h_T^3\right)e^{-\alpha p_1}\right]_{i,j}+\left(h_1^3-h_T^3\right)e^{-\alpha p_1}\Big]_{i-1,j}}{2}\left[\frac{(p_1)_i-(p_1)_{i-1}}{(\Delta x)_{i-1}}\right]$$

$$+6\mu_s(u_1-u_2)\left(\frac{\delta_{i+1,j}-\delta_{i-1,j}}{2}\right) \qquad (4.32)$$

After re-arranging and the following non-dimensional variables are introduced:

$\Delta X=\Delta x/b'$, $\Delta Y=\Delta y/a'$, $\gamma=a'/b'$, $H_T=h_T/h_o$, $H_1=h_1/h_o$, $\bar{c}_1=c_1/h_o$,

$X=x/b$, $X_3=x_3/b$, $Y=y/a'$, $\bar{b}=b'/b$, $P_1=p_1/p_{Hz}$, $\Phi=\phi/p_{Hz}$,

$P_{Hz}=p_{Hz}/E'$, $G=\alpha E'$, $E'=\left[\frac{1}{2}\left(\frac{1-\nu_1^2}{E_1}+\frac{1-\nu_2^2}{E_2}\right)\right]^{-1}$, $\bar{\alpha}=\alpha p_{Hz}$,

$U_D=\dfrac{\mu_s(u_1-u_2)}{2E'R}$, $H_o=h_o/R$, $C_{UD}=48\;U_D/H_o\cdot\bar{b}$,

$$\bar{\delta}=\delta/h=c_1/h_o\left[\left(\frac{x-x_3}{b'}\right)^2+\left(\frac{y}{a'}\right)^2-1\right]=\bar{c}_1\left[\left(\frac{X-X_3}{\bar{b}}\right)^2+(Y)^2-1\right]$$

the governing equation becomes:

$$\left[\frac{(\Delta Y)_{j-1}+(\Delta Y)_j}{(\Delta X)_{i-1}}\right]\left\{\left(H_T^3\, e^{-\bar{\alpha}P_1}\right)_{i,j}+\left(H_T^3\, e^{-\bar{\alpha}P_1}\right)_{i-1,j}\right.$$

$$\left.+\bar{\alpha}\left(H_T^3\, e^{-\bar{\alpha}P_1}\right)_{i-1,j}\left[(P_1)_i-(P_1)_{i-1}\right]\right\}\Phi_{i-1,j} \qquad (4.33)$$

$$+ \frac{1}{\gamma^2}\left[\frac{(\Delta X)_{i-1} + (\Delta X)_i}{(\Delta Y)_{j-1}}\right]\left[\left(H_T^3\, e^{-\bar{\alpha} p_1}\right)_{i,j} + \left(H_T^3\, e^{-\bar{\alpha} p_1}\right)_{i,j-1}\right] \Phi_{i,j-1}$$

$$+ \left\{ - \left[(\Delta Y)_{j-1} + (\Delta Y)_j\right]\left[\frac{\left(H_T^3\, e^{-\bar{\alpha} p_1}\right)_{i+1,j} + \left(H_T^3\, e^{-\bar{\alpha} p_1}\right)_{i,j}}{(\Delta X)_i} + \frac{\left(H_T^3\, e^{-\bar{\alpha} p_1}\right)_{i,j} + \left(H_T^3\, e^{-\bar{\alpha} p_1}\right)_{i-1,j}}{(\Delta X)_{i-1}}\right.\right.$$

$$\left. + \bar{\alpha}\left(H_T^3\, e^{-\bar{\alpha} p_1}\right)_{i,j} \frac{(p_1)_{i+1} - (p_1)_i}{(\Delta X)_i} - \bar{\alpha}\left(H_T^3\, e^{-\bar{\alpha} p_1}\right)_{i,j} \frac{(p_1)_i - (p_1)_{i-1}}{(\Delta X)_{i-1}}\right]$$

$$- \frac{1}{\gamma^2}\left[(\Delta X)_{i-1} + (\Delta X)_i\right]\left[\frac{\left(H_T^3\, e^{-\bar{\alpha} p_1}\right)_{i,j+1} + \left(H_T^3\, e^{-\bar{\alpha} p_1}\right)_{i,j}}{(\Delta Y)_j}\right.$$

$$\left.\left. + \frac{\left(H_T^3\, e^{-\bar{\alpha} p_1}\right)_{i,j} + \left(H_T^3\, e^{-\bar{\alpha} p_1}\right)_{i,j-1}}{(\Delta Y)_{j-1}}\right]\right\} \Phi_{i,j}$$

$$+ \frac{1}{\gamma^2}\left[\frac{(\Delta X)_{i-1} + (\Delta X)_i}{(\Delta Y)_j}\right]\left[\left(H_T^3\, e^{-\bar{\alpha} p_1}\right)_{i,j+1} + \left(H_T^3\, e^{-\bar{\alpha} p_1}\right)_{i,j}\right] \Phi_{i,j+1}$$

$$+ \left[\frac{(\Delta Y)_{j-1} + (\Delta Y)_j}{(\Delta X)_i}\right]\left\{\left(H_T^3\, e^{-\bar{\alpha} p_1}\right)_{i+1,j} + \left(H_T^3\, e^{-\bar{\alpha} p_1}\right)_{i,j}\right.$$

$$\left. - \bar{\alpha}\left(H_T^3\, e^{-\bar{\alpha} p_1}\right)_{i+1,j}\left[(p_1)_{i+1} - (p_1)_i\right]\right\} \Phi_{i+1,j}$$

$$= \left[(\Delta Y)_{j-1} + (\Delta Y)_j\right]\left(\left\{\left[\left(H_1^3 - H_T^3\right) e^{-\bar{\alpha} p_1}\right]_{i+1,j}\right.\right.$$

$$\left. + \left[\left(H_1^3 - H_T^3\right) e^{-\bar{\alpha} p_1}\right]_{i,j}\right\}\left[\frac{(p_1)_{i+1} - (p_1)_i}{(\Delta X)_i}\right] - \left\{\left[\left(H_1^3 - H_T^3\right) e^{-\bar{\alpha} p_1}\right]_{i,j}\right.$$

$$\left.\left. + \left[\left(H_1^3 - H_T^3\right) e^{-\bar{\alpha} p_1}\right]_{i-1,j}\right\}\left[\frac{(p_1)_i - (p_1)_{i-1}}{(\Delta X)_{i-1}}\right] + C_{UD}\left(\bar{\delta}_{i+1,j} - \bar{\delta}_{i-1,j}\right)\right) \tag{4.33}$$

4.2.3 Method of Solution

In Eq. (4.33), $\Phi_{i-1,j}$, $\Phi_{i,j-1}$, $\Phi_{i,j}$, $\Phi_{i,j+1}$, $\Phi_{i+1,j}$ are the only unknowns. H_1 and p_1 considered as known are determined by the method outlined in [22] for the smooth lubricated contacts. Thus, Eq. (4.33) can be re-written in the following matrix form:

$$\left[A_i\right]\left\{\Phi_{i-1}\right\} + \left[B_i\right]\left\{\Phi_i\right\} + \left[c_i\right]\left\{\Phi_{i+1}\right\} = \left\{R_i\right\} \tag{4.34}$$

where $[A_i]$ and $[c_i]$ are M x M diagonal square matrix; $[B_i]$ is a M x M tri-diagonal square matrix; $\{\Phi_{i-1}\}$, $\{\Phi_i\}$, $\{\Phi_{i+1}\}$ and $\{R_i\}$ are M x 1 column matrix; M and N are the number of grids used in the x and y directions.

In prescribing the boundary conditions for Eq. (4.34), it is necessary to assume that the effect of the asperity on the pressure distribution at $|X-x_3/b'| \geq 5$ or $|y/a'| \geq 5$ is negligible. This assumption justifies the prescription of the contact. Thus the boundary conditions are $\Phi = 0$ along $X-x_3/b' = \pm 5$ and along $y/a' = \pm 5$, or

$$\begin{aligned} &\left\{\Phi_1\right\} = \left\{\Phi_N\right\} = 0 \\ &\Phi_{i,j} = 0 \qquad \text{for } j = M \end{aligned} \tag{4.35}$$

Along y=0 or j=1, the flow is considered to be symmetric, and this gives the following additional boundary condition,

$$\Phi_{i,j-1} = \Phi_{i,j+1} \qquad \text{for } j=1 \tag{4.36}$$

Eq. (4.34) is solved numerically by the Columnwise Matrix Inversion Method [25].

4.3 DEFORMED ASPERITY ON THE STATIONARY SURFACE

In the case of simple sliding of a smooth surface against a stationary asperity, the non-dimensional Reynolds equation and elasticity equation are respectively

$$\frac{dP}{dX} = \left(\frac{48}{H_o^2}\right) U \bar{\mu} \left(\frac{H_T - 1}{H_T^3}\right) \tag{4.37}$$

$$H_T = H_1 + \frac{\delta}{h_o} \tag{4.38}$$

In this case, δ is a function of x only. Thus, $\partial\delta/\partial t = 0$. Therefore these coupled equations can be solved simultaneously using the same numerical scheme as described in [22]. The results are compared with those obtained by solving the perturbed Reynolds equation.

4.4 DISCUSSIONS OF RESULTS

The results of the perturbed pressure Φ are presented as Δ_s, which is defined as

$$\Delta_s = (\Phi_{max} - \Phi_{min}) \quad \text{at } j=1 \tag{4.39}$$

where the position j=1 is at the centerline of the asperity along the sliding direction. At this position, the effect of asperity on Φ is most severe. Since Φ is a function of P_{Hz}, G, h_o/R, $\bar{b}$, γ, c_1/h_o, x_3, and the slide to roll ratios, the effects of these variables on Δ_s are studied separately.

(1) Effect of h_o/R

With $P_{Hz} = 0.003$, $G = 100$, $X_3 = -0.5$, $\bar{b} = 1/32$, $c_1/h_o = 0.3$, the results of h_o/R versus Δ_s are shown in Fig. (4.6). In the case of 2-D elastic asperity, the magnitude of Δ_s increases as h_o/R increases from 1.0×10^{-6} to about $h_o/R = 5 \times 10^{-6}$ (approximate) after which the magnitude of Δ_s decreases with further increase in h_o/R. This phenomenon is attributable to the local elastic effect of the asperity. In general, one might imagine that the effect of roughness on Φ should be much more severe as the ratio h_o/R becomes smaller. However, in an elastohydrodynamic contact, the elastic effect becomes more significant as h_o/R becomes smaller. Thus, for a fixed ratio of c_1/h_o, the elastic effect tends to flatten out the asperity and produces a trend which shows a decrease in Δ_s as h_o/R decreases. On the other hand, for the 3D rigid asperity analysis the elastic effect is not accounted; therefore, the magnitude of Δ_s consistently increases with a decrease in h_o/R.

Based on the results shown in Fig. 4.6, it appears that further comparisons between the 2D-elastic asperity and 3D-rigid asperity results are more meaningful for values of h_o/R greater than 1.0×10^{-5}, since below this value no good agreement is expected.

(2) Effect of P_{Hz}

In hydrodynamic lubrication, with a rigid asperity, it is expected that the effect of asperity on Δ_s will become more severe as the load increases. However, for EHD contacts, this simple trend is only expected to be true if the load parameter P_{Hz} is sufficiently small. For very heavy loads, the elastic effect will iron out the asperity and this may decrease the magnitude of Δ_s. Such trend is demonstrated in Fig. (4.7). In the 2D-elastic asperity curve, the magnitude of Δ_s increases with P_{Hz} until $P_{Hz} = 0.0045$. Beyond this point, the magnitude of Δ_s flattens out and shows a tendency to decrease as load further increases. On the other hand, the 3D-rigid asperity curve shows a steady increase in Δ_s with P_{Hz} even for very heavy loads. The lack of agreement at these heavy loads is definitely due to the local elastic effect.

Referring to Fig. (4.8), with the ratio h_o/R changing from 10^{-5} to 10^{-6}, the discrepency between the 3D-rigid asperity results and the 2D-elastic asperity is greatly enlarged. In this regime of extremely thin film, the local elastic effect is so overwhelming that one cannot expect any validity of the 3D-rigid asperity perturbation analysis.

(3) Effect of G

The effect of pressure-viscosity dependence is examined by varying G from 100 to 500 for P_{Hz}= 0.003, $h_o/R = 10^{-5}$, X_3= -0.5, $\bar{b}$ = 1/32, and c_1/h_o= 0.3. The reason for using a mild pressure-viscosity dependence is because recent studies in EHD traction has indicated that the effective pressure-viscosity coefficient within the Hertzian conjunction is only a small fraction of those measured under static equilibrium. For this reason, it is believed that values of G around 500 should not be unreasonable to represent the effective pressure-viscosity dependence in the conjunction. It can be readily seen in Fig. 4.9 that the magnitude of Δ_s increases with G for both 3D-rigid asperity and 2D-elastic asperity cases. However, the rigid-asperity model is slightly more influenced by G than the elastic asperity model. It is also interesting to note that the pressure perturbation Δ_s is depending exponentially on the pressure-viscosity coefficient. This is somewhat expected since pressure is directly portionally to the viscosity.

(4) Effect of X_3

With P_{Hz}= .003, $h_o/R = 10^{-5}$, G = 100, $\bar{b}$ = 1/32, c_1/h_o = 0.3, Fig. (4.10) shows the relation between Δ_s and X_3, the location of the center of the asperity. Qualitatively, the effects on Δ_s due to rigid and elastic asperity have the same trend. The magnitude of Δ_s increases as X_3 moving toward the center of the contact. This trend is certainly expected, since a higher pressure level inevitably would lead to a stronger asperity interaction, hence higher pressure perturbation.

(5) Effect of $\bar{b}$

Fig. (4.11) shows the effect of $\bar{b}$, asperity size, on Δ_s for P_{Hz}= 0.003, $h_o/R = 10^{-5}$, G = 100, X_3= -0.5, c_1/h_o= 0.3. From the two curves shown, a similar trend is seen to exist in the relation between Δ_s and the asperity size for both the rigid model and the elastic model. In both cases, Δ_s increases with the asperity size; however, the increase in Δ_s is much larger in the case of rigid asperity model than that in the elastic-asperity model.

(6) Effect of c_1/h_o

With P_{Hz}= .003, $h_o/R = 10^{-5}$, G = 100, X_3= -0.5, $\overline{b}$ = 1/32, Fig. (4.12) shows the effect of asperity height, c_1/h_o, on Δ_s for both 3D-rigid-asperity and 2D-elastic asperity models. It is readily seen that the two curves almost coincide with each other and the magnitude of Δ_s for both cases increases with c_1/h_o. As c_1/h_o becomes larger, the two curves begin to divert slightly.

(7) Effect of γ

As defined earlier, γ is the ratio of half of the asperity length to half of the asperity width, known as the ellipticity ratio of the asperity. As the 2D elastic asperity model only describes straight asperity ridges, Fig. (4.13) only shows the results for the 3D-rigid-asperity model. It is seen that the magnitude of Δ_s increases with γ as expected. When γ is less than 1, Δ_s increases sharply with a small increase in γ. As γ becomes larger the change of Δ_s becomes much more gentle. In fact, for $\gamma > 5$, the change of γ is practically negligible.

(8) Effect of Slide to Roll Ratio S

Fig. (4.14) shows the effect of S on Δ_s for P_{Hz}= .003, G = 100, $h_o/R = 10^{-5}$, X_3= -0.5, $\overline{b}$ = 1/32 and c_1/h_o= 0.3. For γ = 1,2 and 10, Δ_s decreases when S increases from -2.0 to 0.3, and then increases when S increases from 0.4 to 2.0. These trends show that between S = 0.3 and 0.4, the perturbed pressure Δ_s reaches a minimum. This phenomenon can be explained by Fig. (4.15) in which the perturbed pressures Φ around the asperity center are plotted for S = 0.3 and S = 0.4. In the case of S = 0.3, the value of Φ is mostly negative for $x/b' \leq 0$, and positive for $x/b' \geq 0$.

In the case of $S = 0.4$, the pressure exhibits an opposite trend. Thus, one would expect that between $S = 0.3$, and 0.4, the trend for Φ begins to reverse itself.

With P_{Hz}, h_o/R, X_3, $\bar{b}$, c_1/h_o and γ having the same values as those used for Fig. (4.14), Fig. (4.16) shows the effect of G on S. For $G = 100$ and 500, the qualitative trends of Δ_s versus S are the same. However, for $G = 100$, the minimum Δ_s is located between $S = 0.3$ and 0.4, whereas, for $G = 500$, the minimum Δ_s is shifted to a position between $S = 0.1$ and 0.2. Thus when the magnitude of G is increased, the minimum Δ_s is shifted toward the asperity center. This agrees very well with Lee and Cheng's [5] results in which the G value is equal to 3180, the perturbed pressure is negligibly small when $S=0$.

The pressure profiles obtained from the smooth film theory and the perturbation theory are compared in Fig. (4.17). Again, it shows that in the case of pure rolling ($S=0$), the perturbed pressure can be neglected. For $|S| = 2$, the perturbed pressure is relatively more important.

4.5 CONCLUSIONS

The perturbed pressure distribution around an ellipsoidal asperity tip within an EHD line contact can be calculated by solving the perturbed Reynolds equation based on the assumption of a rigid asperity. The magnitude of the perturbed pressure Δ_s, was found to be a function of the following dimensionless variables: The Hertzian pressure, P_{Hz}, the smooth film center film thickness h_o/R, the pressure viscosity parameter G, the position of the asperity center X_3, the size of the asperity $\bar{b}$, the height of the asperity c_1/h_o, the ellipticity ratio γ and the slide to roll ratio S. Δ_s was shown to increase with an increase of P_{Hz}, G, $\bar{b}$, c_1/h_o, γ, or X_3. However, it decreases as h_o/R increases. The manner in which Δ_s varies with S is dependent upon the pressure viscoisty parameter G. For a large G, Δ_s is at its minimum when S approaches zero (pure rolling condition); it increases as the magnitude of S increases. For a small G, the value of S at which Δ_s reaches a minimum shifts from zero to some small positive values.

A comparison was made between the results obtained by the perturbation analysis based on an ellipsoidal asperity for γ = 10 and S=2, and those obtained by the 2D asperity analysis. The comparison indicated that the perturbation analysis which ignored the local elastic effect yielded a very good approximation on the magnitude of the pressure fluctuation for certain cases, provided that $h_o/R \geq 10^{-5}$, $P_{Hz} \leq 0.003$, $G \simeq 100$, $c_1/h_o \leq 0.3$ and $\bar{b} \simeq 1/32$. Beyond these limitations, the perturbation analysis would over-estimate the pressure fluctuation.

(a)

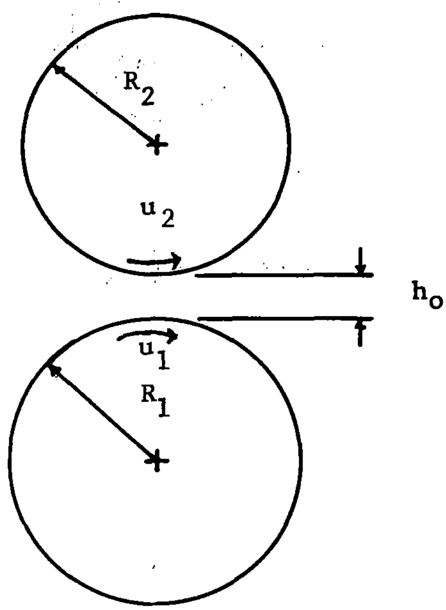

(b)

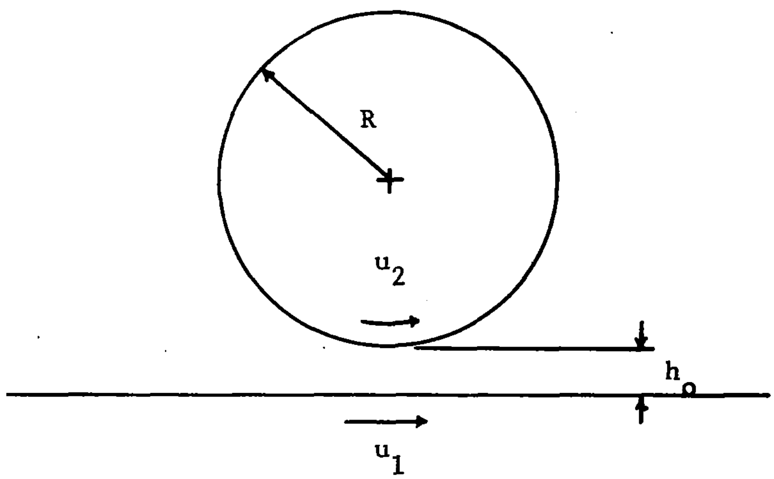

Figure 4-1 Two Lubricated Rollers and the Equivalent Roller-Plane System

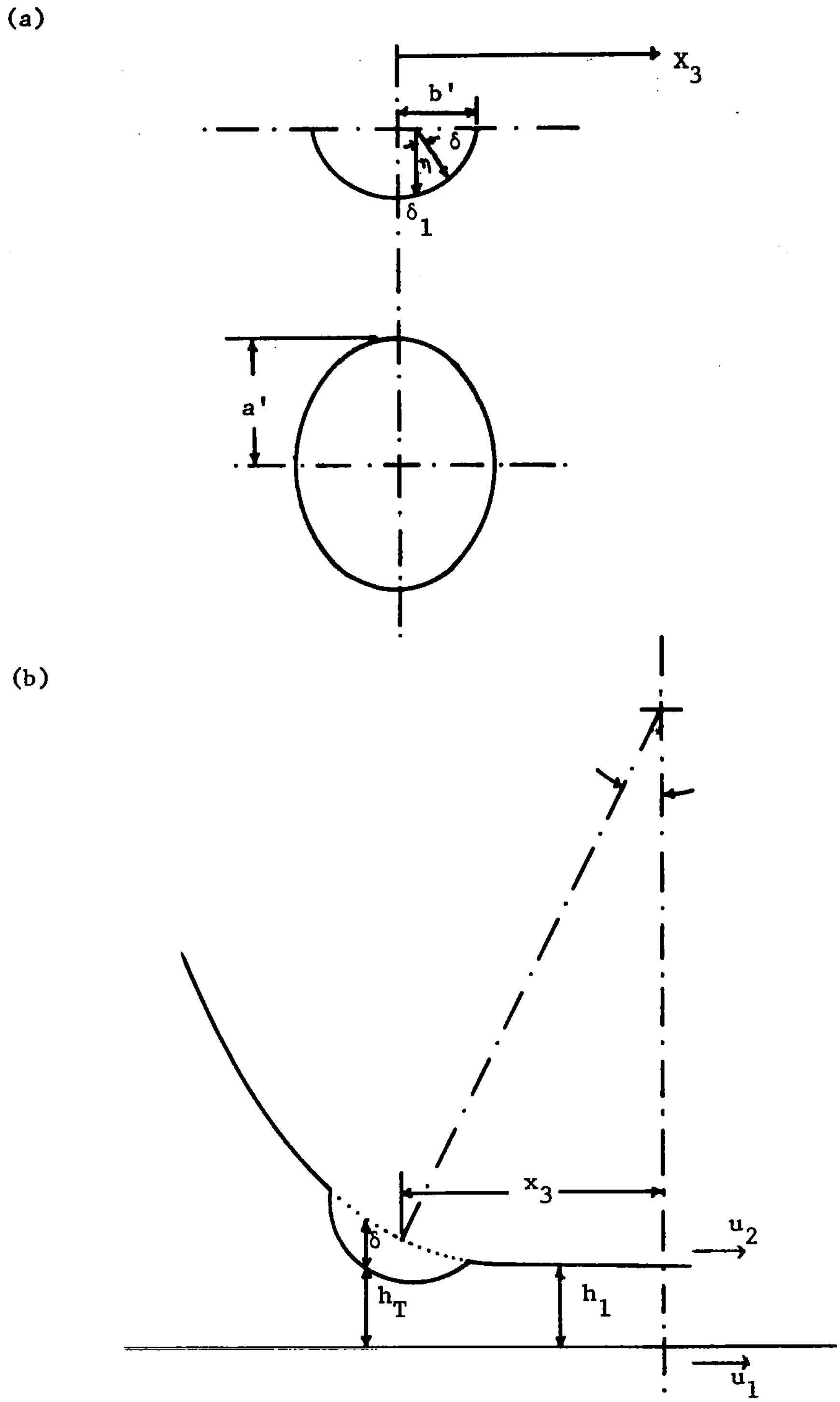

Figure 4-2 A Single Ellipsoidal Rigid Asperity in an EHD Contact

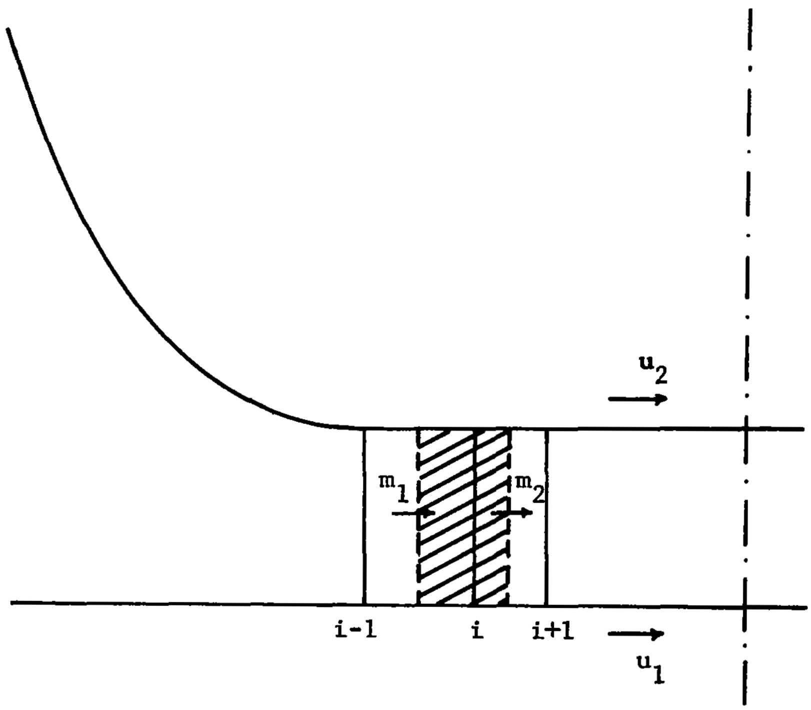

Figure 4-3 One-Dimensional Grids for Smooth Contact

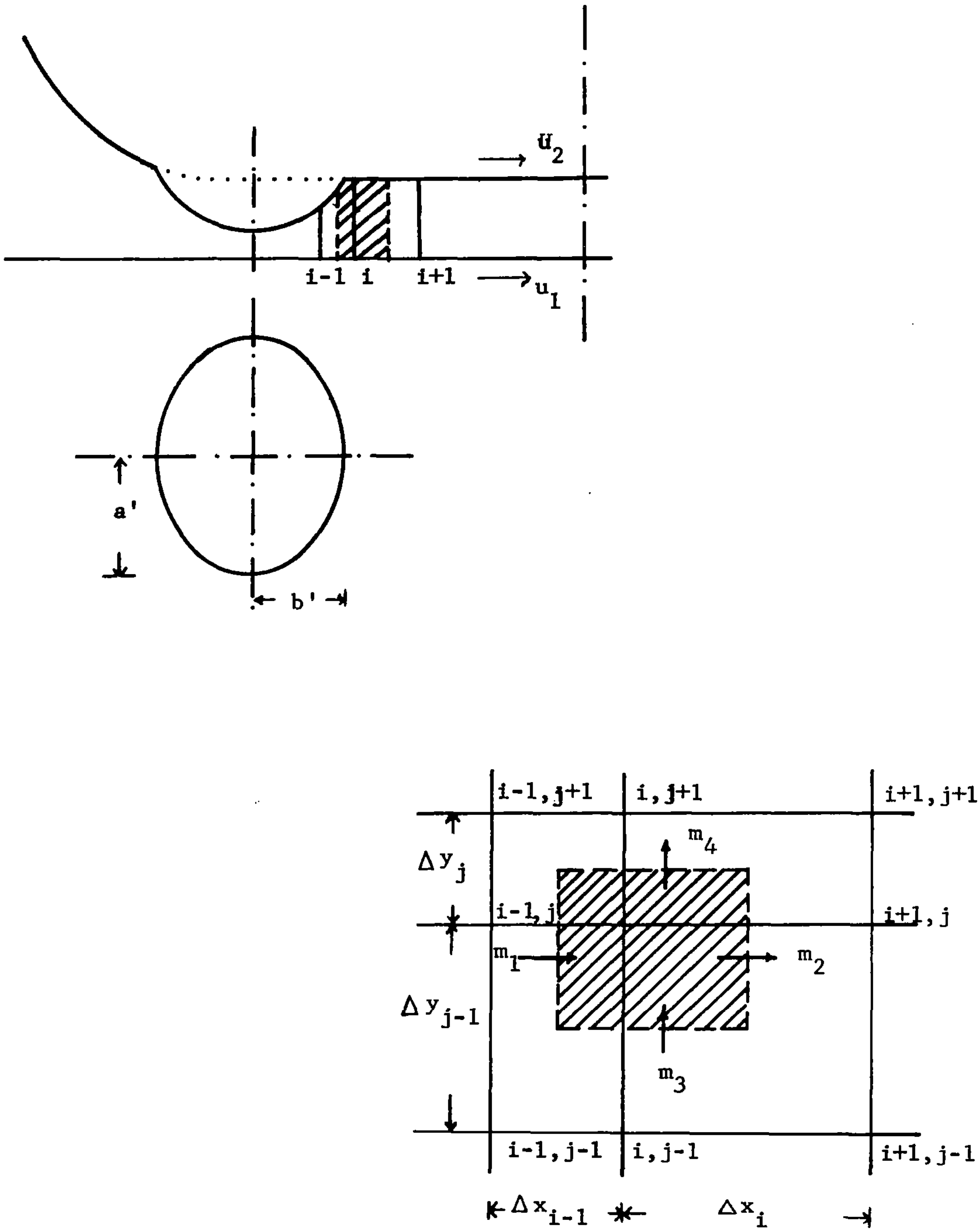

Figure 4-4 Two-Dimensional Grids for Rough Contact

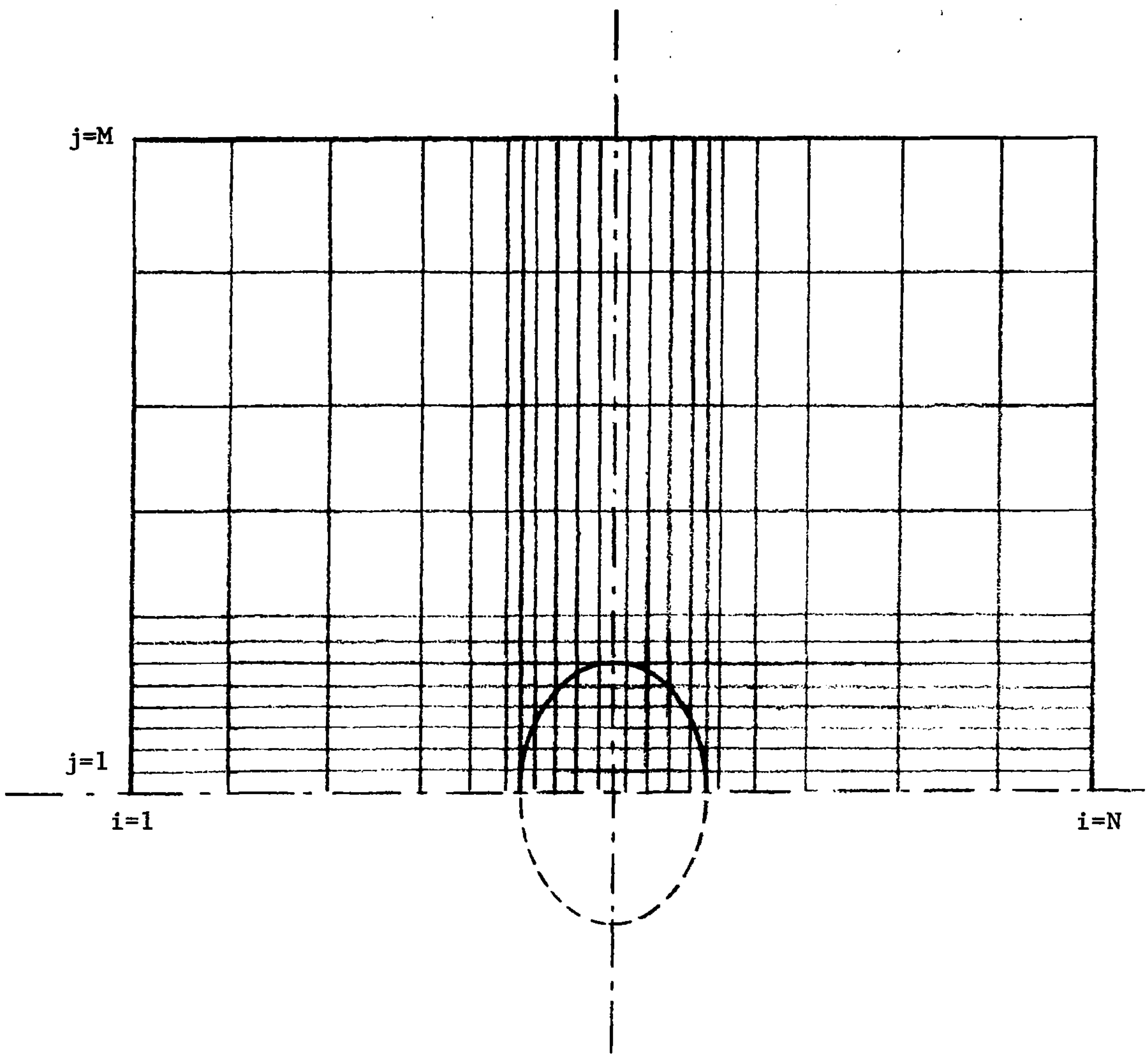

Figure 4-5 Grid Spacing

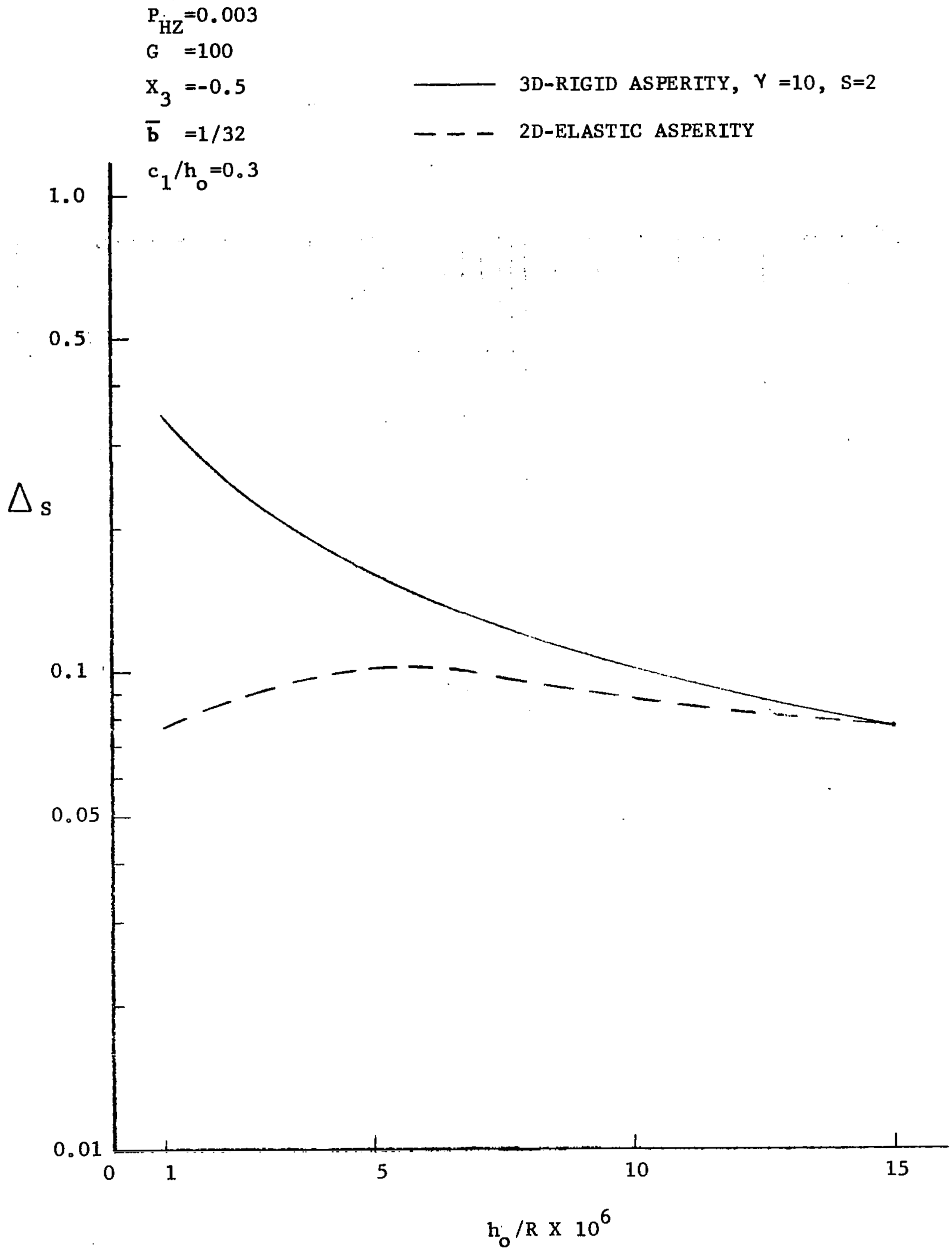

Fig. 4-6 The Effect of the Nominal EHD Center Film Thickness, h_o/R, on the Double Amplitue of the Perturbed Pressure, $\Delta_s = \Phi_{max.} - \Phi_{min.}$

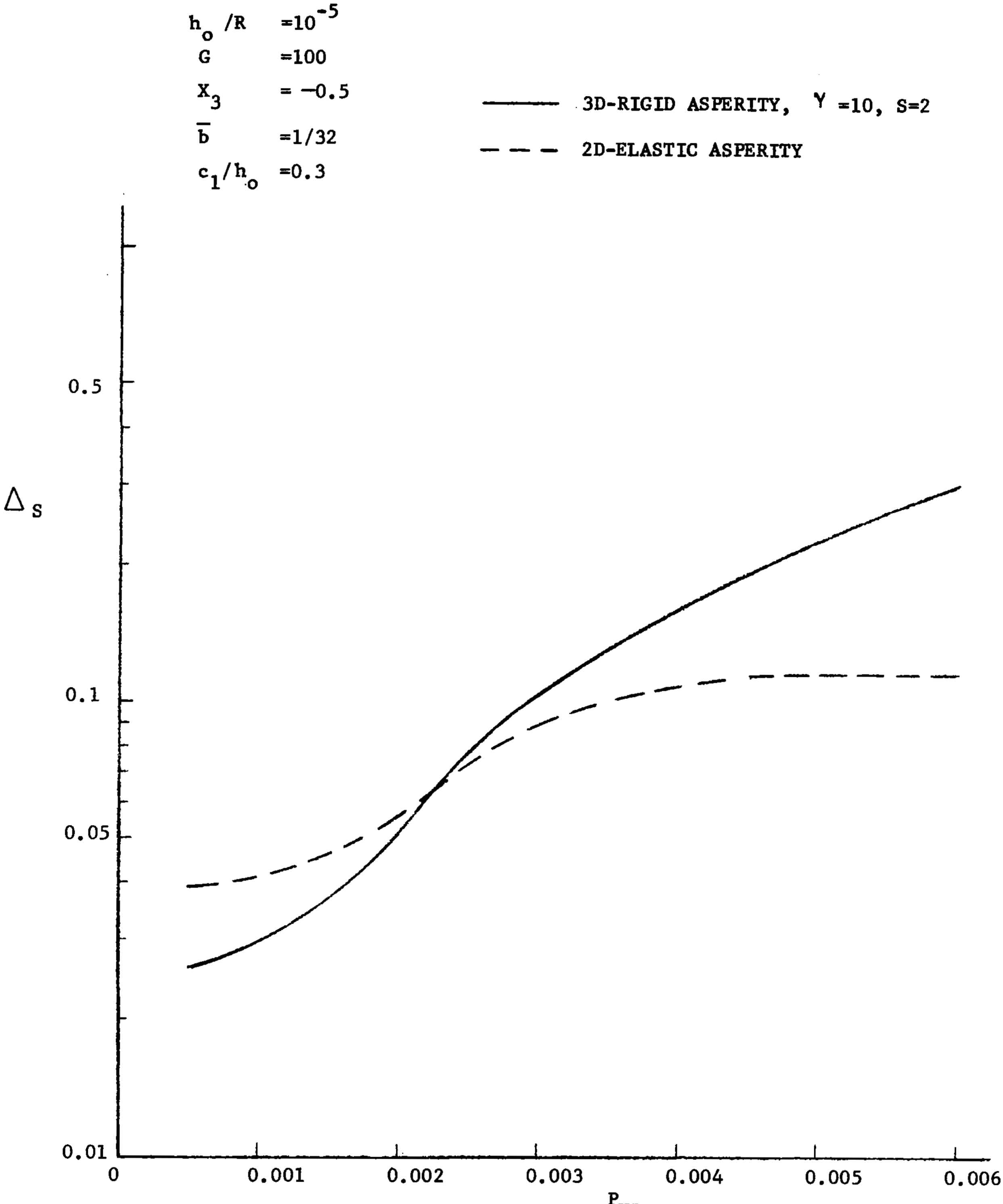

Fig. 4-7 The Effect of the Normalized Hertzian Pressure, $P_{Hz} = p_{Hz}/E'$, on $\Delta_s = \Phi_{max} - \Phi_{min}$, for $h_o/R = 10^{-5}$

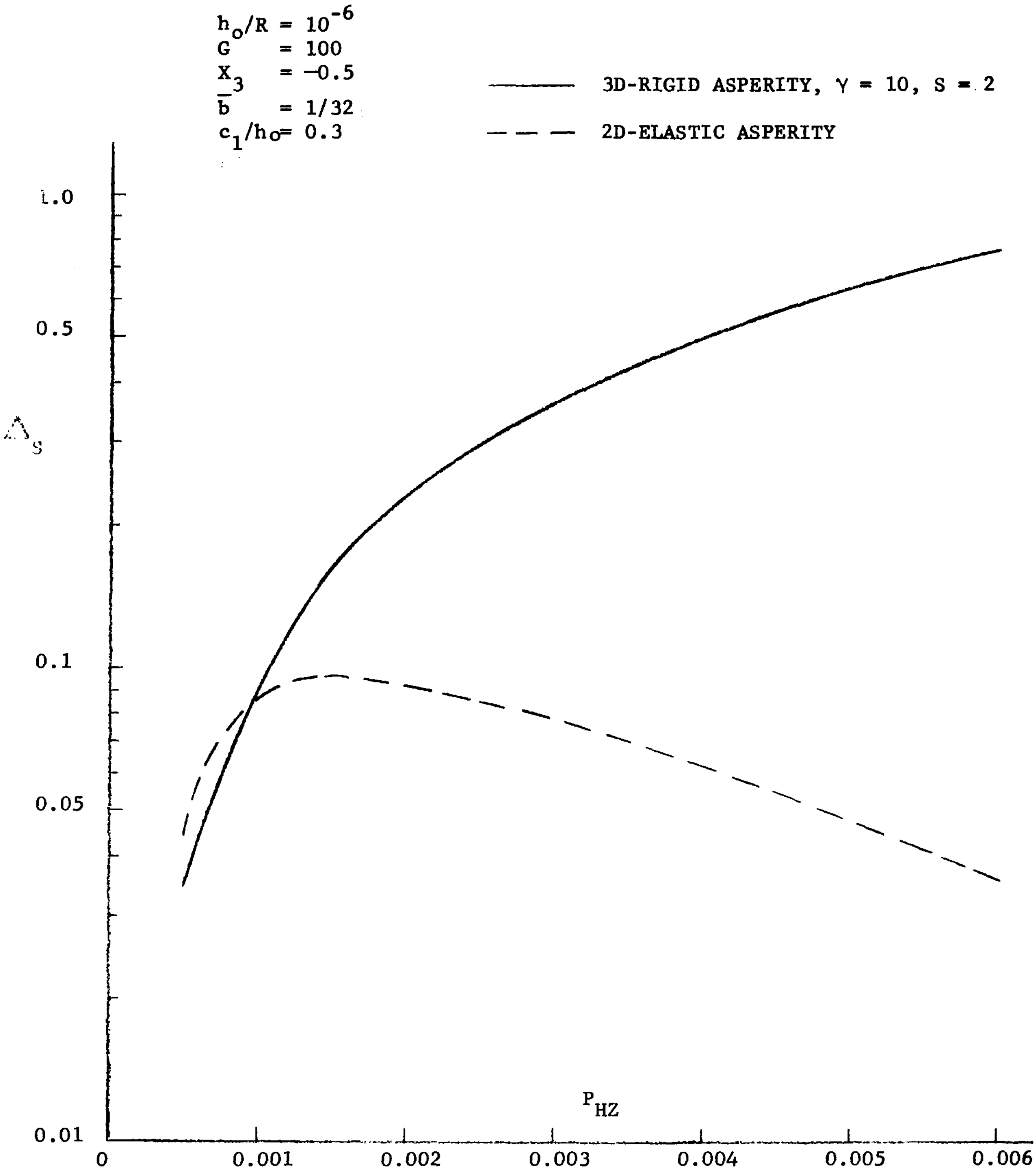

Fig. 4-8 The Effect of the Normalized Hertzian Pressure, $P_{Hz} = p_{Hz}/E'$, on $\Delta_s = \Phi_{max} - \Phi_{min}$, for $h_o/R = 10^{-6}$

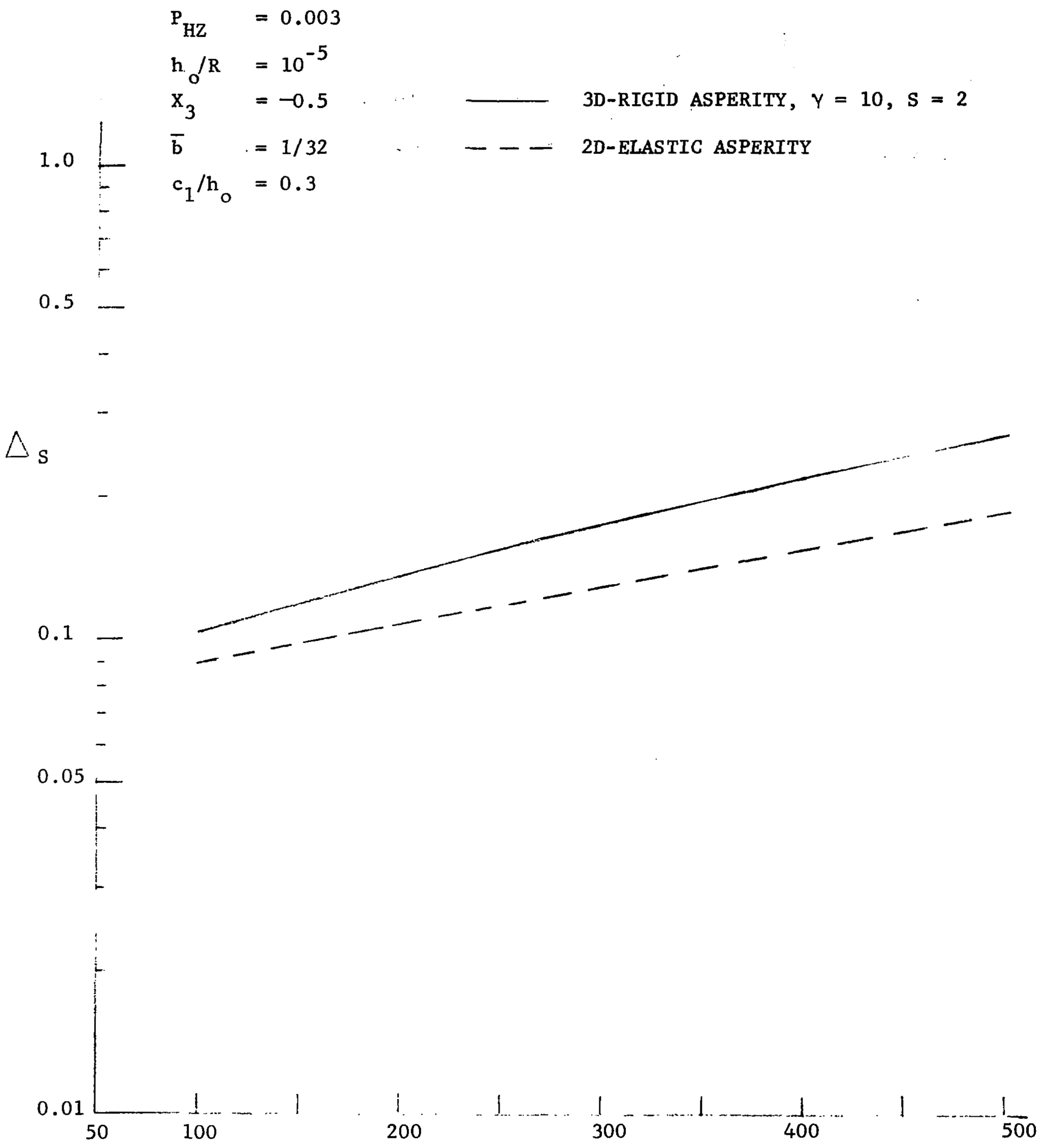

Fig. 4-9 The Effect of the Pressure Viscosity Parameter, $G = \alpha E'$, on $\Delta_S = \Phi_{max.} - \Phi_{min.}$

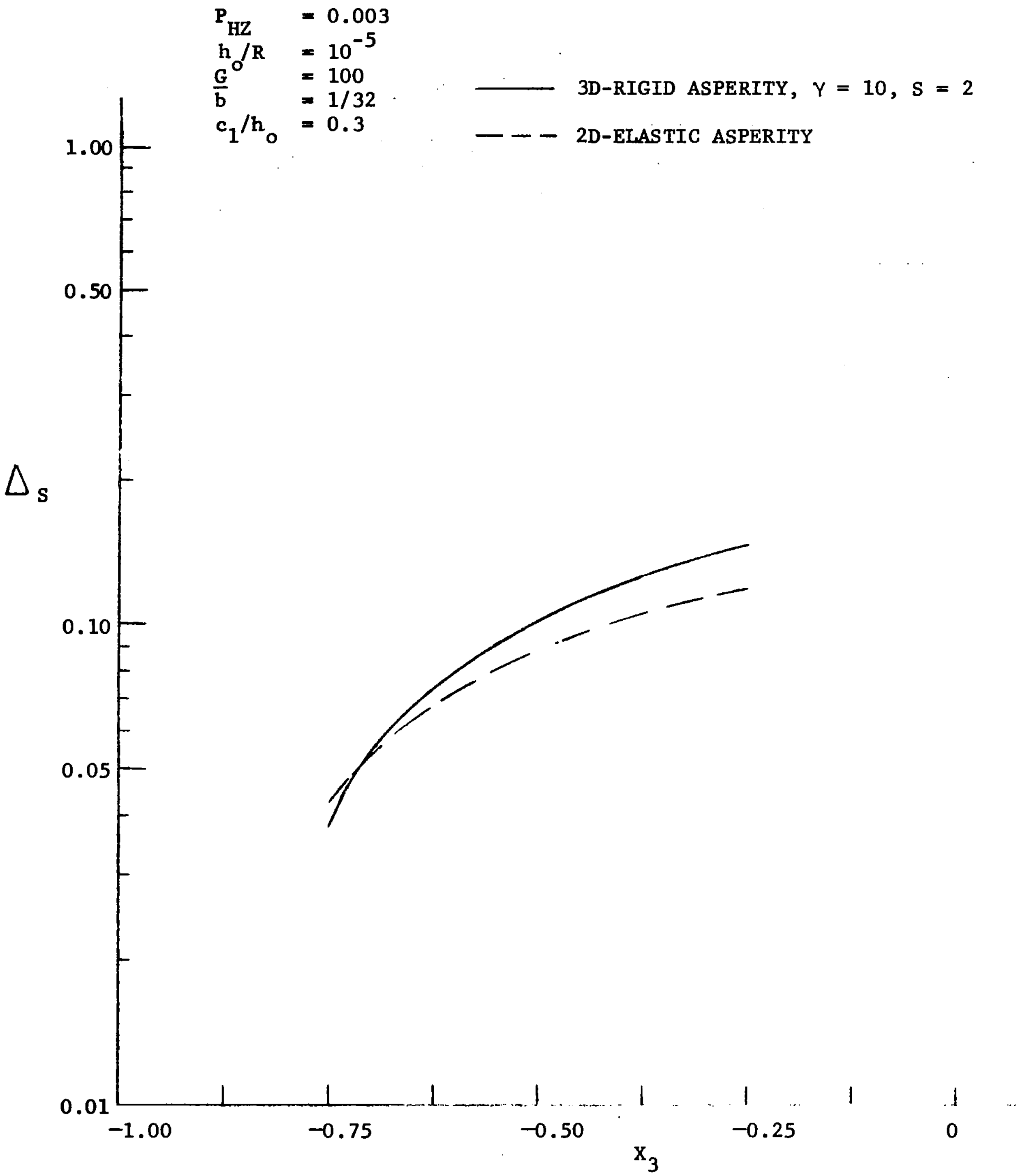

Fig. 4-10 The Effect of the Position of the Asperity Center, X_3, on $\Delta_S = \Phi_{max.} - \Phi_{min}$

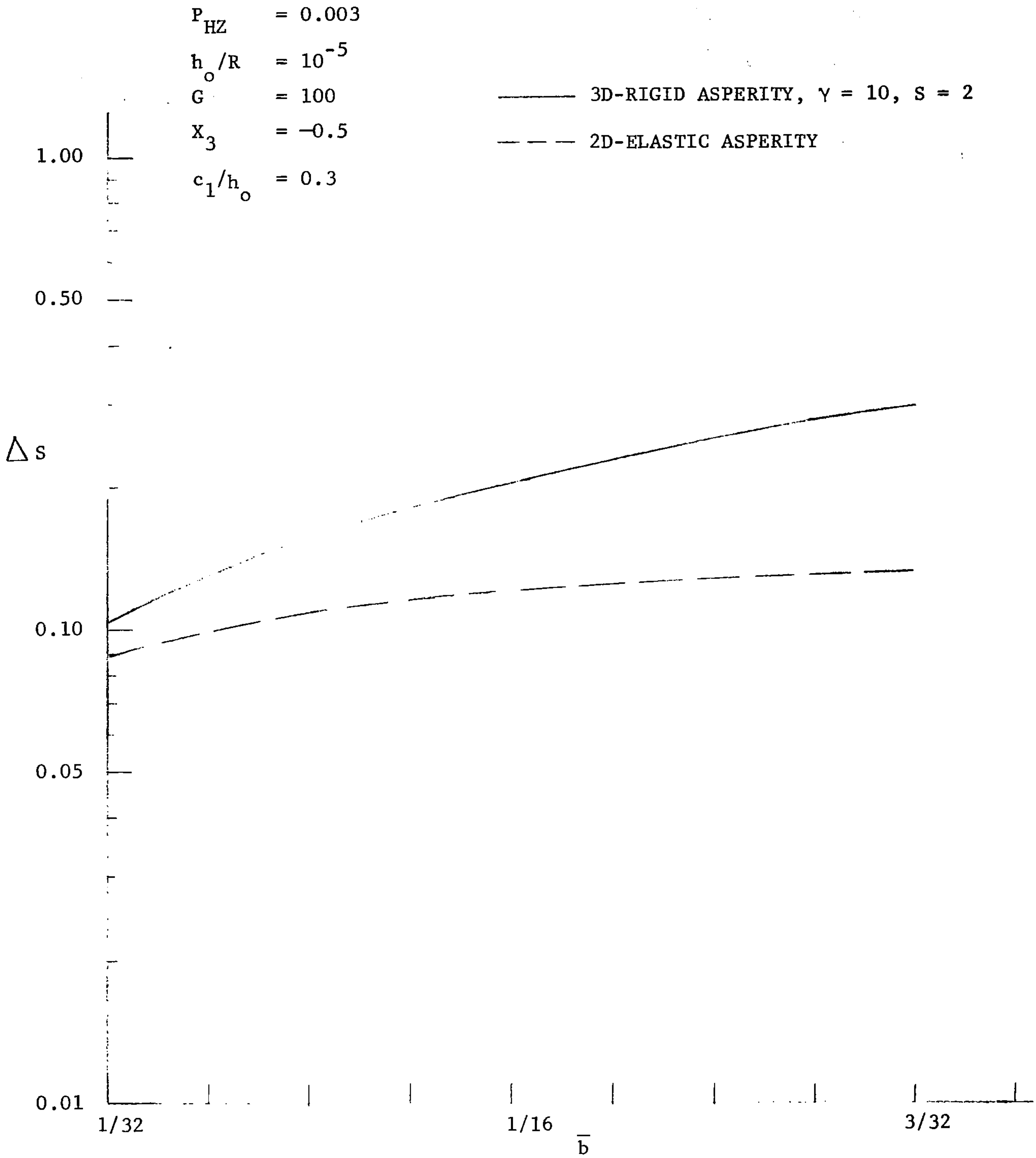

Fig. 4-11 The Effect of the Asperity Size, $\bar{b} = b'/b$, on $\Delta_S = \Phi_{max} - \Phi_{min}$

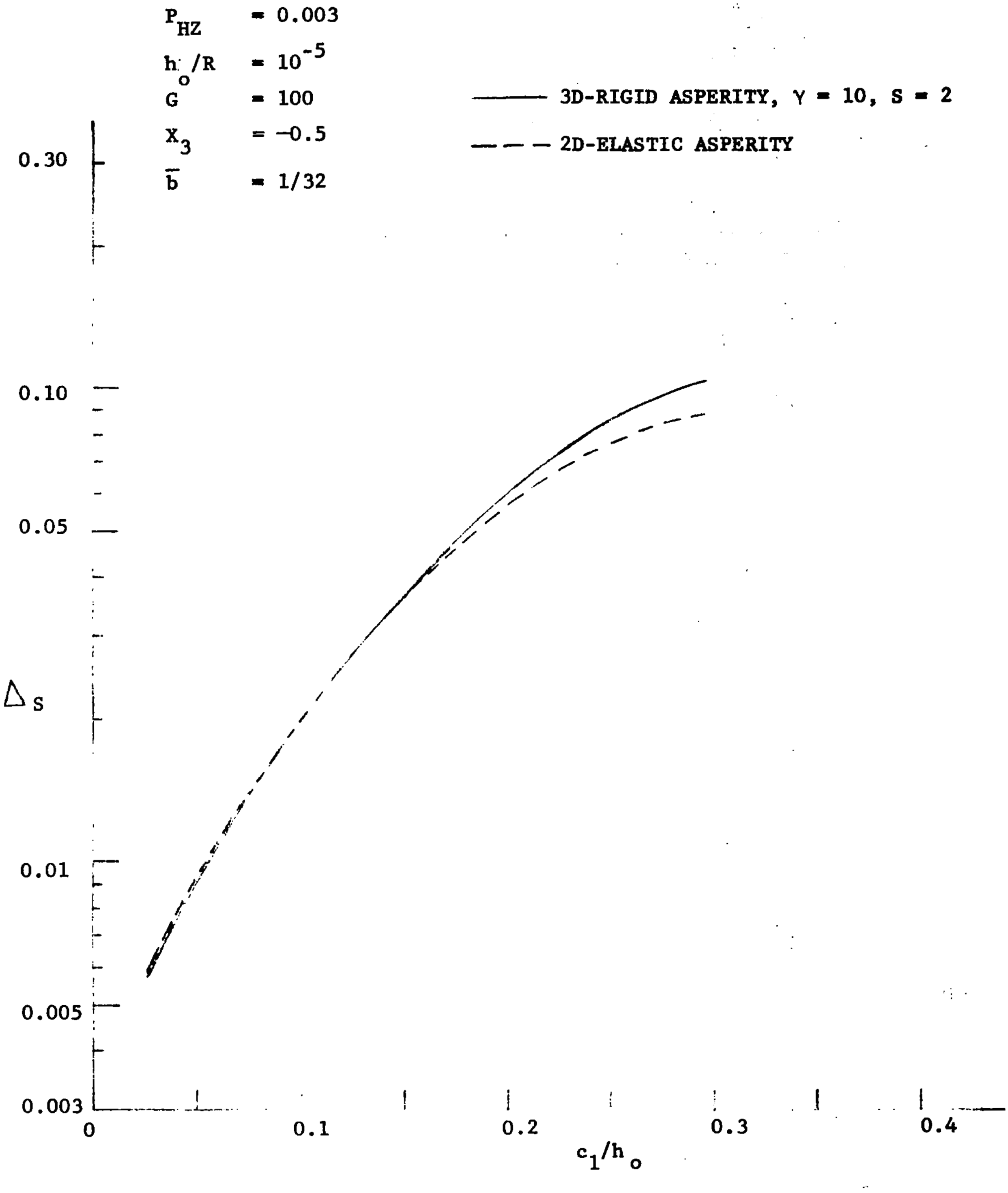

Fig. 4-12 The Effect of the Asperity Height, c_1/h_o, on $\Delta_s = \bar{\Phi}_{max} - \bar{\Phi}_{min}$

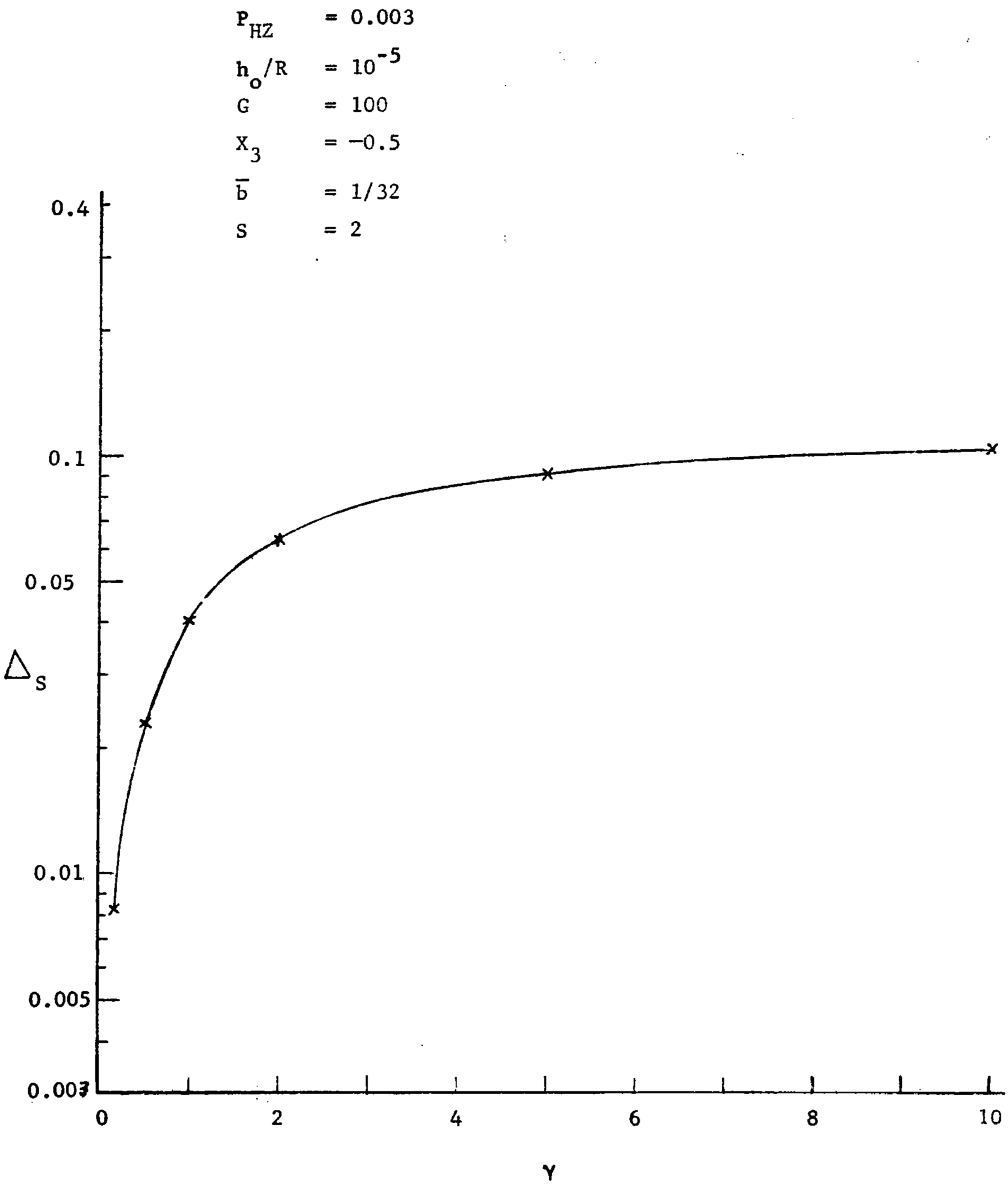

Fig. 4-13 The Effect of the Ellipticity Ratio, $\gamma = a'/b'$, on $\Delta_s = \Phi_{max.} - \Phi_{min}$

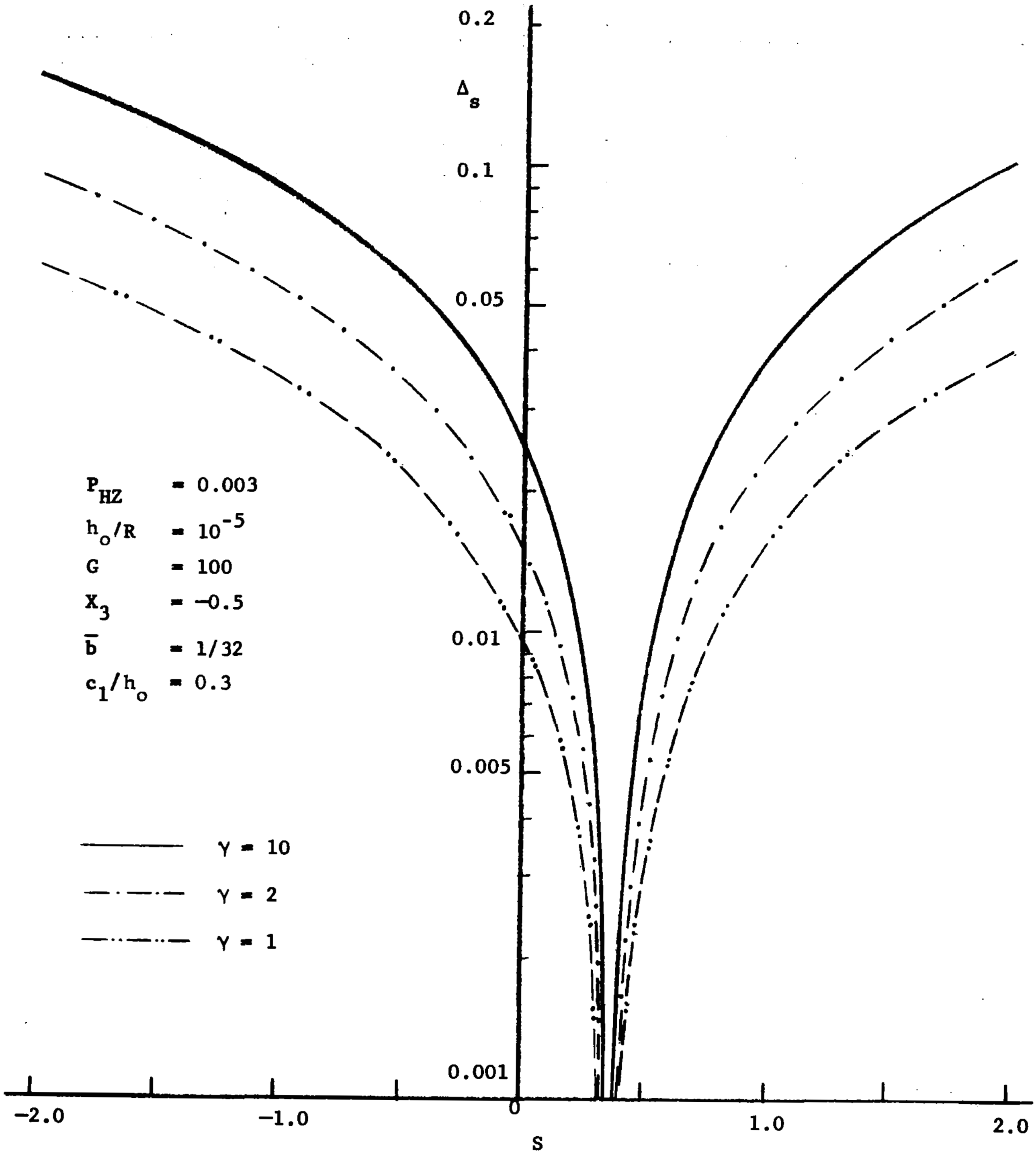

Fig. 4-14 The Effect of the Slide to Roll Ratio, $S = 2(u_1-u_2)/(u_1+u_2)$, on $\Delta_s = \Phi_{max} - \Phi_{min}$ for a Three-dimensional Rigid Asperity with Pressure Viscosity Parameter, $\alpha E' = 100$

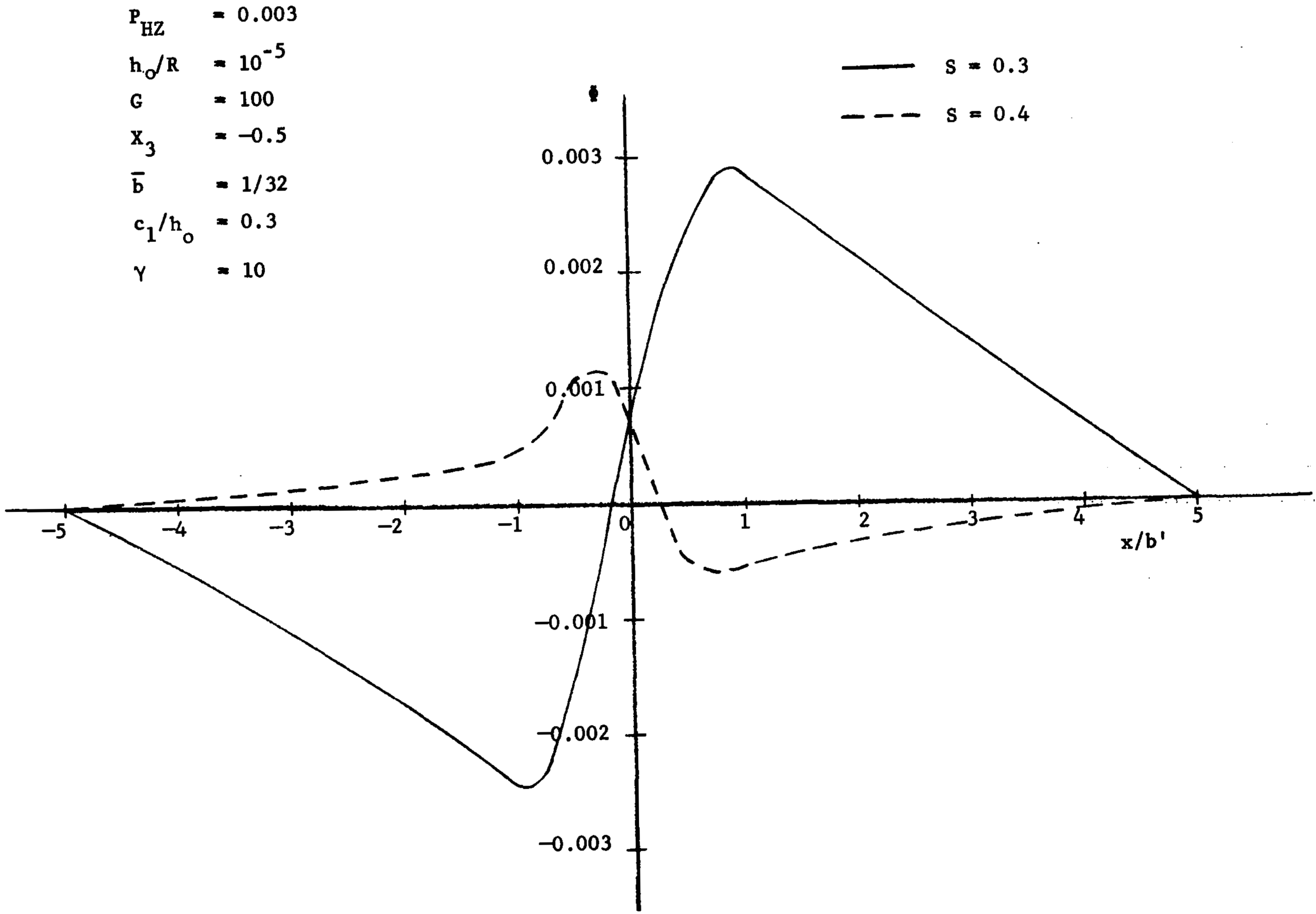

Fig. 4-15 The Perturbed Pressure, Φ, Around the Tip of a Three-dimensional Rigid Asperity

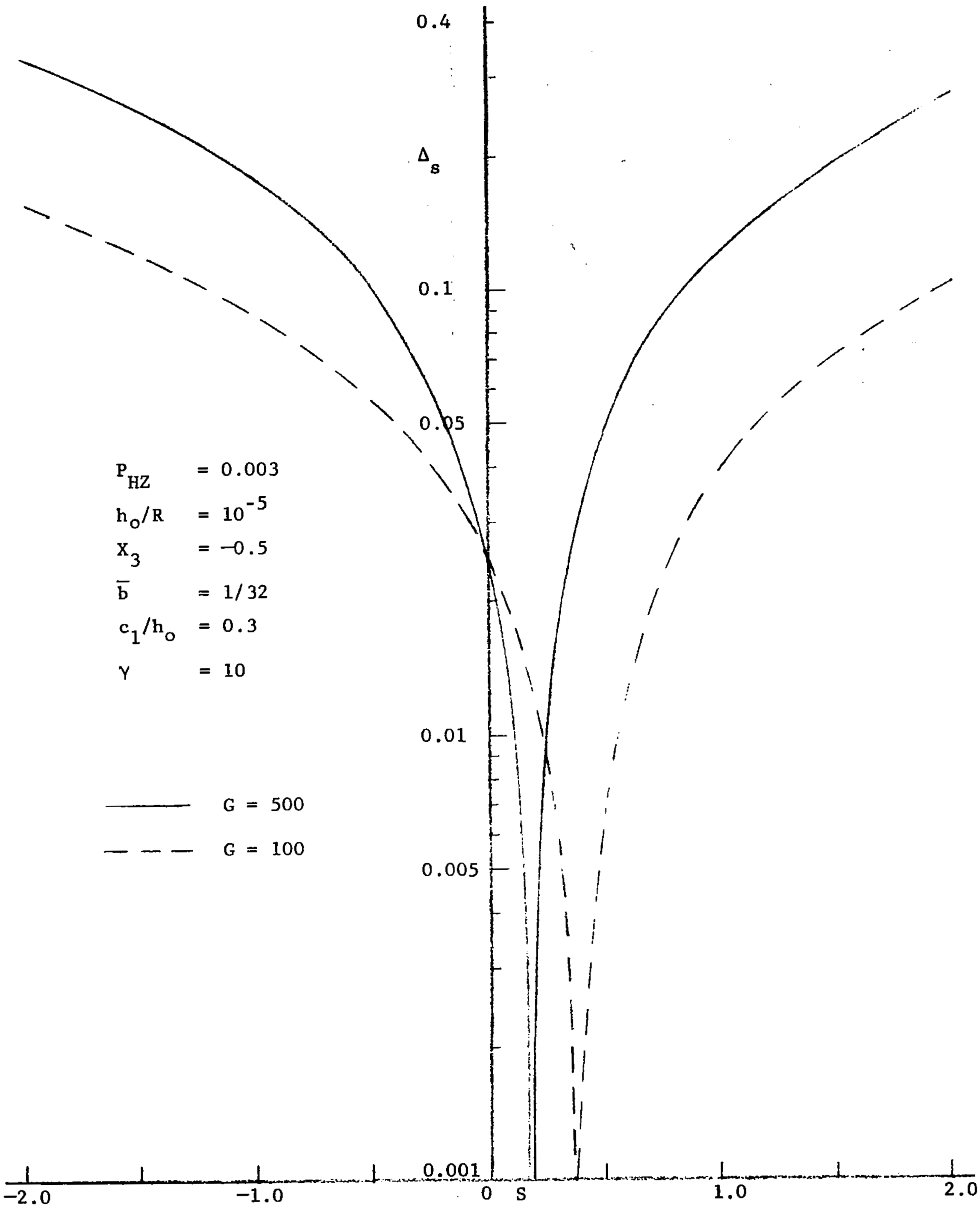

Fig. 4-16 The Effect of Slide to Roll Ratio, $S = 2(u_1-u_2)/(u_1+u_2)$, on $\Delta_S = \Phi_{max} - \Phi_{min}$ for a Three-dimensional Rigid Asperity with Pressure Viscosity Parameter, $\alpha E'$ = 100 and 500

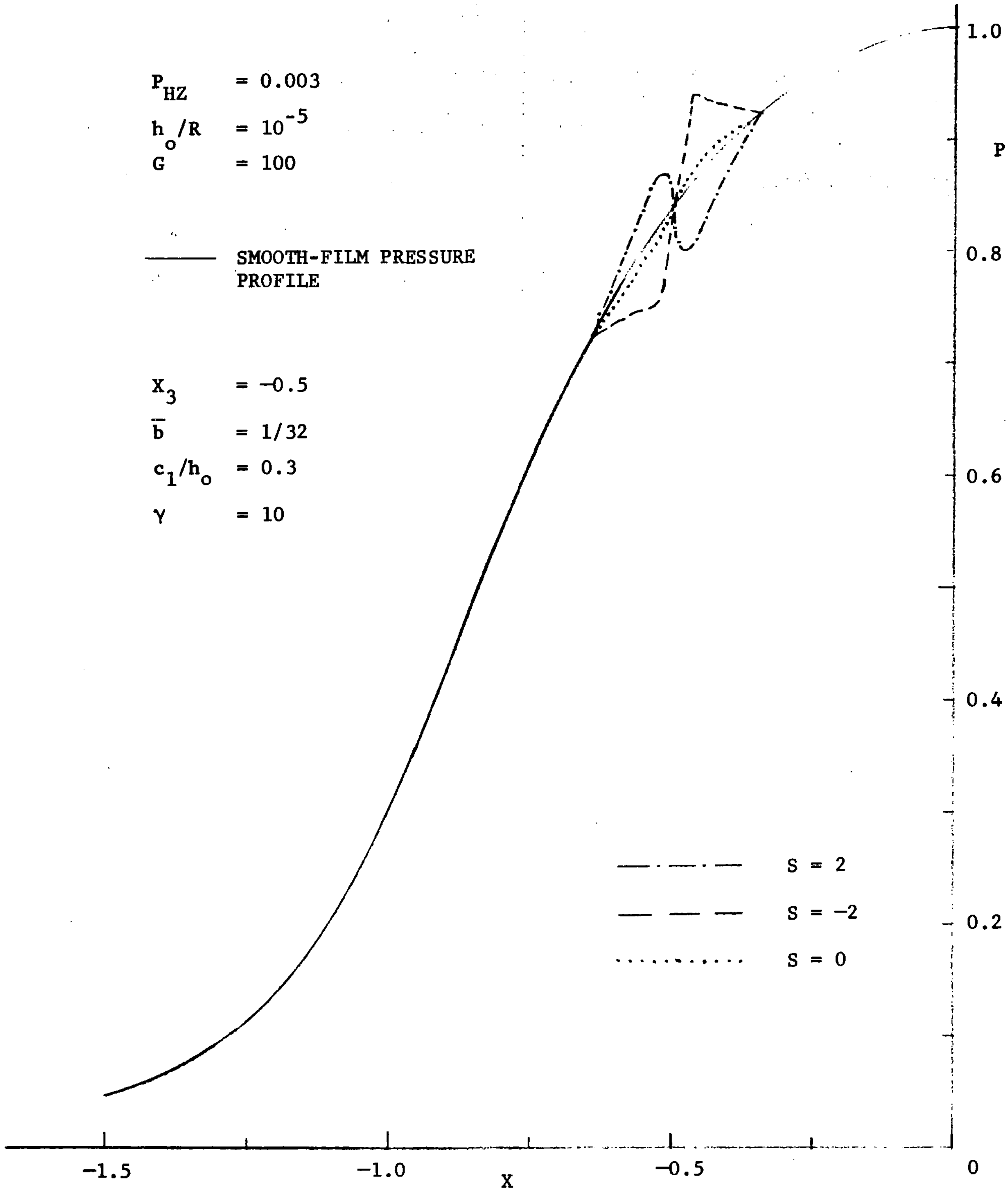

Fig. 4-17 The Smooth-Film and the Perturbed Pressure Profiles for a Three-dimensional Rigid Asperity

CHAPTER V

THE EFFECT OF SINUSOIDAL WAVINESS ON THE PRESSURE FLUCTUATION WITHIN THE HERTZIAN CONTACT

5.1 Introduction

In the previous chapter, the emphasis has been placed on the pressure perturbation around a single asperity. Such analysis with a single asperity is useful only in determining qualitatively the effects of asperity geometry, lubricant property, speed, and load upon the perturbed pressure amplitude; but it is not suitable in making quantitative predictions of pressure fluctuations within these contacts. In order to simulate the effect of continuous transverse ridges on the pressure fluctuation in an elastohydrodynamic contact, one may assume these ridges can be represented by a series of sinusoidal waviness.

In the case the surface roughness is located on the stationary surface only, the pressure and deformation profiles become time-independent, and one can modify the method described in [22] to solve for the compatible pressure and film thickness profiles. The analysis in this chapter is confined to seek the EHD performance at the inlet of a Hertzian contact with a sinusoidal roughness on the stationary surface.

5.2 Mathematical Formulation

The roughness model is assumed to be continuous transverse ridges which can be represented by a sine wave on the stationary side of the contact. Thus the asperity height δ, is a function of x only. Therefore one would obtain the relations

$$\bar{\delta} = c_1/h_o \sin(2n\pi X) \tag{5.1}$$

$$\frac{\partial \bar{\delta}}{\partial t} = 0 \tag{5.2}$$

where $\bar{\delta} = \delta/h_o$

$n = \frac{1}{4} \times \frac{1}{b'/b}$ or $= \frac{1}{4\bar{b}}$

$X = x/b$

h = center film thickness of the smooth-film EHD contact

c_1 = maximum asperity height

b' = half of the asperity width

b = half of the Hertzian contact width

x = coordinate axis along the sliding direction

The Reynolds equation and the elasticity equation are respectively

$$\frac{dP}{dX} = \frac{48}{H_o^2} U \bar{\mu} \left(\frac{H_T - 1}{H_T^3}\right) \tag{5.3}$$

$$H_T = H_1 + \bar{\delta} \tag{5.4}$$

$$H_1 = 1 + \frac{16\, P_{Hz}^2}{H_o^2} \left(\frac{X^2}{2} - \frac{1}{\pi} \int_{-\infty}^{X_f} P(\bar{\xi})\, \ell n \frac{|\bar{\xi} - X|}{|\bar{\xi}|}\, d\bar{\xi}\right) \tag{5.5}$$

where $P = p/p_{Hz}$, $H_o = h_o/R$, $R = \left(\frac{1}{R_1} + \frac{1}{R_2}\right)^{-1}$,

$U = \frac{\mu_s (u_1 + u_2)}{2E'R}$, $H_T = h_T/h_o$, $h_T = h_1 + \delta$, $\bar{\mu} = \frac{\mu}{\mu_s}$

$P_{Hz} = p_{Hz}/E'$, $E' = \left[\frac{1}{2}\left(\frac{1 - \nu_1^2}{E_1} + \frac{1 - \nu_2^2}{E_2}\right)\right]^{-1}$,

$\bar{\xi} = \xi/b$, $G = \alpha E'$

Using the same numerical scheme stated in [22], P(X), $H_T(X)$ and U are solved for a given set of non-dimensional variables, namely nominal center film thickness h_o/R, Hertzian pressure P_{Hz}, pressure viscosity parameter G, maximum asperity height c_1/h_o and asperity width b'/b.

5.3 Discussions of Results

The effect of the pressure viscosity parameter G, the maximum asperity height c_1/h_o, the asperity width b'/b, the nominal center film thickness h_o/R, and the Hertzian pressure P_{Hz}, on the magnitude of the perturbed pressure, Δ_s, (which is defined as the difference between the maximum and the minimum pressure ripples deviated from the nominal smooth-film pressure profile), and the actual pressure distribution will be discussed in the following sections.

5.3.1 The Effect of Pressure Viscosity Parameter G

For $P_{Hz} = 0.003$, $h_o/R = 10^{-5}$, $c_1/h_o = 0.3$ and $n = 2(b'/b = 1/8)$. Fig. (5.1) shows the effect of G on Δ_s. Similar to the results obtained for the single asperity ridge in an EHD contact, as discussed in Chapter IV, the magnitude of Δ_s increases with G for this case with a waviness surface profile. With the same set of values for P_{Hz}, h_o/R, c_1/h_o and b'/b, the effect of G on the pressure profile is shown in Fig. (5.2). As expected, the pressure fluctuation from the nominally smooth-film pressure profile is more pronounced when the value of G is larger and within the Hertzian contact zone. Since G represents a significant parameter, the effects of other parameters on Δ_s are compared in the subsequent sections for G = 100 and G = 1,000. An attempt was made for cases with G greater than 1,000, some of the solutions failed to converge.

5.3.2 The Effect of c_1/h_o

The asperity interaction will be more severe when the amplitude of the asperity is larger. This phenomenon has been shown earlier in the single asperity-ridge analysis and is exhibited again here in Fig. (5.3) for the case of wavy surface roughness with $P_{Hz} = 0.003$, $h_o/R = 10^{-5}$, and $n = 2(b'/b = 1/8)$. For both cases with G = 100 and 1,000, the magnitude of the perturbed pressure increases with the ratio c_1/h_o. This phenomenon can also be observed in Fig. (5.4) with G = 100 and Fig. (5.5) with G = 1,000 in which the perturbed pressure profiles are shown.

5.3.3 The Effect of n

For $P_{Hz} = .003$, $h_o/R = 10^{-5}$ and $c_1/h_o = 0.3$, Fig. (5.6) shows the effect of n on the magnitude of the perturbed pressure Δ_s, for both G = 100 and 1,000. It seems that the two curves shown here do not have the same qualitative trend. However, it is believed that the further increase of n for the case with G = 1,000 will decrease the magnitude of Δ_s due to the elastic effect, so that the shape of the curve in this case will be similar to that with G = 100.

Let's recall that $n = 1/4 \times b/b'$. Thus increasing the value of n implies the closer the distance between the center of each individual asperity ridge and the center of the EHD contact. Therefore the effect of n actually consists of the effects of elastic deformation, the ratio b'/b and the distance between the individual asperity center and the contact center.

The perturbed pressure profiles for G = 100 and 1,000, due to the effect of n, are shown in Figs. (5.7) and (5.8) respectively. The results obtained for these two cases are the same qualitatively. For

$G = 1{,}000$ in which the elastic effect is more severe, the magnitude of the pressure ripple deviated from the nominally smooth-film pressure profile is much larger than those with $G = 100$.

5.3.4 /R Effect

The effect of h_o/R on the magnitude of the perturbed pressure Δ_s, for both $G = 100$ and $1{,}000$ are shown in Fig. (5.9). In these examples, the values of P_{Hz}, c_1/h_o, n and b'/b are 0.003, 0.3, 2 and 1/8 respectively. It is observed that the magnitude of Δ_s increases with the ratio h_o/R. This increase is larger when the magnitude of G is larger.

In Chapter IV, it has been shown that the magnitude of Δ_s decreases with the increase of h_o/R when there is a single 3D rigid asperity within the contact zone. This opposing trend between the case of a single 3D rigid asperity and continuous elastic asperities can be explained in the following manner:

In the case of sinusoidal elastic asperities, the pressure amplitude is reduced by the local elastic deformation of the asperity. If c_1/h_o is held constant, the reduction in pressure due to local elastic deformation becomes much greater as h_o/R decreases, because at a smaller h_o/R, it requires only a very small pressure amplitude to flatten out the asperity. This phenomenon of elastic effect is best illustrated by Fig. (5.10) which shows the perturbed pressure and surface profiles for $h_o/R = 10^{-5}$, 5×10^{-6} and 10^{-6} respectively, for the sinusoidal elastic asperities with $G = 100$. The shapes of these perturbed pressure and surface profiles are consistent with one another. However, the smaller the h_o/R, the more the asperity being flattened out. For the case of a 3D rigid asperity, the effect of local elastic deformation is ignored, and thus the opposing trend is found.

The perturbed pressure and surface profiles for the sinusoidal elastic asperities with G = 1,000 are shown in Fig. (5.11). The results for both G = 100 and 1,000 are shown to have the same characteristics and the magnitude of Δ_s is larger with G = 1,000 as expected.

5.3.5 P_{Hz} Effect

For $h_o/R = 10^{-5}$, $c_1/h_o = 0.3$, n = 2 and b'/b = 1/8, the results of the magnitude of the perturbed pressure Δ_s, versus the nominal value of the maximum Hertzian pressure P_{Hz}, are shown in Fig. (5.12). It is readily seen that, for both cases with G = 100 and 1,000, the increase in P_{Hz} results in a decrease in Δ_s. This phenomenon is due to the reduction of the pressure amplitude caused by the local elastic deformation of the asperity. The larger the P_{Hz}, the easier the asperity being flattened, and thus the smaller the Δ_s.

The perturbed pressure profiles are shown in Figs. (5.13) and (5.14) respectively. The results for G = 100 and 1,000 are found to have the same trend qualitatively. As expected, the magnitude of Δ_s is larger in the case of G = 1,000. In addition the perturbed surface profiles for the case of G = 100 as shown in Fig. (5.13) illustrates the effect of the local elastic deformation of the asperity as explained previously. It tells that the larger the P_{Hz}, the more severe the asperity being deformed.

5.4 CONCLUSIONS

In the case of the simple sliding of a smooth surface against a stationary rough one, the magnitude of the pressure deviation from the nominally smooth-film profile and the perturbed pressure profile in the inlet of an elastohydrodynamic contact, can be determined quantitatively when the undeformed rough surface profile is given.

In the examples given in this chapter, the undeformed rough surface profile is simulated by continuous transverse ridges represented by a series of sinusoidal waviness. The effect of the following non-dimensional parameters on the magnitude of the pressure fluctuation Δ_s and the perturbed pressure profile are obtained: the pressure viscosity parameter G, the maximum height of the asperity c_1/h_o, the number of wave cycles within the contact zone, n, (which in turn determines the width of the asperity, b'/b), the nominal smooth-film center film thickness h_o/R and the Hertzian pressure P_{Hz}.

The effects of G and c_1/h_o on the magnitude of Δ_s for this case with a waviness surface profile have the same characteristics compared to those obtained for the single asperity ridge in an EHD contact as presented in Chapter IV. Namely, the magnitude of Δ_s increases when the magnitude of G or c_1/h_o increases.

The results of Δ_s versus P_{Hz} and h /R are found to be consistent for both G = 100 and 1,000. The magnitude of Δ_s decreases as the magnitude of P_{Hz} or h_o/R becomes larger. These results for the waviness surface profile have the opposing trend when compared to those obtained by the 3D rigid asperity analysis. The reason for the opposing trend is due to the pressure reduction caused by the local elastic deformation of the asperity for the waviness surface profile, whereas the effect of local elastic deformation is ignored for a 3D rigid asperity.

The effect of the number of wave cycles within the contact zone on the magnitude of the perturbed pressure Δ_s is found to be very complicated. The local elastic effect, the ratio b'/b, and the distance between each individual asperity center and the contact center are important factors affecting the magnitude of Δ_s caused by changing the magnitude of n.

$P_{HZ} = 0.003$

$h_o / R = 10^{-5}$

$c_1 / h_o = 0.3$

$n = 2$

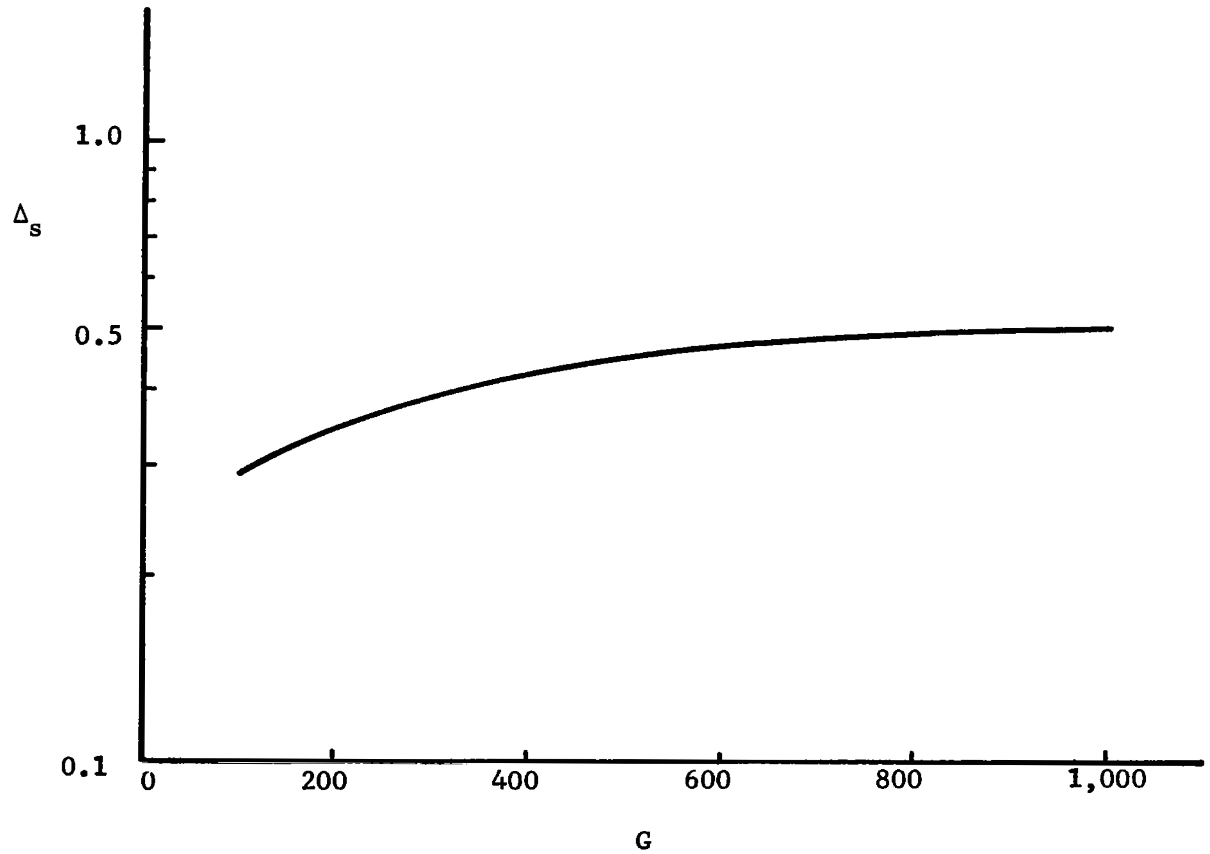

Fig. 5-1 The Effect of the Pressure Viscosity Parameter, $G = \alpha E'$, on the Double Amplitude of the Perturbed Pressure

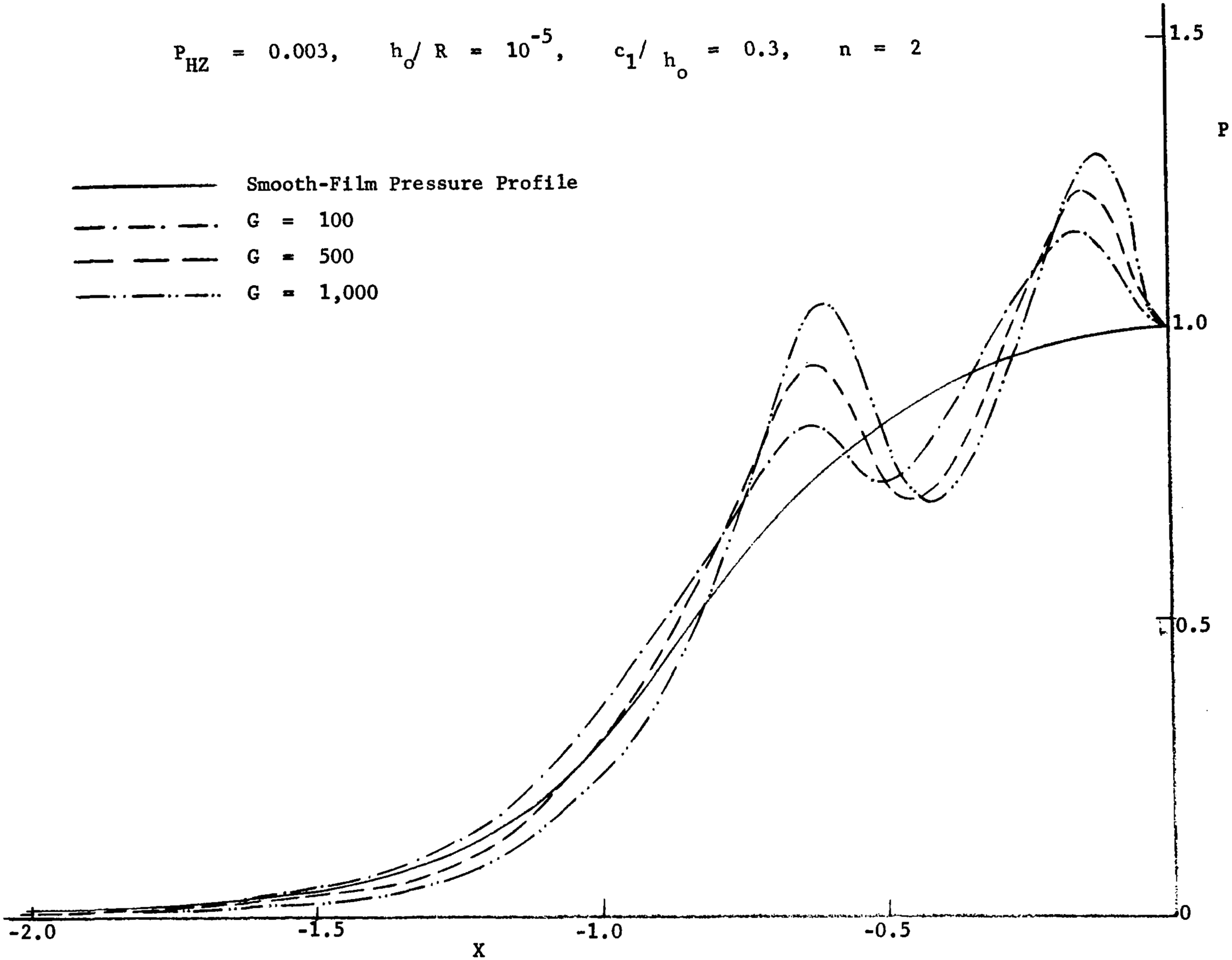

Fig. 5-2 The Effect of the Pressure Viscosity Parameter, $G = \alpha E'$, on the Perturbed Pressure Profiles

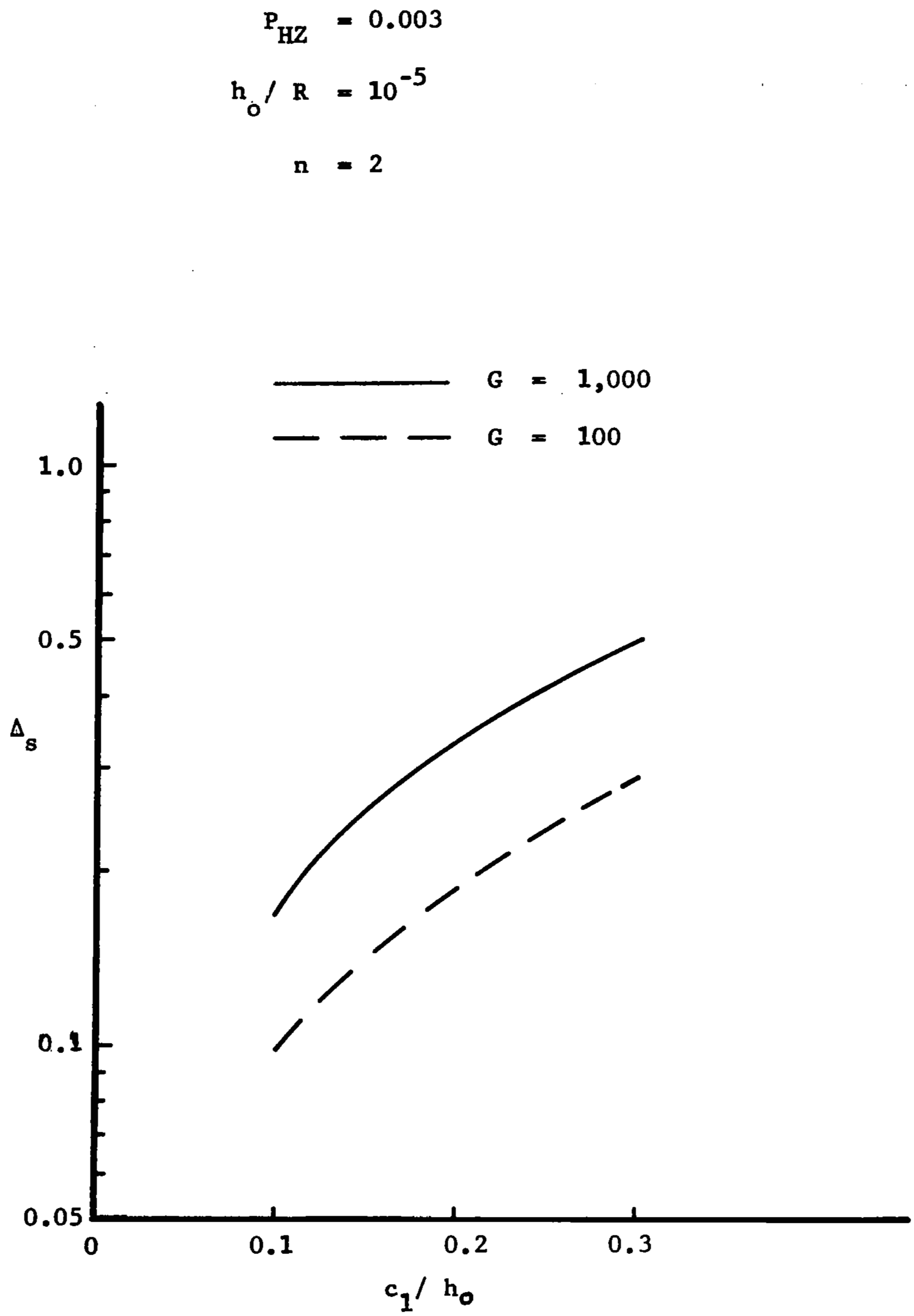

Fig. 5-3 The Effect of the Asperity Height to Film Thickness Ratio, c_1/h_o, on $\Delta_s = \Phi_{max.} - \Phi_{min.}$

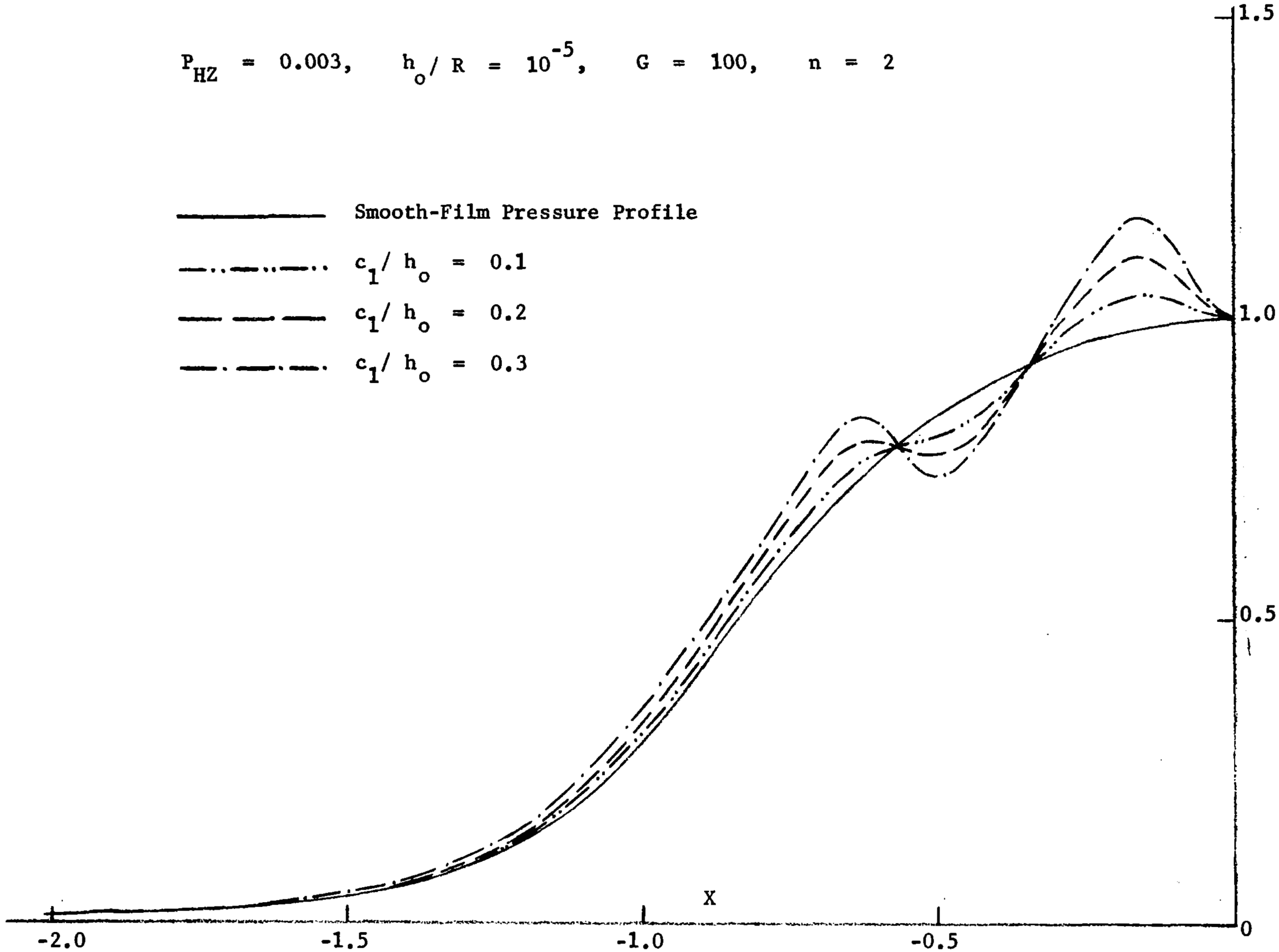

Fig. 5-4 The Effect of the Asperity Height to Film Thickness Ratio, c_1/h_o, on the Perturbed Pressure Profiles for $E' = 100$

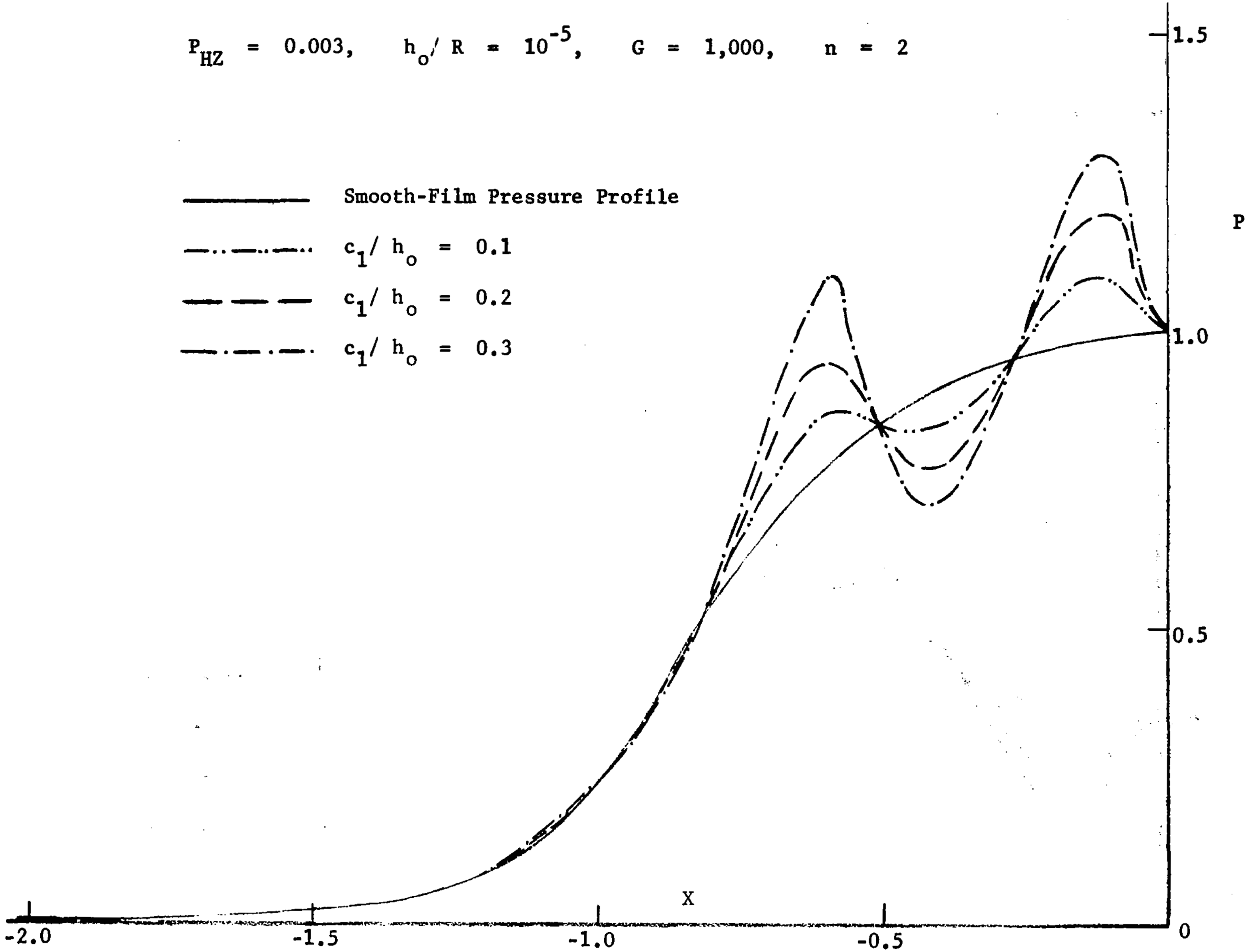

Fig. 5-5 The Effect of the Asperity Height to Film Thickness Ratio, c_1/h_o, on the Perturbed Pressure Profiles for E' = 1000

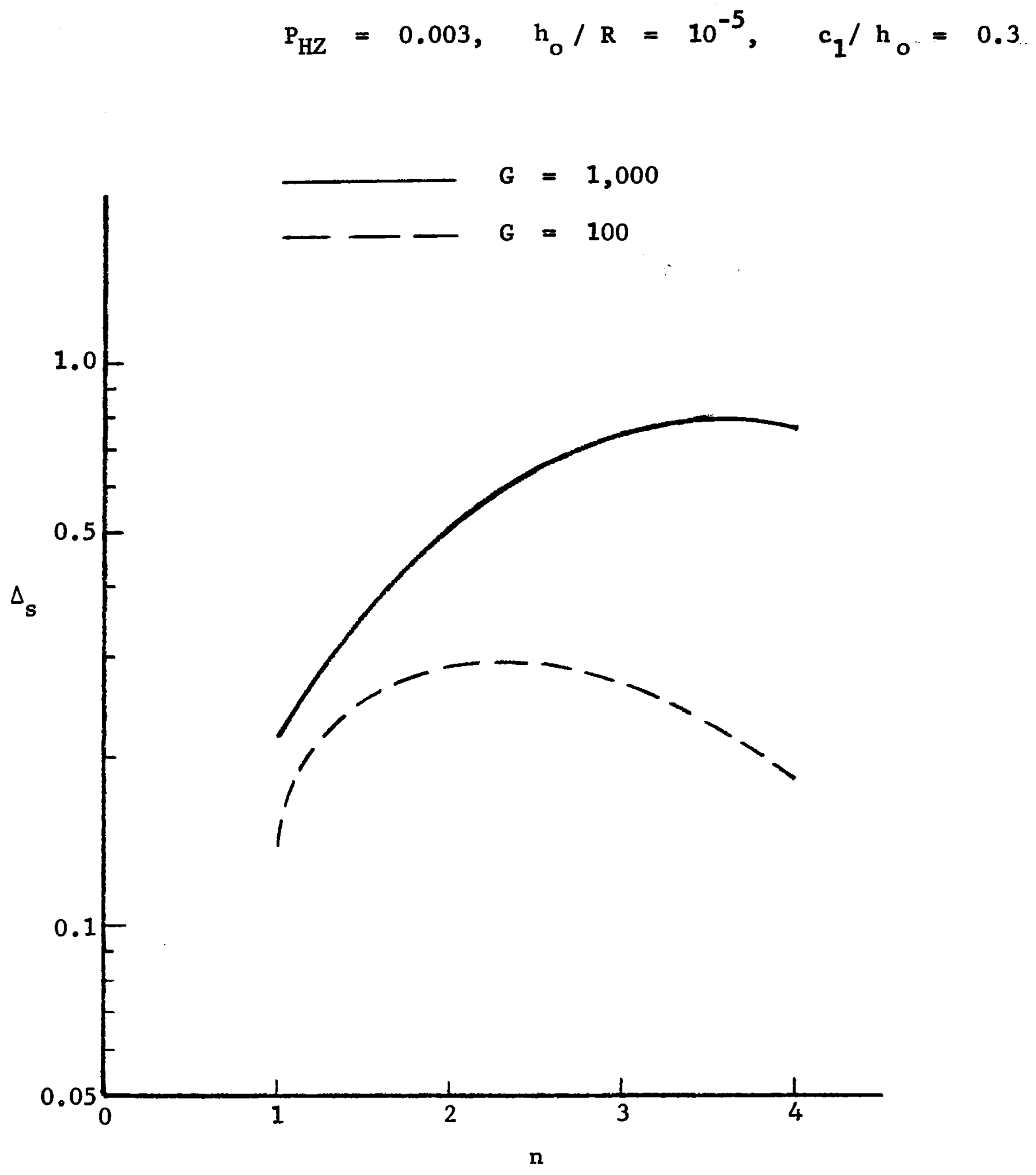

Fig. 5-6 The Effect of the Number of Wave Cycles, n, on $\Delta_s = \Phi_{max.} - \Phi_{min.}$

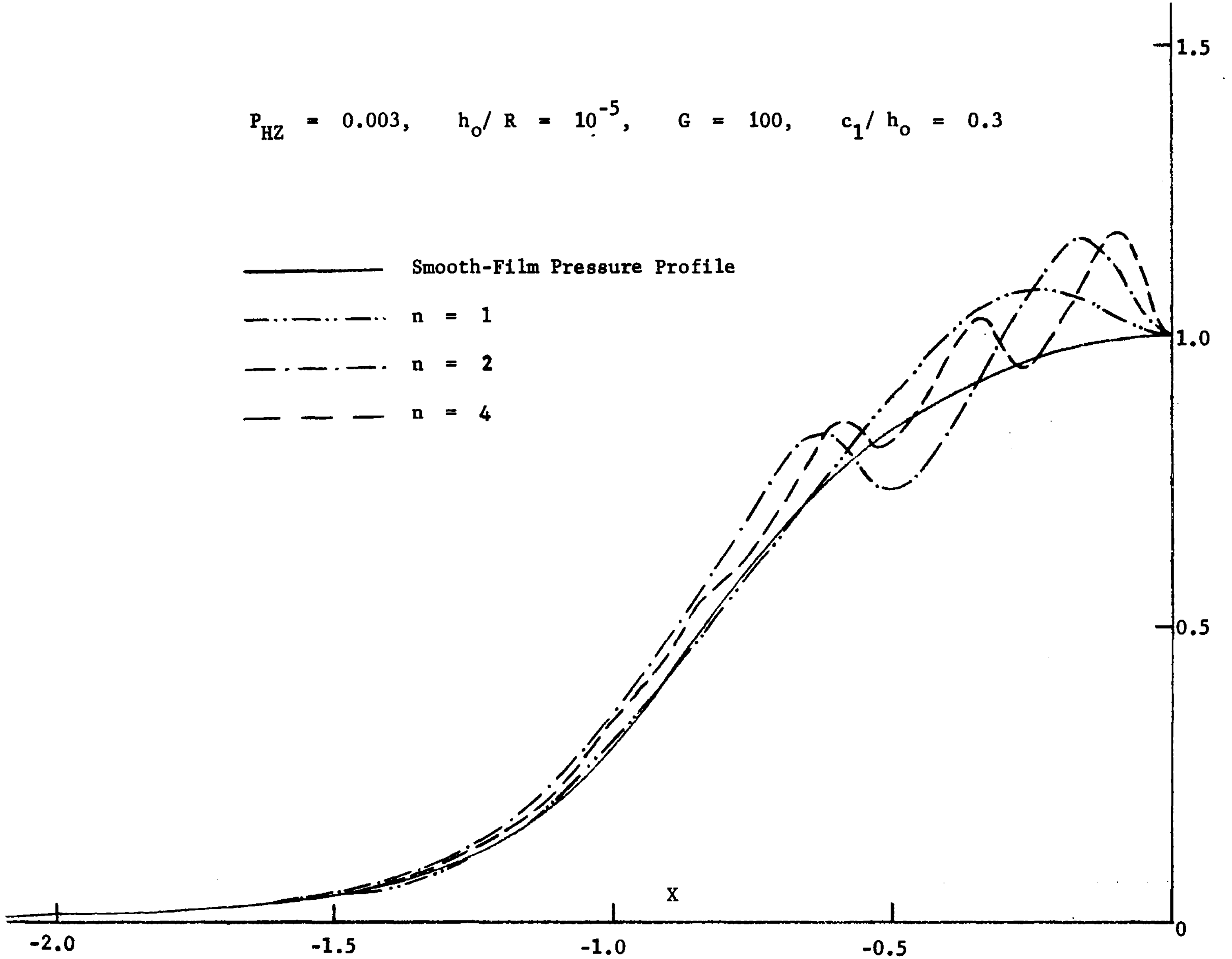

Fig. 5-7 The Effect of the Number of Wave Cycles, n, on the Perturbed Pressure Profiles for Pressure Viscosity Parameter, $\alpha E'$ = 100

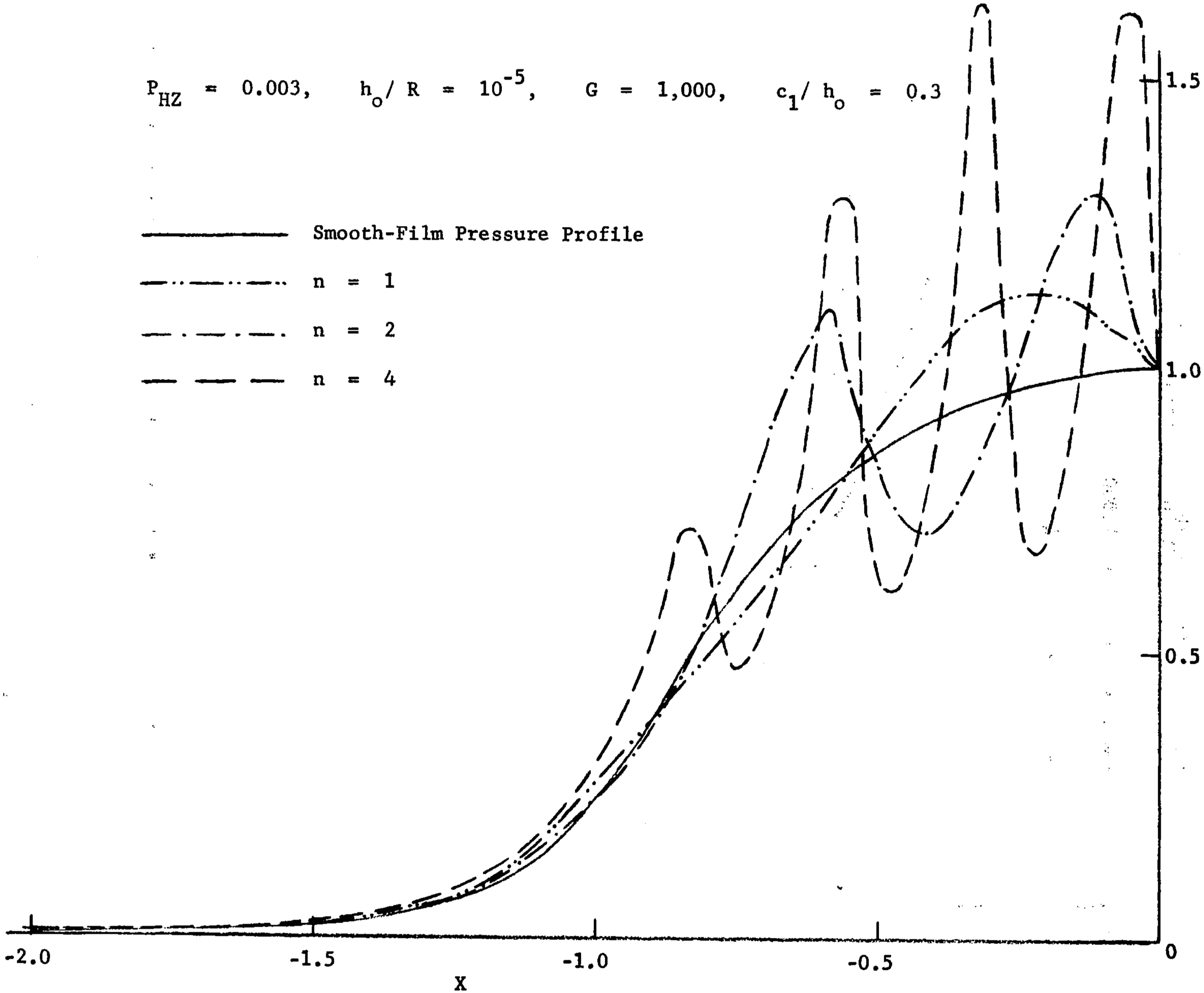

Fig. 5-8 The Effect of n, on the Perturbed Pressure Profiles for Pressure Viscosity Parameter, $\alpha E'$ = 1000

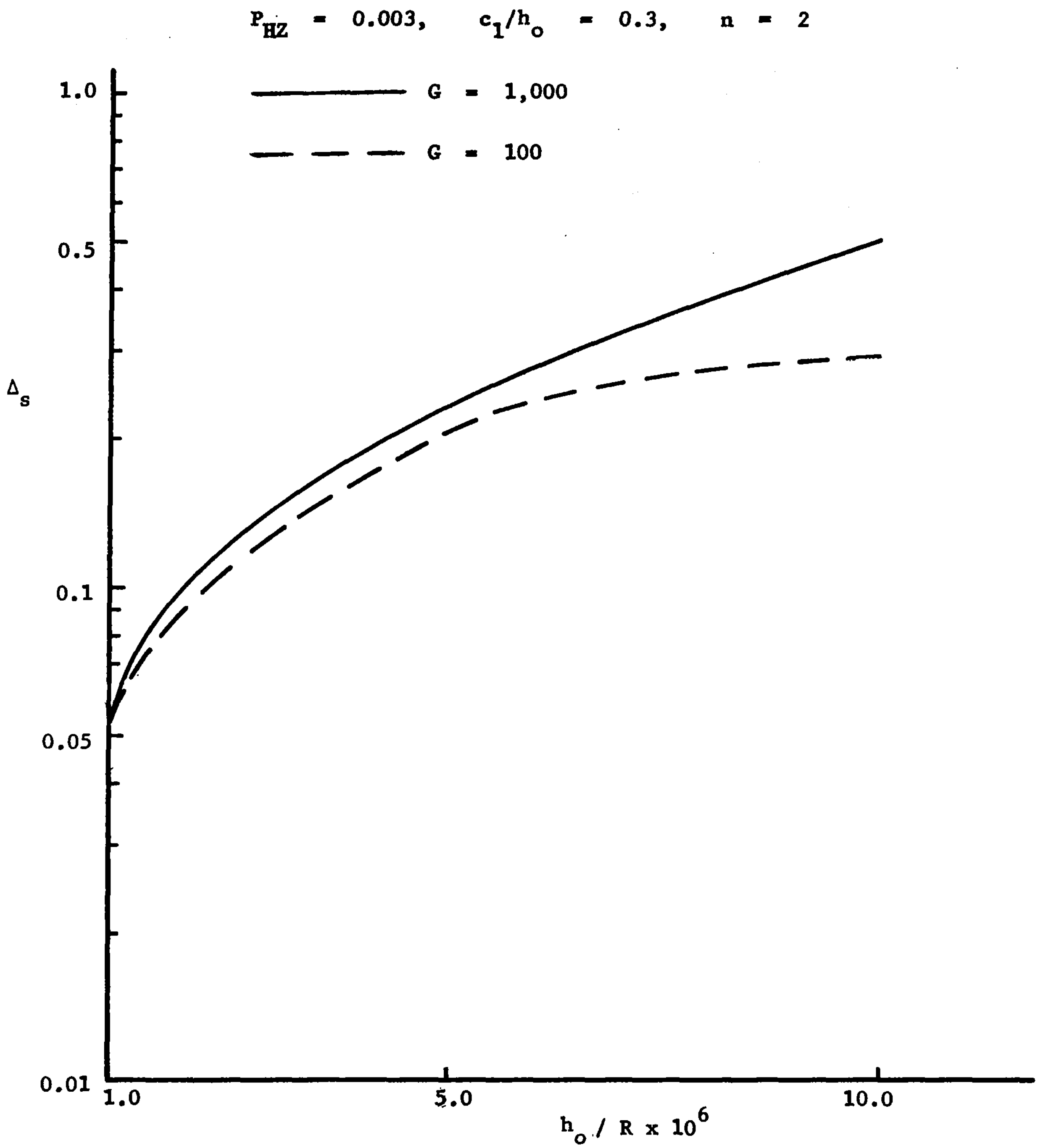

Fig. 5-9 The Effect of the Dimensionless Center Film Thickness, h_o/R, on $\Delta_s = \Phi_{max.} - \Phi_{min.}$

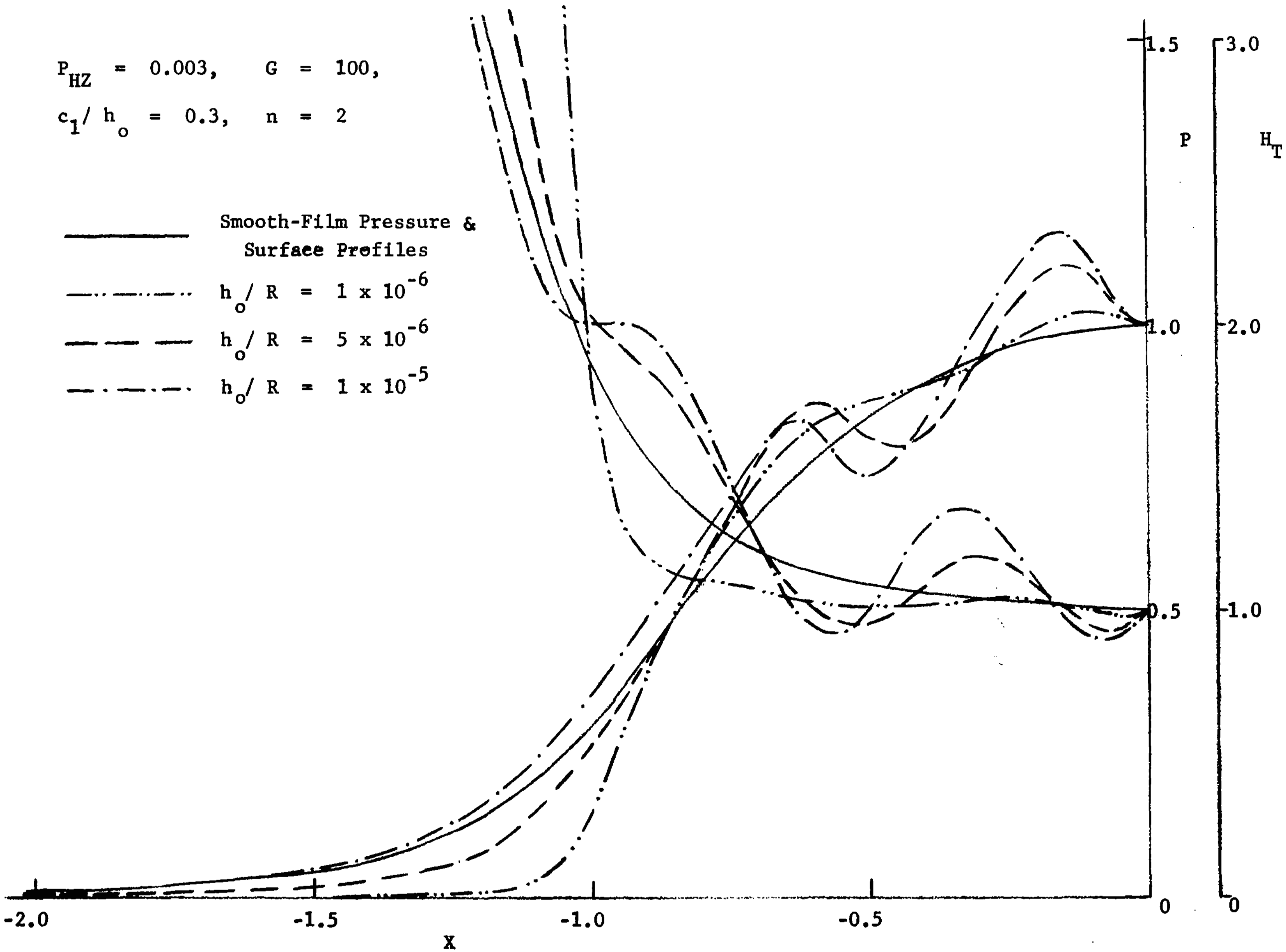

Fig. 5-10 The Effect of the Dimensionless Center Film Thickness, h_o/R, on the Perturbed Pressure Profiles for $\alpha E'$ = 100

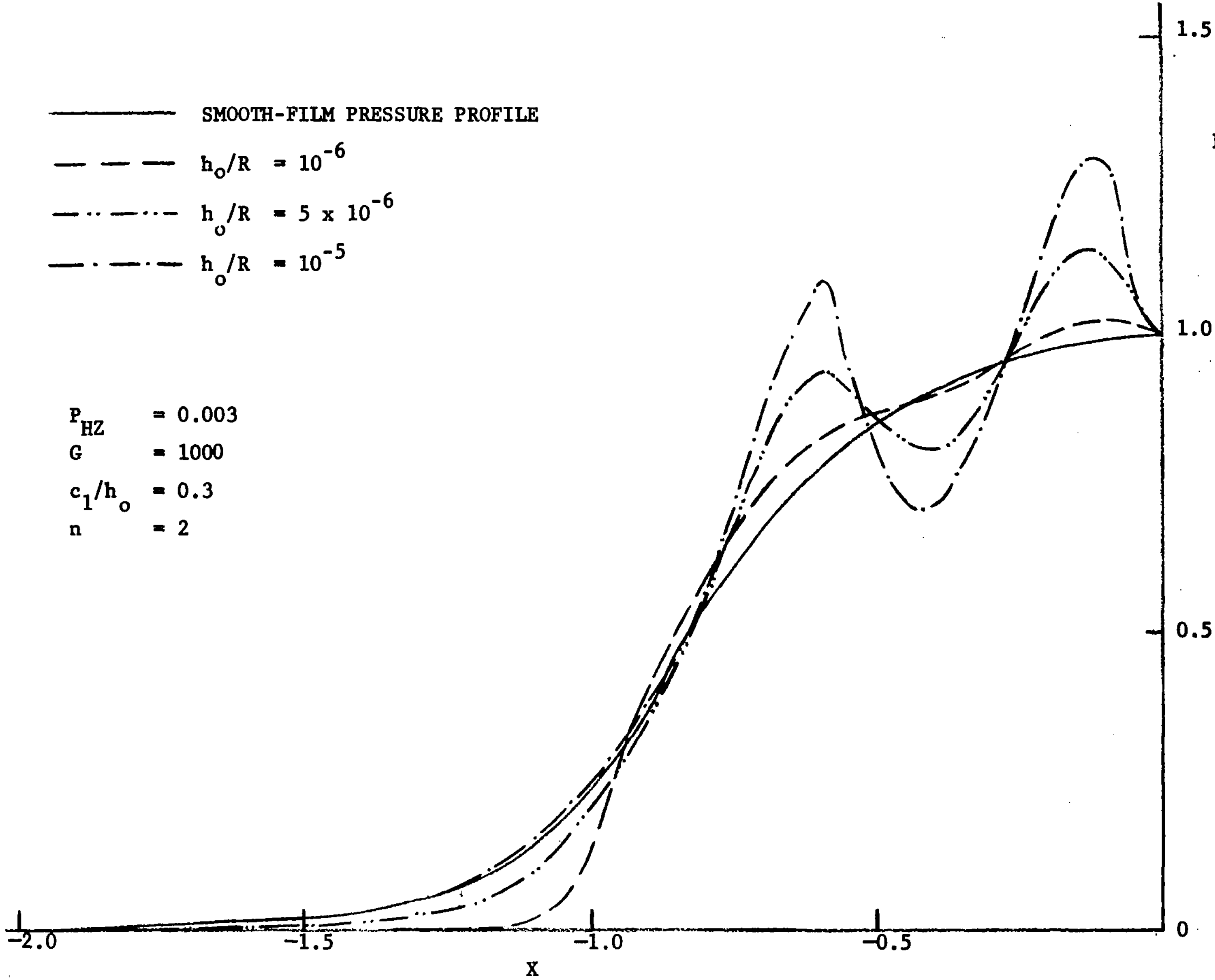

Fig. 5-11 The Effect of the Dimensionless Center Film Thickness, h_o/R, on the Perturbed Pressure Profiles for $\alpha E' = 1000$.

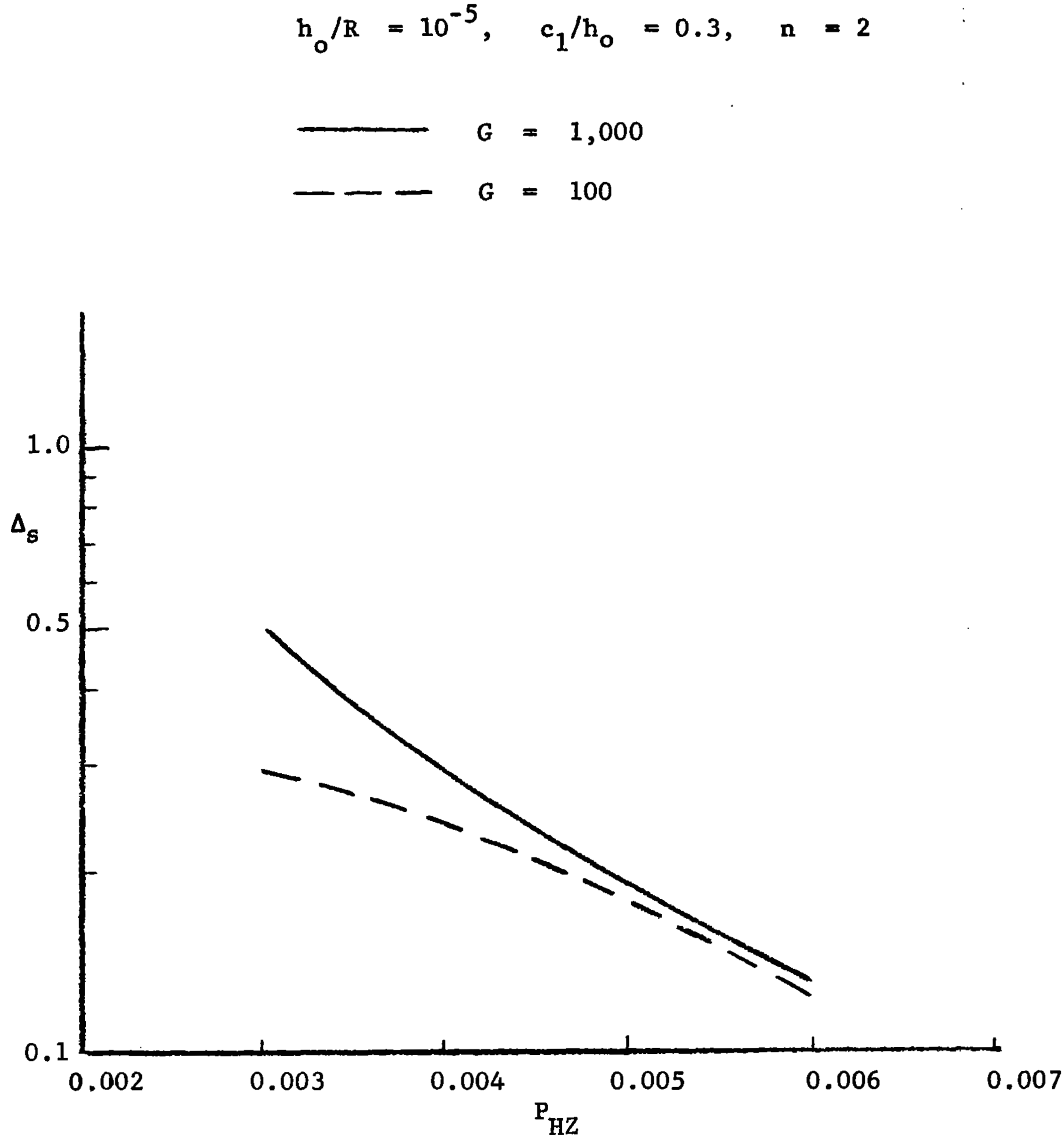

Fig. 5-12 The Effect of the Normalized Hertzian Pressure, $P_{Hz} = p_{Hz}/E'$, on $\Delta_s = \Phi_{max.} - \Phi_{min.}$

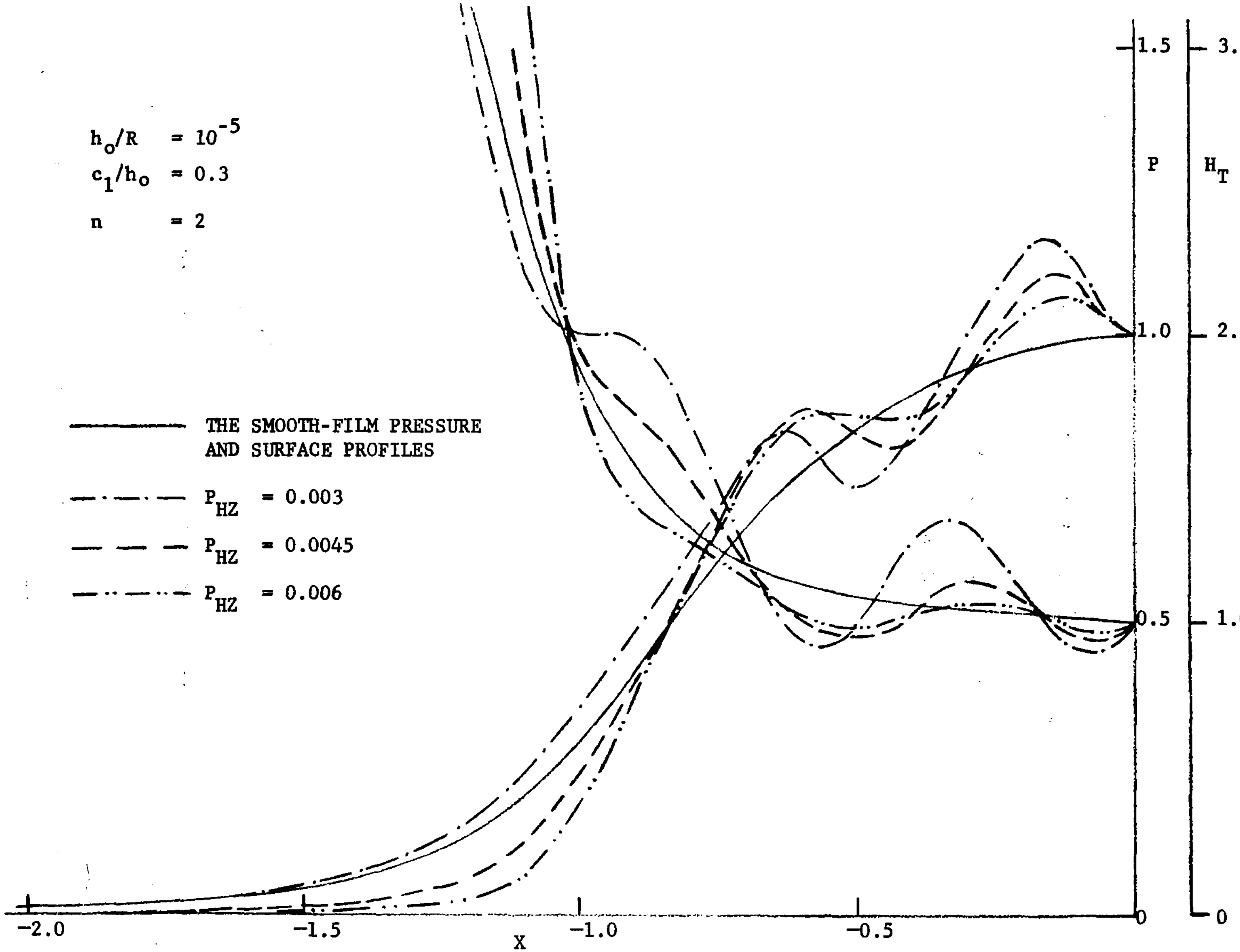

Fig. 5-13 The Effect of the Normalized Hertzian Pressure, $P_{Hz} = p_{Hz}/E'$, on the Perturbed Pressure and Film Profiles for $\alpha E' = 100$

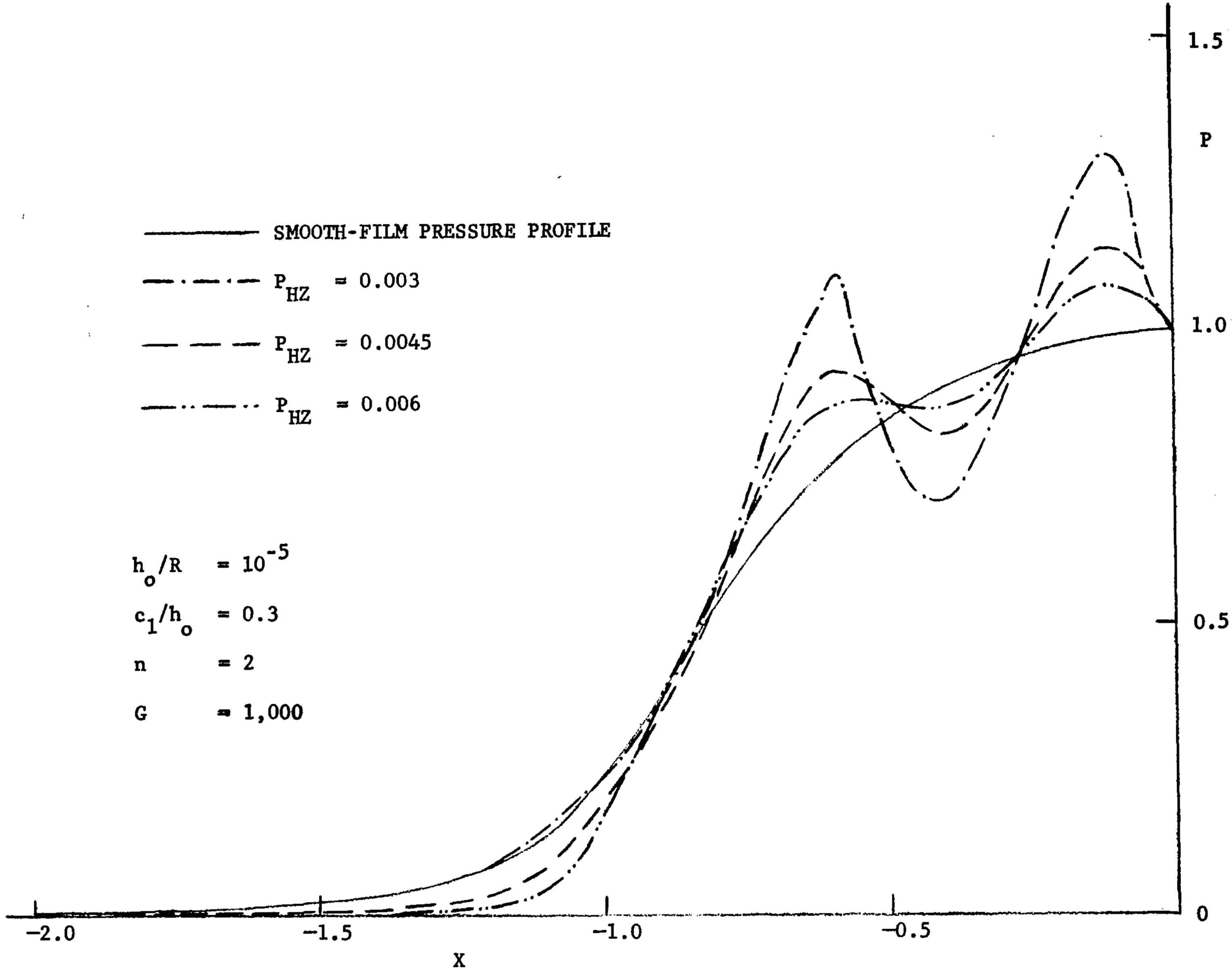

Fig. 5-14 The Effect of the Normalized Hertzian Pressure, $P_{Hz} = p_{Hz}$, on the Perturbed Pressure Profiles for $\alpha E' = 1000$

REFERENCES

1. Citron, S. J., "Slow Viscous Flow Between Rotating Concentric Infinite Cylinder With Axial Roughness," K. Appl. Mech., Trans. ASME, Vol. 29, Ser. E (1962), p. 188.

2. Burton, R. A., "Effect of Two-Dimensional, Sinusoidal Roughness on the Load Support Characteristics of a Lubricant Film," J. Basic Eng., Trans. ASME, Ser. D, 85, (1963), p. 258.

3. Davies, M. G., "The Generation of Pressure Between Rough, Fluid Lubricated, Moving, Deformable Surface," Lub. Engineering, 19, (1963), p. 246.

4. Fowles, P. E., "The Application of Elastohydrodynamic Lubrication Theory to Individual Asperity-Asperity Collisions," Trans, ASME, J. of Lub. Tech., (July 1969), p. 464.

5. Lee, K., and Cheng, H. S., "The Effect of Surface Asperity on the Elastohydrodynamic Lubrication," NASA Report No. CR-2195,(February 1973).

6. Tseng, S. T., and Saibel, E., "Surface Roughness Effect on Slider Lubrication," ASLE Trans, 10, (1967), p. 334.

7. Christensen, H., "Stochastic Models for Hydrodynamic Lubrication of Rough Surfaces," Proc. Instn. Mech. Engrs., Tribology Group, Vol. 184, Pt. 1, 55, (1969-70), p. 1013.

8. Christensen, H., "A Theory of Mixed Lubrication," Proc. Instn. Mech. Engrs., Tribology Group, Vol. 186, 41, (1972), p. 421.

9. Christensen, H., and Tonder, K., "The Hydrodynamic Lubrication of Rough Bearing Surfaces of Finite Width," ASME-ASLE Lub. Conf., Paper No. 70-Lub-7, Cincinnati, Ohio, Oct. 12-15, 1970.

10. Tallian, T. E., "The Theory of Partial Elastohydrodynamic Contacts," Wear, 21, (1972), p. 49.

11. Johnson, K. L., Greenwood, J. A., and Poon, S. Y., "A Simple Theory of Asperity Contact in Elastohydrodynamic Lubrication," Wear, 19, (1972), p. 91.

12. Thompson, R. A., and Bocchi, W., "A Model for Asperity Load Sharing in Lubricated Contacts," ASLE, 71LC-9, p. 67.

13. Greenwood, J. A., and Tripp, J. H., "The Contact of Two Nominally Flat Rough Surfaces," Proc. Instn. Mech. Engrs., Tribology Group, Vol. 135, 48/71, (1970-71), p. 625.

14. Dowson, D., and Higginson, G. R., "Elastohydrodynamic Lubrication," Pergamon Press, New York, 1966.

15. Meyer, P. L., "Introductory Probability and Statistical Application," Addison-Wesley Publishing Co., 1965.

16. Christensen, H., and Tonder, K., "The Hydrodynamic Lubrication of Rough Journal Bearings," Trans, ASME, J. of Lub. Tech., (April 1973), p. 166.

17. Tonder, K., and Christensen, H., "Waviness and Roughness in Hydrodynamic Lubrication," Proc. Instn. Mech. Engrs., Tribology Group, Vol. 186, 72/72, (1972), p. 807.

18. Rhow, S. K., and Elrod, H. G., "The Effects on Bearing Load-Carrying Capacity of Two-Sided Straited Roughness," Trans. ASME, J. of Lub. Tech., Paper No. 73-Lub-42.

19. Tallian, T. E., "Pressure and Traction Rippling in Elastohydrodynamic Contact of Rough Surfaces," Trans. ASME, J. of Lub. Tech., Paper No. 73-Lub-18.

20. Greenwood, J. A., and Williamson, J. B. P., "Contact of Nominally Flat Surfaces," Proc. R. Soc. (1966), p. 295 (Series A), 300.

21. Grubin, A. N., and Vinogradova, I. E., " Central Scientific Research Institute for Technology and Mechanical Engineering, Book No. 30," Moscow, 1949, (D.S.I.R. Translation No. 337)

22. Cheng, H. S., " Isothermal Elastohydrodynamic Theory for the Full Range of Pressure-Viscosity Coefficient," NASA CR-1929 (September 1971).

23. Cheng, H. S., and Sternlicht, B., " A Numerical Solution for the Pressure, Temperature, Film Thickness Between Two Infinitely Long Lubricated Rolling and Sliding Cylinders, Under Heavy Loads," ASME Transaction, Journal of Basic Engineering, Vol.87, 1965, pp.695-707.

24. Dowson, D., and Whitaker, A. V., " A Numerical Procedure for the Solution of Elastohydrodynamic Problem of Rolling and Sliding Contacts Lubricated by Newtonian Fluid," Proceeding of the Institute of Mechanical Engineers, Vol. 180, Part 3, Series B, 1965, pp. 57-71.

25. Castelli, V., and Pirvics, J., "Equilibrium Characteristics of Axial Groove Gas Lubricated Bearings," Trans. ASME, J. of Lub. Tech., Vol. 89, Ser. F, No. 2 (April 1967), pp. 177-196.

APPENDIX A

Justification of M as a Random Quantity of Zero (or Negligible) Variance

When $\frac{\partial h}{\partial t}$ is assumed to be zero, Eq. (2.6) becomes

$$\frac{\partial M}{\partial x} = 0 \tag{A.1}$$

where M is defined by Eqs. (2.7) and (2.10). Hence M is a constant of x. However, this constant can be a stochastic quantity in the time domain.

EHD Contact

Re-arrange Eq. (2.10) to obtain

$$\frac{1}{12\mu_s} \frac{\partial q}{\partial x} = \frac{M}{h_T^3} - \frac{u_1 + u_2}{2} \frac{h}{h_T^3} + \frac{u_1 - u_2}{2}\left(\frac{\delta_1 - \delta_2}{h_T^3}\right) \tag{A.2}$$

At $x = -\infty$, the asperity effect is negligible so that $q = p = 0$. However, the pressure p, must reach a significant fraction of the Hertzian maximum at $x = -1$, such that $e^{-\alpha p} \ll 1$, i.e. $q \approx \frac{1}{\alpha}$. Therefore q at $x = -1$, can be assumed to be a stochastic variable with extremely small variance. Integrate Eq. (A.2) from $x = -\infty$ to -1, and obtain

$$\frac{1}{12\mu_s\alpha} = \int_{-\infty}^{-1} \frac{M}{h_T^3}\, dx - \frac{u_1 + u_2}{2} \int_{-\infty}^{-1} \frac{h}{h_T^3}\, dx + \frac{u_1 - u_2}{2} \int_{-\infty}^{-1} \frac{\delta_1 - \delta_2}{h_T^3}\, dx \tag{A.3}$$

As M is a constant of x, Eq. (A.3) can be re-written as

$$M = \frac{\frac{1}{12\mu_s} \cdot \frac{1}{\alpha} + \frac{u_1}{2} \int_{-\infty}^{-1} \frac{h - \delta_1 + \delta_2}{h_T^3}\, dx + \frac{u_2}{2} \int_{-\infty}^{-1} \frac{h + \delta_1 - \delta_2}{h_T^3}\, dx}{\int_{-\infty}^{-1} \frac{1}{h_T^3}\, dx} \tag{A.4}$$

When there are enough asperities within the contact zone, the integrals in Eq. (A.4) are independent of the precise arrangement of the roughness and also independent on time. Therefore M can be assumed to be a stochastic quantity with zero (or negligible) variance.

Rigid Rollers

Eq. (2.7) can be re-written as

$$\frac{1}{12\mu}\frac{dp}{dx} = \frac{M}{h_T^3} - \frac{u_1 + u_2}{2}\frac{h}{h_T^3} + \frac{u_1 - u_2}{2}\left(\frac{\delta_1 - \delta_2}{h_T^3}\right) \tag{A.5}$$

Integrate Eq. (A.5) with the boundary conditions:

$$\begin{aligned} p &= 0 && \text{at} \quad x = -\infty \\ p &= \frac{dp}{dx} = 0 && \text{at} \quad x = x^* \end{aligned} \tag{A.6}$$

one obtains

$$M = \frac{\dfrac{u_1}{2}\displaystyle\int_{-\infty}^{x^*} \frac{h - \delta_1 + \delta_2}{h_T^3}\,dx + \dfrac{u_2}{2}\displaystyle\int_{-\infty}^{x^*} \frac{h + \delta_1 - \delta_2}{h_T^3}\,dx}{\displaystyle\int_{-\infty}^{x^*} \frac{1}{h_T^3}\,dx} \tag{A.7}$$

Even though x^* is a random quantity, its deviation from the mean is expected to be of the same order of the wavelength of the asperity, and is small compared with the size of the bearings. The integrals in Eq. (A.7) are only slightly affected by x^*, and therefore can be considered as stochastic quantities with negligible variances. Thus, M is also a stochastic quantity with negligible variance.

Infinitely-Wide Slider

Integrate Eq. (A.5) with the boundary conditions:

$$p = 0 \qquad \text{at} \qquad x = 0 \quad \text{and } L \tag{A.8}$$

one obtains

$$M = \frac{\dfrac{u_1}{2}\displaystyle\int_o^L \frac{h - \delta_1 + \delta_2}{h_T^3}\,dx}{\displaystyle\int_o^L \frac{1}{h_T^3}\,dx} \tag{A.9}$$

Following the above argument, M is also a stochastic quantity with zero (or negligible) variance.

APPENDIX B

FORTRAN IV LISTINGS OF COMPUTER PROGRAMS

1. PROGRAM ROLSLIP: This program which is used in Chapters II and III, is to calculate the integrated pressure at the inlet of an EHD contact with random surface roughness by the stochastic approach.

2. PROGRAM RIGROL7: This program which is used in Chapter II, is to compute the load of a rigid roller bearing with random surface roughness by stochastic approach.

3. PROGRAM SLIDER5: This program which is used in Chapter II, is to compute the load of an infinitely-wide slider bearing with random surface roughness by stochastic approach.

4. PROGRAM DAPOL2: This program which is used in Chapters II and III, is to generate data for functions G_2, G_4 and G_5 for the corresponding σ/h_o. These data are input to programs ROLSLIP, RIGROL7 and SLIDER5. The data for functions G_2, G_4 and G_5 in the case when the asperity height distribution functions are in the form of polynominal function as well as sinusoidal function are tabulated respectively.

5. PROGRAM ROLWAV1: This program which is used in Chapter III, is to compute the integrated pressure at the inlet of an EHD contact with waviness surface roughness by the deterministic approach.

6. PROGRAM ASPERITY: This program which is used in Chapter IV, is to compute the perturbed pressure distribution due to a single 3D-Rigid Asperity.

```
      PROGRAM ROLSLIP(INPUT,OUTPUT)
C THIS PROGRAM IS TO CALCULATE THE INTEGRATED PRESSURE AT THE INLET OF AN  EHD
C    CONTACT BY THE STOCHASTIC APPROACH
C THIS PROGRAM CONSISTS OF FIVE SUBROUTINES
C 1 - SUBROUTINE GRUBIN   IS TO CALCULATE THE INLET INTEGRATED PRESSURE OF AN
C   EHD CONTACT BY SMOOTH FILM GRUBIN THEORY
C 2 - SUBROUTINE CONS    IS TO CALCULATE THE CONSTANT  C  FOR VARIOUS DSIG DATA
C 3 - SUBROUTINE FUNC    IS TO EVALUATE FUNCTIONS  F1 AND F2  FOR DIFFERENT  S/H
C 4 - SUBROUTINE TABLE    IS TO SET UP FUNCTIONS F1 AND F2 IN THE FORM OF ARRAYS
C 5 - SUBROUTINE INT   IS AN INTEGRATION ROUTINE TO CALCULATE THE INTEGRATED
C   PRESSURES WLOAD1, WLOAD2, AND WLOAD3
C
C THE PRESSURE IS INTEGRARED FROM  X=-5 TO X=-1.  BECAUSE OF THE NONLINEAR
C   PROPERTY OF THE INTEGRAND NEAR  X=-1, THE INTERVAL OF INTEGRATION IS DIVIDED
C   INTO TWO PARTS, I.E. FROM  X=-5 TO X=-2, AND FROM  X=-2 TO X=-1.
C
C DATA CARD NO. 1
C   KF = TOTAL NO. OF GRIDS
C   KM = GRID NO. AT  X=-2
C   NSIG = NO. OF DSIG(I) DATA
C   NHO = NUMBER OF  HO  DATA
C DATA CARD NO. 2
C   W = LOAD PER UNIT WIDTH
C   SLIP = SLIPPAGE COEFFICIENT
C   PI = 3.141593
C DATA CARD NO. 3
C   DSIG(I) =  DATA FOR  SIGMA/HO
C  DATA CARD NO. 4
C   DHO(I) = VARIOUS  HO  DATA
C DATA CARD NO. 5
C   THESE DATA ARE THE OUTPUT FROM PROGRAM SUCHAS PROGRAM DATPOL2 WHICH EVALUATE
C     THE INTEGRAL OF    ( DISTRIBUTION FUNCTION*HSS)/(1.+SH*HSS)**3  AND
C     (DISTRIBUTION FUNCTION/(1.+SH*HSS)**3
C   THIS DISTRIBUTION FUNCTION CAN BE POLYNOMIAL ,GAUSSIAN, SINUSOIDAL OR ANY
C     OTHER FUNCTION
C   DSH(I) = THE ABSCISSA RANGING FROM  0 TO 0.333
C   DV(I) = THE NONDIMENSIONAL  DSH(I)
C   DG4(I) = THE INTEGRAL OF  35/96*(1.-HSS**2/9)**3/(1+SH*HSS)**3*HSS
C     IN THE CASE OF  POLYNOMIAL DISTRIBUTION
C   DG2(I) = THE INTEGRAL OF  35/96*(1.-HSS**2/9)**3/(1+SH*HSS)**3
C     IN THE CASE OF  POLYNOMIAL DISTRIBUTION
C   DG5(I) = DG2(I)/DG4(I)
C
C THE OUTPUT OF THIS PROGRAM  WGRUB, WLOAD1, WLOAD2, WLOAD3, W1, W2, W3  ARE ALL
C   INTEGRATED PRESSURE AT THE INLET
C
C
      COMMON WLOAD1(14),WLOAD2(14),WLOAD3(14),DSIG(14),T1(14,301),
     1 T2(14,301),XX(301),KK,KF,KM,NF,HO,W,PI,S,X,F1,F2,C,SLIP,
     2 G(301),F,WGRUB(14),DG4(201),DG2(201)
      DIMENSION Q1(14,301),Q2(14,301),Q3(14,301),DSH(201),DV(201) ,
     C DG5(201), DHO(14), W1(14), W2(14), W3(14)
C
```

```
      PRINT 1
      READ  2,KF,KM,NSIG,NHO
      READ  3,W,SLIP,PI
      READ  3,(DSIG(I),I=1,NSIG)
      READ  3,(DHO(I),I=1,NHO)
      DO 100 I=1,201
 100  READ  5,DSH(I),DV(I),DG4(I),DG5(I),DG2(I)
      PRINT 51
      PRINT 2, KF, KM, NSIG, NHO
      PRINT 52
      PRINT 4,W,SLIP,PI
      PRINT 53
      PRINT 4,(DSIG(I),I=1,NSIG)
      PRINT 54
      PRINT 4,(DHO(I),I=1,NHO)
      XX(1) = -5.
      DO 98  I=2,KM
 98   XX(I) = XX(I-1) + 0.015
      KMM = KM + 1
      DO 99  I=KMM,KF
 99   XX(I) = XX(I-1) + 0.01
      PRINT  56
      DO 97  I=1,NHO
      IGRUB = I
      HO = DHO(I)
      CALL  GRUBIN(IGRUB)
 97   PRINT 7,I,DHO(I),WGRUB(I)
      DO 101 LL =1,NSIG
      PRINT 55,DSIG(LL)
      PRINT 6
      CALL CONS(LL)
      DO 103 I=1,NHO
      KK = I
      HO = DHO(KK)
      S = DSIG(LL) * HO
      CALL TABLE
      CALL INT
      W1(I) = WLOAD1(I) / WGRUB(I)
      W2(I) = WLOAD2(I) / WGRUB(I)
      W3(I) = WLOAD3(I) / WGRUB(I)
      PRINT 7,I,DHO(I),WLOAD1(I),WLOAD2(I),WLOAD3(I),W1(I),W2(I),W3(I) ,
     7 WGRUB(I)
 103  CONTINUE
 101  CONTINUE
C
 1    FORMAT(1H1)
 2    FORMAT(20I5)
 3    FORMAT(8F10.8)
 4    FORMAT(9(2X,E13.6))
 5    FORMAT(F10.6,F10.2,3F20.10)
 6    FORMAT(/3X,*I*,6X,*DHO*,9X,*WLOAD1*,9X,*WLOAD2*,9X,*WLOAD3*,13X,
     6 *W1*,13X,*W2*,13X,*W3*,10X,*WGRUB*)
```

```
7       FORMAT(I5,8(2X,E13.6))
51      FORMAT(/3X,*KF*,3X,*KM*,X,*NSIG*,2X,*NHO*)
52      FORMAT(/7X,*W*,11X,*SLIP*,13X,*PI*)
53      FORMAT(/6X,*DSIG(I)*)
54      FORMAT(/6X,*DHO(I)*)
55      FORMAT(///6X,*DSIG=*,F10.6/)
56      FORMAT(/3X,*I*,6X,*DHO*,9X,*WGRUB*)
        STOP
        END
```

```
        SUBROUTINE  GRUBIN(IGRUB)
        COMMON WLOAD1(14),WLOAD2(14),WLOAD3(14),DSIG(14),T1(14,301),
       1 T2(14,301),XX(301),KK,KF,KM,NF,HO,W,PI,S,X,F1,F2,C,SLIP,
       2 G(301),F,WGRUB(14),DG4(201),DG2(201)
        DIMENSION  F3(301)
C
        DO 400  J=1,KF
        X = XX(J)
        H=HO+4.*W/PI*(ABS(X)*SQRT(ABS((-X)**2-1.0))-ALOG(ABS(X)+SQRT(ABS
       1 ((-X)**2-1.0))))
400     F3(J) = (H-HO) / H**3
        WGRUB(IGRUB) = 0.
        KMK = KM - 2
        DO 401 J =1,KMK,2
401     WGRUB(IGRUB)=WGRUB(IGRUB)+ 0.015/3.*(F3(J)+4.*F3(J+1)+F3(J+2))
        KFF = KF - 2
        DO 402  J=KM,KFF,2
402     WGRUB(IGRUB)=WGRUB(IGRUB)+ 0.01 /3.*(F3(J)+4.*F3(J+1)+F3(J+2))
        RETURN
        END
```

```
        SUBROUTINE  CONS(LL)
        COMMON WLOAD1(14),WLOAD2(14),WLOAD3(14),DSIG(14),T1(14,301),
       1 T2(14,301),XX(301),KK,KF,KM,NF,HO,W,PI,S,X,F1,F2,C,SLIP,
       2 G(301),F,WGRUB(14),DG4(201),DG2(201)
C
        V = 1. + DSIG(LL) / 0.001665
        MV = V
        VM = MV
        G2 = (DG2(MV+1) - DG2(MV)) * (V-VM) + DG2(MV)
        G4 = (DG4(MV+1) - DG4(MV)) * (V-VM) + DG4(MV)
        C = G4 / G2
        RETURN
        END
```

```
        SUBROUTINE TABLE
        COMMON WLOAD1(14),WLOAD2(14),WLOAD3(14),DSIG(14),T1(14,301),
       1 T2(14,301),XX(301),KK,KF,KM,NF,HO,W,PI,S,X,F1,F2,C,SLIP,
       2 G(301),F,WGRUB(14),DG4(201),DG2(201)
        DO 201 J=1,KF
        X = XX(J)
        CALL FUNC
        T1(KK,J) = F1
        T2(KK,J) = F2
201     CONTINUE
        RETURN
        END
```

```
      SUBROUTINE FUNC
C
      COMMON WLOAD1(14),WLOAD2(14),WLOAD3(14),DSIG(14),T1(14,301),
     1 T2(14,301),XX(301),KK,KF,KM,NF,HO,W,PI,S,X,F1,F2,C,SLIP,
     2 G(301),F,WGRUB(14),DG4(201),DG2(201)
C
      H=HO+4.*W/PI*(ABS(X)*SQRT(ABS((-X)**2-1.0))-ALOG(ABS(X)+SQRT(ABS
     1 ((-X)**2-1.0))))
      SH = S / H
      V = 1. + S/H/0.001665
      MV = V
      VM = MV
      G2 = (DG2(MV+1) - DG2(MV)) * (V-VM) + DG2(MV)
      G4 = (DG4(MV+1) - DG4(MV)) * (V-VM) + DG4(MV)
      F1 = (H-HO)/H**3*G2
      F2 = (G4 - C*G2) / H**3*S
      RETURN
      END
      SUBROUTINE INT
C
      COMMON WLOAD1(14),WLOAD2(14),WLOAD3(14),DSIG(14),T1(14,301),
     1 T2(14,301),XX(301),KK,KF,KM,NF,HO,W,PI,S,X,F1,F2,C,SLIP,
     2 G(301),F,WGRUB(14),DG4(201),DG2(201)
      DIMENSION P1(14),P2(14)
C
      P1(KK) = 0.
      P2(KK) = 0.
      KMK = KM-2
      DO 301 J=1,KMK,2
      P1(KK) = P1(KK) + 0.015/3.*(T1(KK,J)+4.*T1(KK,J+1)+T1(KK,J+2))
      P2(KK) = P2(KK) + 0.015/3.*(T2(KK,J)+4.*T2(KK,J+1)+T2(KK,J+2))
301   CONTINUE
      KFF = KF-2
      DO 302 J=KM,KFF,2
      P1(KK) = P1(KK) + 0.01/3.*(T1(KK,J)+4.*T1(KK,J+1)+T1(KK,J+2))
      P2(KK) = P2(KK) + 0.01/3.*(T2(KK,J)+4.*T2(KK,J+1)+T2(KK,J+2))
302   CONTINUE
      WLOAD1(KK) = P1(KK) - P2(KK)*SLIP
      WLOAD2(KK) = P1(KK) + P2(KK)*SLIP
      WLOAD3(KK) = P1(KK)
C
      RETURN
      END
00000000000000000000000  END OF RECORD
  301  201     9     6
 0.00003   0.1       3.14159265
 0.05      0.1       0.15      0.2       0.25      0.3       0.31      0.32
 0.33
 0.00001   0.00002   0.00003   0.00005   0.00007   0.00009
C   DATA FOR  DSH(I), DV(I), DG4(I), 4G2(I), DG5(I)   ARE OMITTED
000000000000000000000000END OF INFORMATION
```

```
      PROGRAM RIGROL7(INPUT,OUTPUT)
C
C THIS PROGRAM IS TO COMPUTE THE LOAD OF A RIGID ROLLER BEARING BY STOCHASTIC
C    APPROACH
C
C THIS PROGRAM CONSISTS OF  4  SUBROUTINES
C 1 - SUBROUTINE TABLE   IS TO SET UP A PRESSURE ARRAY CORRESPONDING TO THE GRID
C    POSITIONS
C 2 - SUBROUTINE CONS   IS TO CALCULATE THE CONSTANT  C
C 3 - SUBROUTINE FUNC   IS TO EVALUATE FUNCTIONS  F1, F2, AND  F
C 4 - SUBROUTINE INT  IS A SIMPSON INTEGRATION ROUTINE TO COMPUTE THE LOAD W(KK)
C THE OUTPUT OF THIS PROGRAM IS  W(I)  AND THE CORRESPONDING DSIG(I)
C
C DATA CARD NO. 1
C    NI = NO. OF UNIFORM GRIDS FROM  X=-1  TO X=0
C    NF = NO. OF UNIFORM GRIDS FROM  X=0  TO X=XA
C KO = NI + 1
C KF = NF + 1
C    ND = NO. OF  DSIG(I)  DATA
C DATA CARD NO. 2
C XA(1).XA(2)  INITIAL VALUES ASSIGNED TO XA(I),  ASSUMING THAT THE PRESSURE AT
C    THIS LOCATION IS  0.
C    HO = CENTER FILM THICKNESS
C    SLIP = SLIPPAGE COEFFICIENT
C    PI = 3.141593
C DATA CARD NO. 3
C    DSIG(I) = SIGMA / HO , DATA
C DATA CARD NO. 4
C    THESE DATA ARE THE OUTPUT FROM PROGRAM SUCHAS PROGRAM DATPOL2 WHICH EVALUATE
C       THE INTEGRAL OF   ( DISTRIBUTION FUNCTION*HSS)/(1.+SH*HSS)**3  AND
C       (DISTRIBUTION FUNCTION/(1.+SH*HSS)**3
C    THIS DISTRIBUTION FUNCTION CAN BE POLYNOMIAL ,GAUSSIAN, SINUSOIDAL OR ANY
C       OTHER FUNCTION
C    DSH(I) = THE ABSCISSA RANGING FROM  0 TO 0.333
C    DV(I) = THE NONDIMENSIONAL  DSH(I)
C    DG4(I) = THE INTEGRAL OF  35/96*(1.-HSS**2/9)**3/(1+SH*HSS)**3*HSS
C       IN THE CASE OF  POLYNOMIAL DISTRIBUTION
C    DG2(I) = THE INTEGRAL OF  35/96*(1.-HSS**2/9)**3/(1+SH*HSS)**3
C       IN THE CASE OF  POLYNOMIAL DISTRIBUTION
C    DG5(I) = DG2(I)/DG4(I)
C
      COMMON XX(121),P(20,121),DSIG(10),W(10),HO,HA,KO,KF,K,KK,SO,SF,X,
     C F,F1,F2,DELA,PI,C,DG4(201),DG2(201),SLIP
      DIMENSION XA(21),DSH(201),DV(201),DG5(201),XB(10),IK(10)
C
      PRINT 1
      READ  2,NI,NF,KO,KF,ND
      READ  4,XA(1),XA(2),HO,SLIP,PI
      READ  4,(DSIG(I),I=1,ND)
      DO 95 I=1,201
95    READ  5,DSH(I),DV(I),DG4(I),DG5(I),DG2(I)
      PRINT 51
      PRINT 2,NI,NF,KO,KF,ND
```

```
      PRINT 52
      PRINT 9,XA(1),XA(2),HO,SLIP,PI
      PRINT 53
      PRINT 9,(DSIG(I),I=1,ND)
      SO = 1./NI
      DO 99 J=1,KO
99    XX(J) = -1. + (J-1)*SO
      DO 100 II=1,ND
      KK = II
      PRINT 6,II,DSIG(II)
      XA(1) = 0.01
      XA(2) = 0.02
      DO 101 I=1,2
      K = I
      HA = 1. + 0.5*XA(I)**2/HC
      SF = XA(I) / NF
      PRINT 54
      PRINT 3,I,XA(I),HA,SO,SF
      CALL CONS
      CALL TABLE
101   CONTINUE
      XA(3) = (XA(1)*P(2,KF) - XA(2)*P(1,KF)) / (P(2,KF) - P(1,KF))
      DO 102 I=3,20
      K = I
      HA = 1. + 0.5*XA(I)**2/HC
      SF = XA(I) / NF
      PRINT 54
      PRINT 3,I,XA(I),HA,SO,SF
      CALL CONS
      CALL TABLE
      DIFF = P(I,KF) / P(I,KO)
      IF (ABS(DIFF) .LE. 0.001 ) GO TO 103
      PROD = P(I,KF)*P(I-1,KF)
      IF (PROD .GE. 0.) GO TO 104
      XA(I+1)= (XA(I-1)*P(I,KF)-XA(I)*P(I-1,KF))/(P(I,KF)-P(I-1,KF))
      GO TO 102
104   CONTINUE
      P(I-1,KF) = P(I-2,KF)
      XA(I-1) = XA(I-2)
      XA(I+1)= (XA(I-1)*P(I,KF)-XA(I)*P(I-1,KF))/(P(I,KF)-P(I-1,KF))
102   CONTINUE
103   CONTINUE
      CALL INT
      XB(II) = XA(K)
      IK(II) = K
100   CONTINUE
      PRINT 7
      DO 105 II=1,ND
105   PRINT 8,II,DSIG(II),W(II),XB(II),IK(II)
C
1     FORMAT(1H1)
2     FORMAT(20I5)
3     FORMAT(I5,8(2X,E13.6))
4     FORMAT(8F10.8)
```

```
5       FORMAT(F10.6,F10.2,3F20.10)
6       FORMAT(//////X,*II=*,I4,10X,*DSIG=*,F8.4//)
7       FORMAT(////3X,*II*,10X,*DSIG*,16X,*W*,19X,*XA*,12X,*K*/)
8       FORMAT(I5,3(3X,E17.10),3X,I2)
9       FORMAT(9(2X,E13.6))
51      FORMAT(/3X,*NI*,3X,*NF*,3X,*KO*,3X,*KF*,3X,*ND*)
52      FORMAT(/6X,*XA(1)*,10X,*XA(2)*,13X,*HO*,11X,*SLIP*,13X,*PI*)
53      FORMAT(/6X,*DSIG(I)*)
54      FORMAT(/4X,*I*,6X,*XA(I)*,13X,*HA*,13X,*SO*,13X,*SF*)
C
        RETURN
        END
```

```
        SUBROUTINE TABLE
C
        COMMON XX(121),P(20,121),DSIG(10),W(10),HO,HA,KO,KF,K,KK,SO,SF,X,
      C F,F1,F2,DELA,PI,C,DG4(201),DG2(201),SLIP
        DIMENSION E(121)
C
        PRINT 21
        J = 1
        X = XX(J)
        CALL FUNC
        E(J) = F
        P(K,J) = 0.
        DO 201 J=2,KO
        X = XX(J)
        CALL FUNC
        E(J) = F
        X = (XX(J-1)+XX(J))/2.
        CALL FUNC
        P(K,J) = P(K,J-1) + SO/2./3.*(E(J-1)+4.*F+E(J))
201     CONTINUE
        KO1 = KO + 1
        DO 202 J=KO1,KF
        XX(J) = XX(J-1) + SF
        X = XX(J)
        CALL FUNC
        E(J) = F
        X = (XX(J-1)+XX(J))/2.
        CALL FUNC
        P(K,J) = P(K,J-1) + SF/2./3.*(E(J-1)+4.*F+E(J))
202     CONTINUE
        DO 203 J=1,KO,4
203     PRINT 22,J,XX(J),P(K,J)
        DO 204  J=KO1,KF,2
204     PRINT 22,J,XX(J),P(K,J)
C
21      FORMAT(//3X,*J* ,10X,*XX*,18X,*P*/)
22      FORMAT(I5,2(3X,E17.10))
        RETURN
        END
```

```
      SUBROUTINE CONS
      COMMON XX(121),P(20,121),DSIG(10),W(10),HO,HA,KO,KF,K,KK,SO,SF,X,
     C F,F1,F2,DELA,PI,C,DG4(201),DG2(201),SLIP
      V = 1. + DSIG(KK)/HA/0.001665
      MV = V
      VM = MV
      G2 = (DG2(MV+1)-DG2(MV))*(V-VM) + DG2(MV)
      G4 = (DG4(MV+1)-DG4(MV))*(V-VM) + DG4(MV)
      C = G4/G2
      PRINT 41,KK,K,C
41    FORMAT(/3X,*KK*,4X,*K*,10X,*C*/2I5,3X,E17.10/)
      RETURN
      END
```

```
      SUBROUTINE FUNC
      COMMON XX(121),P(20,121),DSIG(10),W(10),HO,HA,KO,KF,K,KK,SO,SF,X,
     C F,F1,F2,DELA,PI,C,DG4(201),DG2(201),SLIP
C
      H = 1. + 0.5*X**2/HO
      V = 1. + DSIG(KK)/H /0.001665
      MV = V
      VM = MV
      G2 = (DG2(MV+1)-DG2(MV))*(V-VM) + DG2(MV)
      G4 = (DG4(MV+1)-DG4(MV))*(V-VM) + DG4(MV)
      F1 = (H-HA)/H**3*G2
      F2 = (G4-C*G2)/H**3
      F = F1 + DSIG(KK) * F2 * SLIP
      RETURN
      END
```

```
      SUBROUTINE INT
      COMMON XX(121),P(20,121),DSIG(10),W(10),HO,HA,KO,KF,K,KK,SO,SF,X,
     C F,F1,F2,DELA,PI,C,DG4(201),DG2(201),SLIP
C
      W(KK) = 0.
      KO2 = KO-2
      DO 301  J = 1, KO2 ,2
      W(KK) = W(KK) + SO/3.*(P(K,J) + 4.*P(K,J+1) + P(K,J+2))
301   CONTINUE
      KFF = KF - 2
      DO 302 J =KO,KFF,2
      W(KK) = W(KK) + SF/3.*(P(K,J) + 4.*P(K,J+1) + P(K,J+2))
302   CONTINUE
      PRINT 31,KK,W(KK)
C
31    FORMAT(////X,*KK=*,I3,10X,*W=*,E17.10//)
      RETURN
      END
```

```
0000000000000000000000  END OF RECORD
  40    10    41    51    10
 0.01        0.02        0.0005     -0.1        3.14159265
  0.06       0.1         0.14        0.18        0.22        0.26        0.3         0.31
 0.32        0.33
C   DATA FOR  DSH(I), DV(I), DG4(I), 4G2(I), DG5(I)  ARE OMITTED
0000000000000000000000  END OF INFORMATION
```

```
      PROGRAM SLIDER5(INPUT,OUTPUT)
C
C THIS PROGRAM IS TO COMPUTE THE LOAD OF AN INFINITELY-WIDE SLIDER BEARING BY
C    STOCHASTIC APPROACH
C
C THIS PROGRAM CONSISTS OF  3  SUBROUTINES
C 1 - SUBROUTINE TABLE   IS TO FORM THE  T1, T2, T3 ARRAYS WHICH WILL BE USED TO
C    COMPUTE THE PRESSURE PROFILE
C 2 - SUBROUTINE FUNC    IS TO EVALUATE THE FUNCTIONS  F1, F2 AND F3
C 3 - SUBROUTINE INT    IS THE INTEGRATION ROUTINE TO CALCULATE THE PRESSURE
C    PROFILE AND THEN THE TOTAL LOAD
C THE OUTPUT OF THIS PROGRAM ARE  WLOAD1 , WLOAD2 , WLOAD3 AND THE CORRESPONDING
C    DSIG(I)
C      WLOAD1 = LOAD IN SLIDING ROUGH SURFACE,FIXED SMOOTH SURFACE CASE
C      WLOAD2 = LOAD IN FIXED ROUGH SURFACE,SLIDING SMOOTH SURFACE CASE
C      WLOAD3 = LOAD IN BOTH SURFACES WITH SAME ROUGHNESS DISTRIBUTION
C
C DATA CARD NO. 1
C    KF = TOTAL NO. OF GRID POINTS
C    NF = NO. OF DSIG(I) DATA
C    PI = 3.141593
C DATA CARD NO. 2
C    DSIG(I) = DATA FOR  SIGMA / H(MIN) RATIO
C DATA CARD NO.3
C    THESE DATA ARE THE OUTPUT FROM PROGRAM SUCHAS PROGRAM DATPOL2 WHICH EVALUATE
C      THE INTEGRAL OF    ( DISTRIBUTION FUNCTION*HSS)/(1.+SH*HSS)**3  AND
C      (DISTRIBUTION FUNCTION/(1.+SH*HSS)**3
C    THIS DISTRIBUTION FUNCTION CAN BE POLYNOMIAL ,GAUSSIAN, SINUSOIDAL OR ANY
C      OTHER FUNCTION
C    DSH(I) = THE ABSCISSA RANGING FROM  0 TO 0.333
C    DV(I) = THE NONDIMENSIONAL  DSH(I)
C    DG4(I) = THE INTEGRAL OF  35/96*(1.-HSS**2/9)**3/(1+SH*HSS)**3*HSS
C      IN THE CASE OF  POLYNOMIAL DISTRIBUTION
C    DG2(I) = THE INTEGRAL OF  35/96*(1.-HSS**2/9)**3/(1+SH*HSS)**3
C      IN THE CASE OF  POLYNOMIAL DISTRIBUTION
C    DG5(I) = DG2(I)/DG4(I)
C
C
      COMMON DSH(201),DV(201),DG4(201),DG5(201),DG2(201),WLOAD1(14),
     1 WLOAD2(14),WLOAD3(14),DSIG(14),T1(14,101),T2(14,101),T3(14,101),
     2 KK,KF,NF,S,X,F1,F2,F3,C1,C2,C3,PI,XX(101)
      PRINT 1
      READ  2,KF,NF,PI
      PRINT 2,KF,NF,PI
      READ 3,(DSIG(I),I=1,NF)
      PRINT 4,(DSIG(I),I=1,NF)
      DO 100 I=1,201
100   READ  5,DSH(I),DV(I),DG4(I),DG5(I),DG2(I)
      DO 99  J=1,KF
99    XX(J) = (J-1)*0.01
      WREF = ALOG(2.) - 2./3.
```

```
      DO 101 I=1,NF
      KK = I
      S = DSIG(KK)
      CALL TABLE
      C1 = (-T1(KK,KF) + S*T3(KK,KF)) / T2(KK,KF)
      C2 = (-T1(KK,KF) -S*T3(KK,KF)) / T2(KK,KF)
      C3 = -T1(KK,KF) / T2(KK,KF)
      CALL INT
101   CONTINUE
      PRINT 6,WREF
      DO 102 I=1,NF
      PRINT 7,I,DSIG(I),WLOAD1(I),WLOAD2(I),WLOAD3(I)
102   CONTINUE
C
1     FORMAT(1H1/2X,*KF*,3X,*NF*,10X,*PI*/)
2     FORMAT(2I5,F20.14)
3     FORMAT(20F5.3)
4     FORMAT(X,*(DSIG(I),I=1,NF)*,5X,20(X,F5.3)/)
5     FORMAT(F10.6,F10.2,3F20.10)
6     FORMAT(///X,*WREF=*,E17.10/3X,*I*,6X,*DSIG*,12X,*WLOAD1*,14X,
     6 *WLOAD2*,14X,*WLOAD3*/)
7     FORMAT(I5,5X,F5.3,5(3X,E17.10))
      STOP
      END
```

```
      SUBROUTINE TABLE
C
      COMMON DSH(201),DV(201),DG4(201),DG5(201),DG2(201),WLOAD1(14),
     1 WLOAD2(14),WLOAD3(14),DSIG(14),T1(14,101),T2(14,101),T3(14,101),
     2 KK,KF,NF,S,X,F1,F2,F3,C1,C2,C3,PI,XX(101)
C
      DIMENSION  E1(101),E2(101),E3(101)
      J = 1
      X = XX(J)
      CALL FUNC
      E1(J) = F1
      E2(J) = F2
      E3(J) = F3
      T1(KK,J) = 0.
      T2(KK,J) = 0.
      T3(KK,J) = 0.
      DO 201 J =2,KF
      X = XX(J)
      CALL FUNC
      E1(J) = F1
      E2(J) = F2
      E3(J) = F3
      X = (XX(J-1)+XX(J))/2.
      CALL FUNC
      T1(KK,J) = T1(KK,J-1) + 0.01/2./3.*(E1(J-1) + 4.*F1 + E1(J))
      T2(KK,J) = T2(KK,J-1) + 0.01/2./3.*(E2(J-1) + 4.*F2 + E2(J))
      T3(KK,J) = T3(KK,J-1) + 0.01/2./3.*(E3(J-1) + 4.*F3 + E3(J))
201   CONTINUE
      RETURN
      END
```

```
      SUBROUTINE FUNC
      COMMON DSH(201),DV(201),DG4(201),DG5(201),DG2(201),WLOAD1(14),
     1 WLOAD2(14),WLOAD3(14),DSIG(14),T1(14,101),T2(14,101),T3(14,101),
     2 KK,KF,NF,S,X,F1,F2,F3,C1,C2,C3,PI,XX(101)
      H = 2. - X
      SH = S/H
      V = 1.+SH/0.001665
      MV = V
      VM = MV
      D2 = (ALOG(DG2(MV+1))-ALOG(DG2(MV))) * (V-VM) + ALOG(DG2(MV))
      G2 = EXP(D2)
      D4 = (ALOG(-DG4(MV+1))-ALOG(-DG4(MV)))*(V-VM) + ALOG(- DG4(MV))
      G4 = -EXP(D4)
      F1 = G2/H**2
      F2 = G2/H**3
      F3 = G4/H**3
      RETURN
       END
```

```
      SUBROUTINE INT
      COMMON DSH(201),DV(201),DG4(201),DG5(201),DG2(201),WLOAD1(14),
     1 WLOAD2(14),WLOAD3(14),DSIG(14),T1(14,101),T2(14,101),T3(14,101),
     2 KK,KF,NF,S,X,F1,F2,F3,C1,C2,C3,PI,XX(101)
      DIMENSION P1(14,101),P2(14,101),P3(14,101)
      PRINT 31,KK,DSIG(KK)
      DO 301 J=1,KF
      P1(KK,J) = T1(KK,J) + C1*T2(KK,J) - S*T3(KK,J)
      P2(KK,J) = T1(KK,J) + C2*T2(KK,J) + S*T3(KK,J)
      P3(KK,J) = T1(KK,J) + C3*T2(KK,J)
      PRINT 32,J,P1(KK,J),P2(KK,J),P3(KK,J)
301   CONTINUE
      WLOAD1(KK) = 0.
      WLOAD2(KK) = 0.
      WLOAD3(KK) = 0.
      KFF = KF-2
      DO 302 J=1,KFF,2
      WLOAD1(KK) = WLOAD1(KK) + 0.01/3.*(P1(KK,J) + 4.*P1(KK,J+1) +
     1 P1(KK,J+2))
      WLOAD2(KK) = WLOAD2(KK) + 0.01/3.*(P2(KK,J) + 4.*P2(KK,J+1) +
     2 P2(KK,J+2))
      WLOAD3(KK) = WLOAD3(KK) + 0.01/3.*(P3(KK,J) + 4.*P3(KK,J+1) +
     3 P3(KK,J+2))
302   CONTINUE
      PRINT 6
      PRINT 7,KK,DSIG(KK),WLOAD1(KK),WLOAD2(KK),WLOAD3(KK)
C
31    FORMAT(/X,*KK=*,I4,5X,*DSIG=*,F7.4//3X,*J*,10X,*P1*,18X,*P2*,18X,
     C *P3*/)
32    FORMAT(I5,3(3X,E17.10))
6     FORMAT(/3X,*I*,6X,*DSIG*,12X,*WLOAD1*,14X,*WLOAD2*,14X,*WLOAD3*/)
7     FORMAT(I5,5X,F5.3,5(3X,E17.10))
C
      RETURN
      END
```

```
00000000000000000000000.0  END OF RECORD
  101    10    3.14159265359
 0.06 0.1 0.14 0.18 0.22 0.26 0.3  0.31 0.32 0.33
C   DATA FOR  DSH(I), DV(I), DG4(I), 4G2(I), DG5(I)  ARE OMITTED
00000000000000000000000.0  END OF INFORMATION
```

```
      PROGRAM DATPOL2 (INPUT,OUTPUT,PUNCH)
C
C THIS PROGRAM IS TO CALCULATE DATA FOR FUNCTIONS  G2 AND G4  FOR THE CASE WHEN
C   THE ASPERITY HEIGHT DISTRIBUTION FUNCTION IS IN THE FORM OF POLYNOMIAL
C   FUNCTION   35/96*(1-HSS**2/9)**3
C G2 = THE INTEGRAL OF 35/96*(1-HSS**2/9)**3/(1+SH*HSS)**3 FOR HSS = -3 TO 3
C G4 = THE INTEGRAL OF 35/96*(1-HSS**2/9)**3/(1+SH*HSS)**3*HSS FOR HSS = -3 TO 3
C SINCE HSS RANGES FROM  -3 TO 3  , SH  MUST BE LESS THAN  1/3. THUS  SH  VALUES
C   USED IN THIS PROGRAM RANGES FROM  0 TO 0.333
C SH(I), I=1,201,  WITH  200  UNIFORM GRIDS OF SIZE  0.001665
C V(I) = NONDIMENSIONAL  SH(I)
C
C
C THIS PROGRAM CONSISTS OF THREE SUBROUTINES
C 1 - SUBROUTINE MAIN   IS TO CALCULATE  RI1 AND RI2  FROM SUBROUTINES  INT1
C   AND  INT2
C 2 -  SUBROUTINE INT1   IS TO INTEGRATE THE FUNCTION
C       (1.-HSS**2/9.)**3/(1.+SH*HSS)**3*HSS
C 3 - SUBROUTINE INT2   IS TO INTEGRATE THE FUNCTION
C      (1.-HSS**2/9.)**3/(1.+SH*HSS)**3
C
C THE RESULTS OF  G2(I),G4(I), G5(I) TOGETHER WITH THE CORRESPONDING  SH(I),V(I)
C   VALUES  WHICH ARE THE OUTPUT OF THIS PROGRAM ARE IN THE FORM OF DATA CARD
C
C
      COMMON A,B,RI1,RI2,SIMPSON
      DIMENSION G2(201),G4(201),G5(201),V(201),SH(202)
      PRINT 1
      SH(1)=0.0
      DO 10 I=1,201
      CALL MAIN (SH(I))
      G2(I) = 35./96. *RI2
      G4(I) = 35./96. *RI1
      G5(I) = G2(I) /G4(I)
      V(I)=1.0+SH(I)/0.001665
      PRINT 3
      PRINT 4,I,SH(I),V(I),G4(I),G5(I),G2(I)
      SH(I+1)=SH(I)+0.001665
10    CONTINUE
      PRINT 2
      DO 20 I=1,201
      PRINT 5,SH(I),V(I),G4(I),G5(I),G2(I)
      PUNCH 5,SH(I),V(I),G4(I),G5(I),G2(I)
20    CONTINUE
1     FORMAT(1H1)
2     FORMAT(5X,*SH*,8X,*V*,16X,*G4*,18X,*G5*,18X,*G2*/)
3     FORMAT(/2X,*I*,5X,*SH(I)*,5X,*V(I)*,7X,*G4(I)*,15X,*G5(I)*,15X,
     C*G2(I)*/)
4     FORMAT(X,I3,2X,F9.6,2X,F6.1,3(2X,E17.10)/)
5     FORMAT(F10.6,F10.2,3F20.10)
      STOP
      END
```

```
      SUBROUTINE MAIN(SH)
      COMMON A,B,RI1,RI2,SIMPSON
      DIMENSION D(3), E(3), SM(3), SIM(3)
      DATA  (D(I),I=1,2)/-3., -2.8/,(E(I),I=1,2)/-2.8,3./
C
      DO 100  J=1,2
      A=D(J)
      B=E(J)
      CALL INT1(SH)
      SM(J)=SIMPSON
      CALL INT2(SH)
      SIM(J)=SIMPSON
      PRINT 11,J,A,B,SM(J),SIM(J)
100   CONTINUE
      RI1 = SM(1) + SM(2)
      RI2 = SIM(1) + SIM(2)
      PRINT 12,RI1,RI2
C
11    FORMAT(X,*J=*,I1,4X,*A=*,F6.3,4X,*B=*,F6.3,4X,*SM=*,E17.10,4X,
     C*SIM=*,E17.10/)
12    FORMAT(X,*RI1=*,E17.10,5X,*RI2=*,E17.10/)
      RETURN
      END
```

```
      SUBROUTINE INT1(SH)
      COMMON A,B,RI1,RI2,SIMPSON
      PRINT 21
      HSS=A
      FA=(1.0-HSS**2/9.0)**3/(1.0+SH*HSS)**3*HSS
      HSS=B
      FB=(1.0-HSS**2/9.0)**3/(1.0+SH*HSS)**3*HSS
      F1=FA+FB
      F2=0.0
      HSS=(A+B)/2.0
      F4=(1.0-HSS**2/9.0)**3/(1.0+SH*HSS)**3*4.0*HSS
      N=2
      T=(B-A)/N
      SIMPSON=T/3.0*(F1+F2+F4)
      DO 10 K=1,500
      T=(B-A)/N
      TN=T/2.0
      F2=F2+F4/2.0
      F4=0.0
      DO 20 J=1,N
      HSS=A-TN+J*T
      F4=(1.0-HSS**2/9.0)**3/(1.0+SH*HSS)**3*4.0*HSS + F4
20    CONTINUE
      SIMP=SIMPSON
      SIMPSON=TN/3.0*(F1+F2+F4)
      DELTA=ABS((SIMPSON-SIMP)/(SIMPSON+SIMP))
      PRINT 22,N,SIMP,DELTA
      N=2*N
```

```
      IF(DELTA.LE.0.0005) GO TC 26
10    CONTINUE
26    PRINT 22,N,SIMPSON
C
21    FORMAT(4X,*N*,6X,*SIMPSON*,10X,*DELTA*/)
22    FORMAT(X,I4,4X,E17.10,4X,F8.5)
      RETURN
      END
```

```
      SUBROUTINE INT2(SH)
      COMMON A,B,RI1,RI2,SIMPSCN
      PRINT 21
      HSS=A
      FA=(1.0-HSS**2/9.0)**3/(1.0+SH*HSS)**3
      HSS=B
      FB=(1.0-HSS**2/9.0)**3/(1.0+SH*HSS)**3
      F1=FA+FB
      F2=0.0
      HSS=(A+B)/2.0
      F4=(1.0-HSS**2/9.0)**3/(1.0+SH*HSS)**3*4.0
      N=2
      T=(B-A)/N
      SIMPSON=T/3.0*(F1+F2+F4)
      DC 10 K=1,500
      T=(B-A)/N
      TN=T/2.0
      F2=F2+F4/2.0
      F4=0.0
      DO 20 J=1,N
      HSS=A-TN+J*T
      F4=(1.0-HSS**2/9.0)**3/(1.0+SH*HSS)**3*4.0+F4
20    CONTINUE
      SIMP=SIMPSON
      SIMPSON=TN/3.0*(F1+F2+F4)
      DELTA=ABS((SIMPSON-SIMP)/(SIMPSON+SIMP))
      PRINT 22,N,SIMP,DELTA
      N=2*N
      IF(DELTA.LE.0.0005) GO TC 26
10    CONTINUE
26    PRINT 22,N,SIMPSON
C
21    FORMAT(4X,*N*,6X,*SIMPSON*,10X,*DELTA*/)
22    FORMAT(X,I4,4X,E17.10,4X,F8.5)
      RETURN
      END
0000000000000000000000  END OF RECORD
0000000000000000000000  END OF INFORMATION
```

Data for G_2, G_4 and G_5 with polynomial distribution of the asperity height.

SH $= \bar{\sigma}/H$

V = non-dimensional SH

$$G_2 = \int_{-\infty}^{\infty} \frac{g(\delta^*)}{\left[1 + \delta^*(\bar{\sigma}/H)\right]^3} \, d\delta^*$$

$$G_4 = \int_{-\infty}^{\infty} \frac{\delta^* g(\delta^*)}{\left[1 + \delta^*(\sigma/H)\right]^3} \, d\delta^*$$

$$G_5 = G_2/G_4$$

$$g(\delta^*) = \begin{cases} \frac{35}{96}\left(1 - \frac{\delta^{*2}}{9}\right)^3 & -3 \le \delta^* \le 3 \\ 0 & \text{elsewhere} \end{cases}$$

SH	V	G4	G5	G2
0.000000	1.00	.0000000008	*73508622.8972244263	.9999937040
.001665	2.00	-.0049951360	-200.1968247935	1.0000103701
.003330	3.00	-.0099912933	-100.0931790408	1.0000603055
.004995	4.00	-.0149884332	-66.7276896773	1.0001435203
.006660	5.00	-.0199876140	-50.0439939147	1.0002600317
.008325	6.00	-.0249895170	-40.0331812483	1.0004098635
.009990	7.00	-.0299948249	-33.3588560485	1.0005930462
.011655	8.00	-.0350042216	-28.5911118930	1.0008096174
.013320	9.00	-.0400183928	-25.0149881471	1.0010596214
.014985	10.00	-.0450380259	-22.2332815146	1.0013431094
.016650	11.00	-.0500638108	-20.0076686839	1.0016601395
.018315	12.00	-.0550964396	-18.1864886970	1.0020107769
.019980	13.00	-.0601366075	-16.6686338844	1.0023950934
.021645	14.00	-.0651850124	-15.3841064170	1.0028131682
.023310	15.00	-.0702461021	-14.2821460160	1.0032650874
.024975	16.00	-.0753129297	-13.3277373168	1.0037509442
.026640	17.00	-.0803901121	-12.4924672077	1.0042708389
.028305	18.00	-.0854783624	-11.7553127078	1.0048248792
.029970	19.00	-.0905783984	-11.0999222553	1.0054131799
.031635	20.00	-.0956909428	-10.5133864718	1.0060358632
.033300	21.00	-.1008167234	-9.9853776741	1.0066930586
.034965	22.00	-.1059564734	-9.5075352232	1.0073849032
.036630	23.00	-.1111109320	-9.0730184962	1.0081115416
.038295	24.00	-.1162808444	-8.6761764664	1.0088731260
.039960	25.00	-.1214669623	-8.3122998848	1.0096698164
.041625	26.00	-.1266700439	-7.9774329347	1.0105017804
.043290	27.00	-.1318908551	-7.6682283475	1.0113691938
.044955	28.00	-.1371301688	-7.3818347149	1.0122722402
.046620	29.00	-.1423887658	-7.1158079458	1.0132111113
.048285	30.00	-.1476674354	-6.8680410430	1.0141860071

.049950	31.00	-.1529669751	-5.6367079229	1.0151971358
.051615	32.00	-.1582881916	-6.4202181087	1.0162447141
.053280	33.00	-.1636319007	-6.2171799186	1.0173289673
.054945	34.00	-.1689989282	-6.0263703463	1.0184501295
.056610	35.00	-.1743901098	-5.8467102566	1.0196084435
.058275	36.00	-.1798062917	-5.6772438332	1.0208041609
.059940	37.00	-.1852483314	-5.5171214518	1.0220375429
.061605	38.00	-.1907170973	-5.3655853297	1.0233088596
.063270	39.00	-.1962134701	-5.2215363317	1.0245357631
.064935	40.00	-.2017383425	-5.0802341398	1.0248780151
.066600	41.00	-.2072926201	-4.9508585771	1.0262764462
.068265	42.00	-.2128772216	-4.8277327210	1.0277143282
.069930	43.00	-.2184930795	-4.7104100548	1.0291919985
.071595	44.00	-.2241411406	-4.6027585049	1.0316675410
.073260	45.00	-.2298223663	-4.4957019781	1.0332128666
.074925	46.00	-.2355377334	-4.3933455139	1.0347986442
.076590	47.00	-.2412882345	-4.2953824033	1.0364252365
.078255	48.00	-.2470748786	-4.2015320339	1.0380930172
.079920	49.00	-.2528986917	-4.1115371720	1.0398023717
.081585	50.00	-.2587607174	-4.0251615764	1.0415536970
.083250	51.00	-.2646620173	-3.9421878997	1.0433474022
.084915	52.00	-.2706036722	-3.8624158356	1.0451839087
.086580	53.00	-.2765867821	-3.7856604805	1.0470636503
.088245	54.00	-.2826124672	-3.7117508799	1.0489870739
.089910	55.00	-.2886818687	-3.6405287375	1.0509546391
.091575	56.00	-.2947961494	-3.5718472638	1.0529668195
.093240	57.00	-.3009564942	-3.5055701487	1.0550241022
.094905	58.00	-.3071641114	3.4415706427	1.0571269883
.096570	59.00	-.3134202331	-3.3797307319	1.0592759937
.098235	60.00	-.3197261160	-3.3199403982	1.0614716488
.099900	61.00	-.3260830426	-3.2620969524	1.0637144994
.101565	62.00	-.3324923217	-3.2061044340	1.0660051069
.103230	63.00	-.3389552897	-3.1518730679	1.0683440488
.104895	64.00	-.3454733110	-3.0993187738	1.0707319187
.106560	65.00	-.3520477796	-3.0483627208	1.0731693274
.108225	66.00	-.3586801197	-2.9989309240	1.0756569029
.109890	67.00	-.3653717869	-2.9509538769	1.0781952911
.111555	68.00	-.3721242692	-2.9043662172	1.0807851561
.113220	69.00	-.3789390883	-2.8591064219	1.0834271808
.114885	70.00	-.3858178006	-2.8151165293	1.0861220677
.116550	71.00	-.3927619984	-2.7723418840	1.0888705387
.118215	72.00	-.3997733116	-2.7307309043	1.0916733368
.119880	73.00	-.4068534083	-2.6902348687	1.0945312255
.121545	74.00	-.4140039967	-2.6508077195	1.0974449905
.123210	75.00	-.4212268264	-2.6124058831	1.1004154394
.124875	76.00	-.4285236897	-2.5749881038	1.1034434032
.126540	77.00	-.4358964234	-2.5385152918	1.1065297365
.128205	78.00	-.4433469102	-2.5029503817	1.1096753182
.129870	79.00	-.4508770805	-2.4682582034	1.1128810527
.131535	80.00	-.4584889140	-2.4344053612	1.1161478703

.133200	81.00	-.4661844416	-2.4013601233	1.1194767281
.134865	82.00	-.4739657472	-2.3690923186	1.1228686109
.136530	83.00	-.4818349697	-2.3375732418	1.1263245322
.138195	84.00	-.4897943053	-2.3067755645	1.1298455350
.139860	85.00	-.4978460090	-2.2766732533	1.1334326929
.141525	86.00	-.5059923974	-2.2472414935	1.1370871108
.143190	87.00	-.5142358509	-2.2184566178	1.1408099265
.144855	88.00	-.5225788159	-2.1902960406	1.1446023114
.146520	89.00	-.5310238076	-2.1627381961	1.1484654718
.148185	90.00	-.5395734124	-2.1357624808	1.1524006499
.149850	91.00	-.5482302910	-2.1093491998	1.1564091255
.151515	92.00	-.5569971807	-2.0834795170	1.1604922170
.153180	93.00	-.5658768992	-2.0581354079	1.1646512829
.154845	94.00	-.5748723473	-2.0332996159	1.1688877229
.156510	95.00	-.5839865120	-2.0089556112	1.1732029801
.158175	96.00	-.5932224706	-1.9850875521	1.1775985421
.159840	97.00	-.6025833939	-1.9616802495	1.1820759426
.161505	98.00	-.6120725501	-1.9387191326	1.1866367633
.163170	99.00	-.6216933087	-1.9162541838	1.1913224038
.164835	100.00	-.6314491450	-1.8941383961	1.1960520706
.166500	101.00	-.6413436442	-1.8724283612	1.2008700286
.168165	102.00	-.6513805062	-1.8511116757	1.2057780603
.169830	103.00	-.6615635504	-1.8301764135	1.2107780060
.171495	104.00	-.6718967209	-1.8096111019	1.2158717656
.173160	105.00	-.6823840917	-1.7894047000	1.2210613009
.174825	106.00	-.6930298724	-1.7695465774	1.2263486387
.176490	107.00	-.7038384143	-1.7500264946	1.2317358729
.178155	108.00	-.7148142166	-1.7308345845	1.2372251675
.179820	109.00	-.7259619328	-1.7119613347	1.2428187595
.181485	110.00	-.7372863781	-1.6933975710	1.2485189617
.183150	111.00	-.7487925362	-1.6751344411	1.2543281667
.184815	112.00	-.7604855676	-1.6571634006	1.2602488493
.186480	113.00	-.7723708173	-1.6394761979	1.2662835709
.188145	114.00	-.7844538238	-1.6220648613	1.2724349830
.189810	115.00	-.7967403281	-1.6049216864	1.2787058309
.191475	116.00	-.8092362831	-1.5880392234	1.2850989587
.193140	117.00	-.8219478646	-1.5714102663	1.2916173128
.194805	118.00	-.8348814812	-1.5550278414	1.2982639475
.196470	119.00	-.8480437864	-1.5388851972	1.3050420294
.198135	120.00	-.8614416905	-1.5229757946	1.3119548430
.199800	121.00	-.8750823736	-1.5072932970	1.3190057961
.201465	122.00	-.8889732995	-1.4918315618	1.3261984258
.203130	123.00	-.9031222298	-1.4765846316	1.3335364049
.204795	124.00	-.9175372398	-1.4615467257	1.3410235485
.206460	125.00	-.9322267347	-1.4467122327	1.3486638207
.208125	126.00	-.9471994673	-1.4320757029	1.3564613430
.209790	127.00	-.9624645568	-1.4176318408	1.3644204014
.211455	128.00	-.9780315083	-1.4033754984	1.3725454555
.213120	129.00	-.9939102345	-1.3893016685	1.3808411471
.214785	130.00	-1.0100755107	-1.3754539099	1.3893123104

.216450	131.00	-1.0266066512	-1.3617328315	1.3979639819
.218115	132.00	-1.0434818142	-1.3481800950	1.4068014115
.219780	133.00	-1.0607127742	-1.3347911976	1.4158300742
.221445	134.00	-1.0783118426	-1.3215617472	1.4250556828
.223110	135.00	-1.0962918997	-1.3084874581	1.4344842012
.224775	136.00	-1.1146664290	-1.2955641449	1.4441218590
.226440	137.00	-1.1334495539	-1.2827877178	1.4539751665
.228105	138.00	-1.1526560771	-1.2701541777	1.4640509318
.229770	139.00	-1.1723015235	-1.2576596113	1.4743562783
.231435	140.00	-1.1924021855	-1.2453001863	1.4848986638
.233100	141.00	-1.2129751731	-1.2330721471	1.4956859011
.234765	142.00	-1.2340384668	-1.2209718099	1.5067261804
.236430	143.00	-1.2556109760	-1.2089955583	1.5180280930
.238095	144.00	-1.2777126009	-1.1971398388	1.5296006572
.239760	145.00	-1.3003643011	-1.1854011565	1.5414533464
.241425	146.00	-1.3235881683	-1.1737760706	1.5535961192
.243090	147.00	-1.3474075073	-1.1622611896	1.5660394524
.244755	148.00	-1.3718469225	-1.1508531677	1.5787943763
.246420	149.00	-1.3969324127	-1.1395486991	1.5918725137
.248085	150.00	-1.4226914752	-1.1283445145	1.6052861219
.249750	151.00	-1.4491532185	-1.1172373758	1.6190481389
.251415	152.00	-1.4763484864	-1.1062240711	1.6331722330
.253080	153.00	-1.5043099939	-1.0953014106	1.6476728583
.254745	154.00	-1.5689740923	-1.0596512219	1.6625653141
.256410	155.00	-1.5626728537	-1.0737153380	1.6778658113
.258075	156.00	-1.5931508057	-1.0630453430	1.6935915447
.259740	157.00	-1.6245474222	-1.0524535936	1.7097607724
.261405	158.00	-1.6569077095	-1.0419365718	1.7263929044
.263070	159.00	-1.6902793368	-1.0314913997	1.7435085990
.264735	160.00	-1.7247132771	-1.0211145788	1.7611298714
.266400	161.00	-1.7602641108	-1.0108030863	1.7792803959
.268065	162.00	-1.7969903641	-1.0005534568	1.7979849206
.269730	163.00	-1.8349548881	-.9903624798	1.8172704733
.271395	164.00	-1.8742252835	-.9802267910	1.8371658353
.273060	165.00	-1.9148743788	-.9776494784	1.8720759376
.274725	166.00	-1.9569807696	-.9601074765	1.8789118683
.276390	167.00	-2.0006294286	-.9501167408	1.9008315122
.278055	168.00	-2.0459123983	-.9401670450	1.9234994137
.279720	169.00	-2.0929295794	-.9302545583	1.9469572815
.281385	170.00	-2.1417896321	-.9203043272	1.9710982664
.283050	171.00	-2.1926110099	-.9104513037	1.9962655525
.284715	172.00	-2.2455231493	-.9006231018	2.0223700238
.286380	173.00	-2.3006678470	-.8908152164	2.0494699260
.288045	174.00	-2.3582008586	-.8810229024	2.0776289650
.289710	175.00	-2.4182937643	-.8712411387	2.1069170130
.291375	176.00	-2.4811361584	-.8614645864	2.1374109344
.293040	177.00	-2.5533905657	-.8495353536	2.1691955570
.294705	178.00	-2.6222448358	-.8399676355	2.2026007943
.296370	179.00	-2.6883841314	-.8321982189	2.2372684858
.298035	180.00	-2.7645820112	-.8231330153	2.2756187270

.299700	181.00	-2.8448574004	-.8132303512	2.3135243828
.301365	182.00	-2.9295837773	-.8026515603	2.3514349899
.303030	183.00	-3.0191861865	-.7927200956	2.3933695625
.304695	184.00	-3.1148547519	-.7825532498	2.4375397086
.306360	185.00	-3.2157067681	-.7725087533	2.4841616264
.308025	186.00	-3.3231128883	-.7623829977	2.5334847655
.309690	187.00	-3.4377280336	-.7521826144	2.5857992600
.311355	188.00	-3.5607511491	-.7418116002	2.6414065078
.313020	189.00	-3.6926708634	-.7314022390	2.7008277372
.314685	190.00	-3.8356120648	-.7207272646	2.7644301914
.316350	191.00	-3.9907195912	-.7098576193	2.8328427082
.318015	192.00	-4.1600027090	-.6987670850	2.9068729666
.319680	193.00	-4.3459461393	-.6873990259	2.9873991428
.321345	194.00	-4.5517992396	-.6756874658	3.0755936932
.323010	195.00	-4.7819084722	-.6635495434	3.1730331832
.324675	196.00	-5.0423682502	-.6508665451	3.2819088021
.326340	197.00	-5.3418762853	-.6374769757	3.4053231387
.328005	198.00	-5.6942797548	-.6231104791	3.5481653859
.329670	199.00	-6.1236624056	-.6072920562	3.7188515337
.331335	200.00	-6.6809166008	-.5889847030	3.9349576800
.333000	201.00	-7.5462070183	-.5642247053	4.2577564311

Data for G_2 and G_4 with sinusoidal distribution of the asperity height

SH $= \bar{\sigma}/H$

V = non-dimensional SH

$$G_2 = \int_{-\infty}^{\infty} \frac{g(\delta^*)}{\left[1 + \delta^*(\bar{\sigma}/H)\right]^3} \, d\delta^*$$

$$G_4 = \int_{-\infty}^{\infty} \frac{g(\delta^*)}{\left[1 + \delta^*(\bar{\sigma}/H)\right]^3} \, d\delta^*$$

$$g(\delta^*) = \begin{cases} \frac{1}{\pi} \cdot \sqrt{\frac{1}{9 - \delta^{*2}}} & -3 \le \delta^* \le 3 \\ 0 & \text{elsewhere} \end{cases}$$

SH	V	G2	G4
0.000000	1.000	.99701659	-.00000000
.001665	2.000	.99709099	-.02234477
.003330	3.000	.99731426	-.04469788
.004995	4.000	.99768650	-.06706769
.006660	5.000	.99820793	-.08946258
.008325	6.000	.99887885	-.11189092
.009990	7.000	.99969962	-.13436115
.011655	8.000	1.00067771	-.15688172
.013320	9.000	1.00179267	-.17946112
.014985	10.000	1.00306613	-.20210792
.016650	11.000	1.00449180	-.22483071
.018315	12.000	1.00607050	-.24763819
.019980	13.000	1.00780312	-.27053911
.021645	14.000	1.00969063	-.29354229
.023310	15.000	1.01173413	-.31665667
.024975	16.000	1.01393476	-.33989127
.026640	17.000	1.01629380	-.36325523
.028305	18.000	1.01881259	-.38675779
.029970	19.000	1.02149259	-.41040833
.031635	20.000	1.02433534	-.43421635
.033300	21.000	1.02734249	-.45819150
.034965	22.000	1.03051580	-.48234358
.036630	23.000	1.03385712	-.50668256
.038295	24.000	1.03736840	-.53121856
.039960	25.000	1.04105172	-.55596191
.041625	26.000	1.04490926	-.58092311
.043290	27.000	1.04894331	-.60611288
.044955	28.000	1.05315628	-.63154212
.046620	29.000	1.05755072	-.65722201
.048285	30.000	1.06212927	-.68314392

.049950	31.000	1.06689471	-.70937950
.051615	32.000	1.07184996	-.73588063
.053280	33.000	1.07699806	-.76267951
.054945	34.000	1.08234221	-.78978859
.056610	35.000	1.08788571	-.81722065
.058275	36.000	1.09363206	-.84498877
.059940	37.000	1.09958486	-.87310638
.061605	38.000	1.10574791	-.90158725
.063270	39.000	1.11212514	-.93044553
.064935	40.000	1.11872667	-.95969572
.066600	41.000	1.12553877	-.98935276
.068265	42.000	1.13258391	-1.01943200
.069930	43.000	1.13986673	-1.04994923
.071595	44.000	1.14737407	-1.08092068
.073260	45.000	1.15512896	-1.11236311
.074925	46.000	1.16313064	-1.14429373
.076590	47.000	1.17138457	-1.17673032
.078255	48.000	1.17989642	-1.20969119
.079920	49.000	1.18867210	-1.24319525
.081585	50.000	1.19771776	-1.27726198
.083250	51.000	1.20703979	-1.31191154
.084915	52.000	1.21664484	-1.34716471
.086580	53.000	1.22653083	-1.38304300
.088245	54.000	1.23673196	-1.41956861
.089910	55.000	1.24722873	-1.45676454
.091575	56.000	1.25803794	-1.49465454
.093240	57.000	1.26916770	-1.53326325
.094905	58.000	1.28062644	-1.57261613
.096570	59.000	1.29242297	-1.61273958
.098235	60.000	1.30456643	-1.65366096
.099900	61.000	1.31706633	-1.69540864
.101565	62.000	1.32993260	-1.73891201
.103230	63.000	1.34317556	-1.78159161
.104895	64.000	1.35680597	-1.82599909
.106560	65.000	1.37083501	-1.87126736
.108225	66.000	1.38527437	-1.91761056
.109890	67.000	1.40013620	-1.96497420
.111555	68.000	1.41543317	-2.01339517
.113220	69.000	1.43117849	-2.06291185
.114885	70.000	1.44738594	-2.11356416
.116550	71.000	1.46406988	-2.16539364
.118215	72.000	1.48124530	-2.21844354
.119880	73.000	1.49892783	-2.27275893
.121545	74.000	1.51713379	-2.32838673
.123210	75.000	1.53588622	-2.38537588
.124875	76.000	1.55518490	-2.44377740
.126540	77.000	1.57506642	-2.50364450
.128205	78.000	1.59554418	-2.56593274
.129870	79.000	1.61663849	-2.62890009
.131535	80.000	1.63837654	-2.69263711

.133200	81.000	1.66076253	-2.75891710
.134865	82.000	1.68383765	-2.82699619
.136530	83.000	1.70762621	-2.89691354
.138195	84.000	1.73213561	-2.96874153
.139860	85.000	1.75741049	-3.04255588
.141525	86.000	1.78347273	-3.11843590
.143190	87.000	1.81035156	-3.19646464
.144855	88.000	1.83807763	-3.27672915
.146520	89.000	1.86668306	-3.35932070
.148185	90.000	1.89620158	-3.44433502
.149850	91.000	1.92666857	-3.53187256
.151515	92.000	1.95812119	-3.62203880
.153180	93.000	1.99059848	-3.71494450
.154845	94.000	2.02414147	-3.81070609
.156510	95.000	2.05879328	-3.90944596
.158175	96.000	2.09459929	-4.01129286
.159840	97.000	2.13160725	-4.11638229
.161505	98.000	2.16986742	-4.22485692
.163170	99.000	2.20943277	-4.33686705
.164835	100.000	2.25035910	-4.45257112
.166500	101.000	2.29270526	-4.57213622
.168165	102.000	2.33653334	-4.69573865
.169830	103.000	2.38190886	-4.82356456
.171495	104.000	2.42890103	-4.95581058
.173160	105.000	2.47758298	-5.09268455
.174825	106.000	2.52803203	-5.23440629
.176490	107.000	2.58032998	-5.38120841
.178155	108.000	2.63456340	-5.53333721
.179820	109.000	2.69082401	-5.69105368
.181485	110.000	2.74920898	-5.85463449
.183150	111.000	2.80982139	-6.02437319
.184815	112.000	2.87277059	-6.20058137
.186480	113.000	2.93817273	-6.38359008
.188145	114.000	3.00615122	-6.57375121
.189810	115.000	3.07683725	-6.77143911
.191475	116.000	3.15037046	-6.97705228
.193140	117.000	3.22689952	-7.19101528
.194805	118.000	3.30658286	-7.41378073
.196470	119.000	3.38958944	-7.64583158
.198135	120.000	3.47609959	-7.88768351
.199800	121.000	3.56630592	-8.13988760
.201465	122.000	3.66041432	-8.40303329
.203130	123.000	3.75864509	-8.67775152
.204795	124.000	3.86123411	-8.96471827
.206460	125.000	3.96843423	-9.26465845
.208125	126.000	4.08051663	-9.57835008
.209790	127.000	4.19777255	-9.90662902
.211455	128.000	4.32051495	-10.25039412
.213120	129.000	4.44908055	-10.61061292
.214785	130.000	4.58383198	-10.98833794

.216450	131.000	4.72516011	-11.38466369
.218115	132.000	4.87348682	-11.80083438
.219780	133.000	5.02926786	-12.23815257
.221445	134.000	5.19299615	-12.69803867
.223110	135.000	5.36520547	-13.18203168
.224775	136.000	5.54647449	-13.69180103
.226440	137.000	5.73743136	-14.22915989
.228105	138.000	5.93875877	-14.79609008
.229770	139.000	6.15119970	-15.39470873
.231435	140.000	6.37556380	-16.02738708
.233100	141.000	6.61273463	-16.69667155
.234765	142.000	6.86367781	-17.40535760
.236430	143.000	7.12945016	-18.15653662
.238095	144.000	7.41121018	-18.95347641
.239760	145.000	7.71022979	-19.79995575
.241425	146.000	8.02790777	-20.70003374
.243090	147.000	8.36578505	-21.65809460
.244755	148.000	8.72556215	-22.67916889
.246420	149.000	9.10911916	-23.76869212
.248085	150.000	9.51853870	-24.93272211
.249750	151.000	9.95613223	-26.17799642
.251415	152.000	10.42447057	-27.51197185
.253080	153.000	10.92641907	-28.94302792
.254745	154.000	11.46517847	-30.48048703
.256410	155.000	12.04433247	-32.13480440
.258075	156.000	12.66790326	-33.91772149
.259740	157.000	13.34041657	-35.84245750
.261405	158.000	14.06697811	-37.92393465
.263070	159.000	14.85336381	-40.17904399
.264735	160.000	15.70612666	-42.62696030
.266400	161.000	16.63272364	-45.28951665
.268065	162.000	17.64166741	-48.19165169
.269730	163.000	18.74270805	-51.36194621
.271395	164.000	19.94705202	-54.83326960
.273060	165.000	21.26762710	-58.64356254
.274725	166.000	22.71940469	-62.83678936
.276390	167.000	24.31979390	-67.46410309
.278055	168.000	26.08912611	-72.58527861
.279720	169.000	28.05125438	-78.27049609
.281385	170.000	30.23429958	-84.60249937
.283050	171.000	32.67158524	-91.67946432
.284715	172.000	35.40281739	-99.61839362
.286380	173.000	38.47558456	-108.55961214
.288045	174.000	41.94728049	-118.67245693
.289710	175.000	45.88758960	-130.16264897
.291375	176.000	50.38173002	-143.28191516
.293040	177.000	55.53472677	-158.34067222
.294705	178.000	61.47710291	-175.72493607
.296370	179.000	68.37254675	-195.91904829
.298035	180.000	76.42837128	-219.53685932

.299700	181.000	85.90997735	-247.36462767
.301365	182.000	97.16115232	-280.42144202
.303030	183.000	110.63302537	-320.04536453
.304695	184.000	126.92611767	-368.01859650
.306360	185.000	146.85263210	-426.75296340
.308025	186.000	171.53078349	-499.57092217
.309690	187.000	202.53122672	-591.14194190
.311355	188.000	242.11078656	-708.17933905
.313020	189.000	293.59756930	-860.58890020
.314685	190.000	362.04904862	-1063.43246201
.316350	191.000	455.42518837	-1340.42966098
.318015	192.000	586.78626400	-1730.52105087
.319680	193.000	778.66214058	-2300.92092246
.321345	194.000	1072.38841174	-3175.01959219
.323010	195.000	1549.93125683	-4597.63681103
.324675	196.000	2391.14703390	-7106.29179548
.326340	197.000	4049.10940934	-12055.84967513
.328005	198.000	7919.06795274	-23621.17873278
.329670	199.000	19947.59913754	-59606.81488887
.331335	200.000	88627.89187290	-265304.23173560
.333000	201.000	6822046.68510997	-20457670.58057237

```
      PROGRAM ROLWAVI (INPUT,OUTPUT)
C
C THIS PROGRAM IS TO COMPUTE THE EFFECT OF SURFACE ROUGHNESS AND WAVINESS ON THE
C   INTEGRATED PRESSURE OF AN  EHD  CONTACT
CONLY THE CASE OF PURE ROLLING IS STUDIED
C ASSUMING SINUSOIDAL WAVINESS AND SINUSOIDAL ROUGHNESS DISTRIBUTION
C
C THIS PROGRAM CONSISTS OF   3  SUBROUTINES
C 1 - SUBROUTINE GRUBIN   IS TO CALCULATE  WGRUB , THE REDUCED PRESSURE AT THE
C   INLET BY THE SMOOTH FILM GRUBIN APPROACH
C 2 - SUBROUTINE ROUGH   IS TO CALCULATE  WROUGH(I) , THE REDUCED PRESSURE AT
C   THE INLET BY STOCHASTIC THEORY FOR ROUGH SURFACES
C 3 - SUBROUTINE WAVI   IS TO CALCULATE  WSIN(I) , THE REDUCED PRESSURE AT THE
C   INLET FOR THE SINUSOIDAL WAVINESS SURFACE PROFILE
C
C DATA CARD NO. 1
C   KF = TOTAL NUMBER OF GRID POINTS
C   KM = GRID NUMBER , XX(KM) = -2.0
C   NAMP = NUMBER OF AMPLITUDE DATA
C   NCYC = NUMBER OF WAVINESS CYCLES DATA
C DATA CARD NO. 2
C   HO = CENTER FILM THICKNESS
C   W = DIMENSIONLESS CONTACT LOAD
C   PI = 3.141593
C DATA CARD NO. 3
C   DCYC(I) = WAVINESS CYCLES DATA
C DATA CARD NO. 4
C   DAMP(I) = AMPLITUDE DATA
C DATA CARD NO. 5
C   THESE DATA ARE THE OUTPUT FROM PROGRAM SUCHAS PROGRAM DATPOL2 WHICH EVALUATE
C     THE INTEGRAL OF   ( DISTRIBUTION FUNCTION*HSS)/(1.+SH*HSS)**3  AND
C     (DISTRIBUTION FUNCTION/(1.+SH*HSS)**3
C   THIS DISTRIBUTION FUNCTION CAN BE POLYNOMIAL ,GAUSSIAN, SINUSOIDAL OR ANY
C     OTHER FUNCTION
C   DSH(I) = THE ABSCISSA RANGING FROM  0 TO 0.333
C   DV(I) = THE NONDIMENSIONAL  DSH(I)
C   DG4(I) = THE INTEGRAL OF  35/96*(1.-HSS**2/9)**3/(1+SH*HSS)**3*HSS
C     IN THE CASE OF  POLYNOMIAL DISTRIBUTION
C   DG2(I) = THE INTEGRAL OF  35/96*(1.-HSS**2/9)**3/(1+SH*HSS)**3
C     IN THE CASE OF  POLYNOMIAL DISTRIBUTION
C   DG5(I) = DG2(I)/DG4(I)
C
C
      COMMON KF,KM,NAMP,NCYC,KMM,KMK,KFF
      COMMON HO,W,PI,WGRUB,CYC,AMP,KK,S ,DG2(201),DG4(201)
      COMMON XX(1501),H(1501),WSIN(16),WROUGH(16),G(1501)
      DIMENSION DCYC(20),DAMP(16),SWSIN(16),SWRO(16),PERR(16),DSH(201),
     : DV(201)
C
      PRINT 1
      READ  2,KF,KM,NAMP,NCYC
      READ  3,HO,W,PI
      READ  3,(DCYC(I),I=1,NCYC)
      READ  3,(DAMP(I),I=1,NAMP)
      DO 100  I=1,201
100   READ  5,DSH(I),DV(I),DG2(I),DG4(I)
```

```
      PRINT 51
      PRINT 2,KF,KM,NAMP,NCYC
      PRINT 52
      PRINT 4,HO,W,PI
      PRINT 53
      PRINT 4,(DCYC(I),I=1,NCYC)
      PRINT 54
      PRINT 4,(DAMP(I),I=1,NAMP)
      KMM = KM + 1
      KMK = KM - 2
      KFF = KF - 2
      XX(1) = -5.
      DO 101  J =2,KM
101   XX(J) = XX(J-1) + 0.003
      DO 102  J =KMM,KF
102   XX(J) = XX(J-1) + 0.002
      DO 103  J=1,KF
      X = XX(J)
      H(J) = HO + 4.*W/PI*(ABS(X)*SQRT(ABS((-X)**2-1.)) - ALOG(ABS(X) +
     H SQRT(ABS((-X)**2-1. ))))
103   CONTINUE
      PRINT 55
      PRINT 4,XX(KM),XX(KF)
C
      CALL GRUBIN
      DO 104  I=1,NAMP
      KK = I
      S = DAMP(I) / 3. * HO
      CALL ROUGH
      SWRO(I) = WROUGH(I) / WGRUB
104   CONTINUE
      DO 1000  II=1,NCYC
      CYC = DCYC(II)
      PRINT 7, II,CYC
      DO 105 I = 1,NAMP
      KK = I
      AMP = DAMP(I) * HO
      CALL WAVI
      SWSIN(I) = WSIN(I) / WGRUB
      PERR(I) = (WSIN(I) - WROUGH(I)) / WROUGH(I)
      PRINT 6, I,AMP    ,WSIN(I),SWSIN(I),WROUGH(I),SWRO(I),PERR(I)
105   CONTINUE
      DO 106 I=1,NAMP
      KK = I
      AMP = -DAMP(I) * HO
      CALL WAVI
      SWSIN(I) = WSIN(I) / WGRUB
      PERR(I) = (WSIN(I) - WROUGH(I)) / WROUGH(I)
      PRINT 6, I,AMP    ,WSIN(I),SWSIN(I),WROUGH(I),SWRO(I),PERR(I)
106   CONTINUE
1000  CONTINUE
```

```
C
1     FORMAT(1H1)
2     FORMAT(2015)
3     FORMAT(8F10.7)
4     FORMAT(9(2X,E13.6))
5     FORMAT(2F10.6,3F20.10)
6     FORMAT(I5,8(2X,E13.6))
7     FORMAT(//////////3X,*II=*,I3,10X,*CYC=*,F6.1//4X,*I*,6X,*DAMP*,11X
     7 ,*WSIN*,10X,*SWSIN*,9X,*WROUGH*,11X,*SWRO*,11X,*PERR*/)
51    FORMAT(/3X,*KF*,3X,*KM*,X,*NAMP*,X,*NCYC*)
52    FORMAT(/6X,*HO*,14X,*W*,13X,*PI*)
53    FORMAT(/6X,*DCYC(I)*)
54    FORMAT(/6X,*DAMP(I)*)
55    FORMAT(/6X,*XX(KM)*,9X,*XX(KF)*)
C
      STOP
      END
      SUBROUTINE GRUBIN
C
      COMMON KF,KM,NAMP,NCYC,KMM,KMK,KFF
      COMMON HO,W,PI,WGRUB,CYC,AMP,KK,S ,DG2(201),DG4(201)
      COMMON XX(1501),H(1501),WSIN(16),WROUGH(16),G(1501)
C
      DO 401  J=1,KF
      G(J) = (H(J) - HO) / H(J)**3
401   CONTINUE
      WGRUB = 0.
      DO 402  J=1,KMK,2
402   WGRUB = WGRUB + 0.003/3.*(G(J) + 4.*G(J+1) + G(J+2))
      DO 403  J=KM,KFF,2
403   WGRUB = WGRUB + 0.002/3.*(G(J) + 4.*G(J+1) + G(J+2))
      PRINT 41, HO,WGRUB
41    FORMAT(/////5X,*HO=*,F10.6,20X,*WGRUB=*,E13.6//)
C
      RETURN
      END
      SUBROUTINE ROUGH
      COMMON KF,KM,NAMP,NCYC,KMM,KMK,KFF
      COMMON HO,W,PI,WGRUB,CYC,AMP,KK,S ,DG2(201),DG4(201)
      COMMON XX(1501),H(1501),WSIN(16),WROUGH(16),G(1501)
      DIMENSION TR(1501)
      DO 301  J=1,KF
      V = 1. + S / H(J) / 0.001665
      MV = V
      VM = MV
      D2 = (ALOG(DG2(MV+1)) - ALOG(DG2(MV))) * (V-VM) + ALOG(DG2(MV))
      G2 = EXP(D2)
301   TR(J) = G(J) * G2
      WROUGH(KK) = 0.
      DO 302  J= 1,KMK,2
302   WROUGH(KK) = WROUGH(KK) + 0.003/3.*(TR(J) + 4.*TR(J+1) + TR(J+2))
      DO 303  J =KM,KFF,2
303   WROUGH(KK) = WROUGH(KK) + 0.002/3.*(TR(J) + 4.*TR(J+1) + TR(J+2))
      RETURN
      END
```

```
      SUBROUTINE WAV1
C
      COMMON KF,KM,NAMP,NCYC,KMM,KMK,KFF
      COMMON HO,W,PI,WGRUB,CYC,AMP,KK,S ,DG2(201),DG4(201)
      COMMON XX(1501),H(1501),WSIN(16),WROUGH(16),G(1501)
      DIMENSION T(1501)
C
      DO 201    J = 1,KF
      DEL = AMP * COS(2.*CYC*PI*XX(J))
      T(J) = (H(J) - HO) / (H(J) + DEL)**3
201   CONTINUE
      WSIN(KK) = 0.
      DO 202   J=1,KMK,2
202   WSIN(KK) = WSIN(KK) + 0.003/3.*(T(J) + 4.*T(J+1) + T(J+2))
      DO 203   J=KM,KFF,2
203   WSIN(KK) = WSIN(KK) + 0.002/3.*(T(J) + 4.*T(J+1) + T(J+2))
C
      RETURN
      END
```

```
0000000000000000000000   END OF RECORD
 1501 1001      9    14
 0.00001    0.00003   3.14159265
 1.         2.        3.         4.         5.         10.        15.        20.
 25.        30.       35.        40.        45.        50.
 0.15       0.3       0.45       0.6        0.75       0.9        0.93       0.96
 0.99
C    DATA FOR  DSH(I), DV(I), DG4(I), DG2(I), DG5(I)   ARE OMITTED
0000000000000000000000   END OF INFORMATION
```

```
      PROGRAM ASPERTY (INPUT,OUTPUT,PUNCH)
C THIS PROGRAM IS TO SOLVE FOR THE PERTURBED PRESSURE DUE TO A SINGLE  3-D
C   RIGID ASPERITY WITHIN AN ELASTOHYDRODYNAMIC CONTACT
C THIS PROGRAM CONSISTS OF  4 SUBROUTINES
C 1 - SUBROUTINE TRANSFN   IS USED TO TRANSORM THE INPUT DATA OF CHENG PROGRAM
C   FROM GLOBAL COORDINATE TO ASPERITY COORDINATE
C 2 - SUBROUTINE INTERPN   IS USED TO INTERPOLATE SOME NEW DATA IN ASPERITY
C   COORDINATE BY SECOND ORDER INTERPOLATION  ROUTINE
C 3 - SUBROUTINE ABCR   IS TO FORM THE  A(29,14,14),B(29,14,14), C(29,14,14) AND
C   R(29,14)    MATRICES
C 4 - SUBROUTINE TEFPHI   IS TO FORM MATRICES  T(29,14,14), E(30,14,14),F(30,14)
C   AND SOLVE FOR THE PERTURBED PRESSURE  PHI(29,14)  BY THE COLUMNWISE MATRIX
C   INVERSION METHOD
C
C
C DATA CARD NO. 1
C   NC1 = NUMBER OF THE MAXIMUM ASPERITY AMPLITUDE
C   NUB = NUMBER OF DIFFERENT VELOCITIES DATA
C   NGAMAR = NUMBER OF THE ELLIPSTICITY RATIO OF ASPERITY
C   NPLOT = 0 ,DO NOT PLOT THE RESULTS
C   NPRINT2 = 0 , DO NOT PRINT  THE RESULTS
C   NPRINT = 0 , DO NOT PRINT THE RESULTS
C
C DATA CARD NO. 2
C   BSTAR = THE RATIO OF THE MINOR AXIS OF THE ASPERITY TO THE HALF HERTZIAN
C     CONTACT WIDTH
C   X3 = THE DISTANCE BETWEEN THE ASPERITY CENTER AND THE CONTACT CENTER
C   DI = THE DISTANCE IN X-DIRECTION WHERE THE PERTURBED PRESSURE  PHI  IS
C     ASSUMED TO BE ZERO
C
C DATA CARD NO. 3
C   GAMMA(I) = ELLIPSTICITY RATIO DATA
C DATA CARD NO. 4
C1H(I) = ASPERITY AMPLITUDE DATA
C DATA CARD NO. 5
C   U1(I),U2(I) = VELOCITY DATA
C DATA CARD NO. 6
C   PHZ = HERTIZIAN PRESSURE
C   AL3E = THE PRODUCT OF PRESSURE VISCOSITY COEFFICIENT AND THE EQUIVALENT
C     YOUNGS MODULUS,
C DATA CARD NO. 7
C   HO = CENTER FILM THICKNESS
C
C DATA CARD NO. 8
C   KO = IN GLOBAL COORDINATES, THE GRID NO. OF HERTZIAN CONTACT CENTER WITH
C     XS(KO) = 0
C   KF = IN GLOBAL COORDINATES, THE GRID NO. OF CONTACT EXITWITH  XS(KF) = 1
C   NC = IN ASPERITY COORDINATE, THE GRID NO. OF HERTZIAN CONTACT CENTER
C   NX,NY = THE NO. OF TOTAL GRID POINTS IN X AND Y DIRECTION OF ASPERITY COORD.
C   IDEG=2  MEANS A PARABOLIC INTERPOLATION ROUTINE  USED IN SUBROUTINE INTERPN
C
```

```
C DATA CARD NO. 9
C    DXS(I) = GRID SIZES DATA IN GLOBAL COORD.(FROM CHENG PROGRAM)
C DATA CARD NO. 10
C    PS(I) = STEADY STATE PRESSURE DATA FROM CHENG PROGRAM
C DATA CARD NO. 11
C    HS(I) = STEADY STATE FILM THICKNESS DATA FROM CHENG PROGRAM
C DATA CARD NO. 12
C    DX(I) = GRID SIZES DATA IN X-DIRECTION OF ASPERITY COORD.
C DATA CARD NO. 13
C    DY(I) = GRID SIZES DATA IN Y-DIRECTION OF ASPERITY COORD.
C DATA CARD NO. 14
C    MIN(I) = NO. USED IN SUBROUTINE INTERPN  TO IDENTIFY THE GRID POSITION
C
C
      COMMON BSTAR,X3,C1
      COMMON ALPHA,ALAMDA,GINV
      COMMON NX,NX1,NY,NY1,DI,DX(28), DY(14),DEL(29,15), HTEP(29,15),
     C H1HTEP(29,15), P1(29), H1(29), X(29)
      COMMON A(29,14,14), B(29,14,15), C(29,14,14), R(29,14)
      COMMON PHI(29,14),P1PHI(29,14),HT(29,15),NPRINT,NPRINT2
C
      DIMENSION DXS(80),XS(80),XXS(80),PS(80),HS(80),MIN(29),
     1XOC(29),PPLOT(29),Y(15),H1EP(29),C1H(5),EP1(29),U1(3),U2(3)
      DIMENSION GAMAR(5)
C
C     READ CONSTANT
C
      READ  5,NC1,NUB,NGAMAR,NPLOT,NPRINT2,NPRINT
      READ  2,BSTAR,X3,DI
      READ  2,(GAMAR(I),I=1,NGAMAR)
      READ  2,(C1H(I),I=1,NC1)
      DO  100 I=1,NUB
100   READ  3,U1(I), U2(I)
      READ  2,PHZ,AL3E
      READ 2,HO
      READ  5,KO,KF,NC,NX,NY,IDEG
      KFF = KF-1
      NX1 = NX-1
      NY1 = NY-1
      NCC = NC +1
      ALPHA = AL3E*PHZ
C     READ SMOOTH FILM SOLUTION DATA
      READ  2,(DXS(I),I=1,KFF)
      READ  3,(PS(I),I=1,KO)
      READ  3,(HS(I),I=1,KO)
      READ  2,(DX(I),I=1,NX1)
      READ  2,(DY(I),I=1,NY1)
      READ  5,(MIN(I),I=1,NC)
      PRINT 1
      PRINT 53
      PRINT 6,NC1,NUB,NGAMAR,NPLOT,NPRINT2,NPRINT
      PRINT 31
      PRINT 4,BSTAR,X3,DI
      PRINT 44
```

```
      PRINT 4,(GAMAR(I),I=1,NGAMAR)
      PRINT 35
      PRINT 4,(C1H(I),I=1,NC1)
      PRINT 32
      DO 99 I=1,NUB
99    PRINT 9,I,U1(I),U2(I)
      PRINT 33
      PRINT 4,PHZ,AL3E,ALPHA
      PRINT 34
      PRINT 4,HO
      PRINT 36
      PRINT 6,KO,KF,NC,NX,NY,IDEG,KFF,NCC,NX1,NY1
      XS(1) = -5.
      DO 101 I=2,KF
101   XS(I) = XS(I-1) + DXS(I-1)
      DO 102 I=1,KO
102   XXS(I) = (XS(I)-X3)/BSTAR
      X(1) = DI
      DO 103 I=2,NX
103   X(I) = X(I-1) + DX(I-1)
      DO 106 I=1,NX
106   XOC(I) = X(I)*BSTAR + X3
      Y(1) = 0.
      DO 110 J=2,NY
110   Y(J) = Y(J-1) + DY(J-1)
      PRINT 38
      PRINT 7,(I,PS(I),I=1,KO)
      PRINT 39
      PRINT 7,(I,HS(I),I=1,KO)
      PRINT 40
      PRINT 7,(I,DXS(I),I=1,KFF)
      PRINT 37
      PRINT 7,(I,XS(I),I=1,KO)
      PRINT 45
      PRINT 7,(I,XXS(I),I=1,KO)
      PRINT 42
      PRINT 7,(I,DX(I),I=1,NX1)
      PRINT 43
      PRINT 7,(I,DY(I),I=1,NY1)
      PRINT 47
      PRINT 7,(I,X(I),I=1,NX)
      PRINT 50
      PRINT 7,(I,XOC(I),I=1,NX)
      PRINT 51
      PRINT 7,(J,Y(J),J=1,NY)
      PRINT 41
      PRINT 6,(MIN(I),I=1,NC)
C
      DO 104 I=1,NC
104   CALL TRANSFN(XXS,PS,HS,KO,X(I),P1(I),H1(I),MIN(I),IDEG)
      IF (NC .EQ. NX) GO TO 107
      DO 105 I=NCC,NX
      P1(I) = SQRT(ABS(1. - XOC(I)**2))
105   H1(I) = 1.
107   CONTINUE
```

```
      DO 111 I=1,NX
      EP1(I) = EXP(-P1(I)*ALPHA)
111   H1EP(I) = H1(I)**3*EP1(I)
      PRINT 48
      PRINT 7,(I,P1(I),I=1,NX)
      PRINT 49
      PRINT 7,(I,H1(I),I=1,NX)
      PRINT 54
      PRINT 7,(I,EP1(I),I=1,NX)
      PRINT 55
      PRINT 7,(I,H1EP(I),I=1,NX)
C
      DO  1000  IIK=1,NGAMAR
      GAMMA = GAMAR(IIK)
      GINV = 1./GAMMA**2
      DO 1000   IIJ=1,NUB
      UD = (U1(IIJ)-U2(IIJ))*0.5
      US = (U1(IIJ)+U2(IIJ))*0.5
      ALAMDA = 48.*UD/HO**2*BSTAR
      ALAM2 = 48.*US/HO**2*BSTAR
      ALAM3 = 46./32./ALAM2
      ALAM4 = ALAM3 / GAMMA
C
      DO 1000   III=1,NC1
      C1 = C1H(III)
      PRINT 56
      PRINT 9,IIJ, UD, US, ALAMDA, ALAM2, ALAM3, ALAM4
      PRINT 52
      PRINT 9,III, C1, PHZ, UD, AL3E, BSTAR, GAMMA, X3
C
C     TO TRANSFORM KNOWN DATA TC NEW COORDINATES
C     TO INTERPOLATE NEW RESULTS FRON KNOWN DATA AT NEW COORDINATES
      CALL INTERPN(Y,H1EP,EP1)
C
C     TO FORM MATRICES  A(I,J,K), B(I,J,K), C(I,J,K), R(I,J)
      CALL ABCR
C
C     TO FORM MATRICES  T(I,J,K), E(I,J,K), F(I,J) AND
C     SOLVE FOR  PHI(I,J),  P1PHI(I,J)
      CALL TEFPHI
C
      J = 1
      PRINT 8,J
      DO 108 I=1,NX
108   PPLOT(I) = PHI(I,J)
C STPLT1   IS A LIBRARY SUBROUTINE TO PLOT RESULTS
      CALL STPLT1(1,X,PPLOT,29,1H*,5,5HPHI-X)
      CALL STPLT1(1,XOC,PPLOT,29,1H*,7,7HPHI-XOC)
      DO 109 I=1,NX
109   PPLOT(I) = P1PHI(I,J)
      CALL STPLT1(1,X,PPLOT,29,1H*,7,7HP1PHI-X)
      CALL STPLT1(1,XOC,PPLOT,29,1H*,9,9HP1PHI-XOC)
1000  CONTINUE
```

```
C
1      FORMAT(1H1)
2      FORMAT(8F10.6)
3      FORMAT(5(2X,E13.6))
4      FORMAT(9(2X,E13.6))
5      FORMAT(16I5)
6      FORMAT(18(2X,I5))
7      FORMAT(8(X,I2,X,E13.6))
8      FORMAT(////6X,*J=*,I3////)
9      FORMAT(I5,8(2X,E13.6))
10     FORMAT(10X,2F10.6)
11     FORMAT(X,14E9.2)
31     FORMAT(7X,*BSTAR*,13X,*X3*,13X,*DI*)
32     FORMAT(4X,*I*,7X,*U1(I)*,11X,*U2(I)*)
33     FORMAT(7X,*PHZ*,11X,*AL3E*,10X,*ALPHA*)
34     FORMAT(//7X,*H0*/)
35     FORMAT(6X,*C1H(I)*)
36     FORMAT(4X,*K0*,5X,*KF*,5X,*NC*,5X,*NX*,5X,*NY*,3X,*IDEG*,4X,*KFF*,
      6 4X,*NCC*,4X,*NX1*,4X,*NY1*)
37     FORMAT(//6X,*XS(I)*/)
38     FORMAT(//6X,*PS(I)*/)
39     FORMAT(//6X,*HS(I)*/)
40     FORMAT(//6X,*DXS(I)*/)
41     FORMAT(6X,*MIN(I)*)
42     FORMAT(//6X,*DX(I)*/)
43     FORMAT(//6X,*DY(I)*/)
44     FORMAT(6X,*GAMMA(I)*)
45     FORMAT(//6X,*XXS(I)*/)
47     FORMAT(//6X,*X(I)*/)
48     FORMAT(//6X,*P1(I)*/)
49     FORMAT(//6X,*H1(I)*/)
50     FORMAT(//6X,*X0C(I)*/)
51     FORMAT(//6X,*Y(J)*/)
52     FORMAT(//2X,*II1*,7X,*C1*,12X,*PHZ*,14X,*UD*,14X,*G*,10X,*BSTAR
      2 *,10X,*GAMMA*,12X,*X3*/)
53     FORMAT(4X,*NC1*,4X,*NUB*,X,*NGAMAR*,2X,*NPLOT*,X,*NPRINT2*,X,
      3 *NPRINT*)
54     FORMAT(//6X,*EP1(I)*/)
55     FORMAT(//6X,*H1EP(I)*/)
56     FORMAT(//////////2X,*IIJ*,8X,*UD*,13X,*US*,9X,*ALAMDA*,10X,*ALAM2*
      6 ,10X,*ALAM3*,10X,*ALAM4*/)
C
C
       STOP
C
       END
```

```
      SUBROUTINE TRANSFN(XXS,PS,HS,KU,X,P1,H1,MIN,IDEG)
      DIMENSION XXS(60), PS(60), HS(80)
      IF (X .NE. XXS(MIN)) GO TC 755
      P1 = PS(MIN)
      H1 = HS(MIN)
      GO TO 756
755   FACTOR = 1.
      MAX = MIN + IDEG
      DO 701 J=MIN,MAX
701   FACTOR = FACTOR*(X-XXS(J))
C     EVALUATE INTERPOLATING PCLYNOMIAL
      P1 = 0.
      H1 = 0.
      DO 702 I=MIN,MAX
      TERMP = PS(I)*FACTOR/(X-XXS(I))
      TERMH = HS(I)*FACTOR/(X-XXS(I))
      DO 703 J=MIN,MAX
      IF(I . NE. J) GO TO 757
      GO TO 703
757   TERMP = TERMP/(XXS(I)-XXS(J))
      TERMH = TERMH/(XXS(I)-XXS(J))
703   CONTINUE
      P1 = P1 + TERMP
      H1 = H1 + TERMH
702   CONTINUE
756   RETURN
C
      END
```

```
      SUBROUTINE INTERPN(Y,H1EP,EP1)
C
      COMMON BSTAR,X3,C1
      COMMON ALPHA,ALAMDA,GINV
      COMMON NX,NX1,NY,NY1,DI,DX(28), DY(14),DEL(29,15), HTEP(29,15),
     C H1HTEP(29,15), P1(29), H1(29), X(29)
      COMMON A(29,14,14), B(29,14,15), C(29,14,14), R(29,14)
      COMMON PHI(29,14),P1PHI(29,14),HT(29,15),NPRINT,NPRINT2
      COMMON PHIOP(29)
      DIMENSION Y(15),H1EP(29), EP1(29)
C
      DO 406 I=1,NX
      DO 407 J=1,NY
      XYI = X(I)**2 + Y(J)**2 - 1.
      IF(XYI .GE. 0.) GO TO 451
      DEL(I,J) = C1*XYI
      GO TO 452
451   DEL(I,J) = 0.
452   HT(I,J) = H1(I) + DEL(I,J)
      HTEP(I,J) = HT(I,J)**3*EP1(I)
      H1HTEP(I,J) = H1EP(I) - HTEP(I,J)
407   CONTINUE
406   CONTINUE
      J=1
      PRINT 416
      PRINT 7,(I,DEL(I,J),I=1,NX)
```

```
      PRINT 417
      PRINT 7,(I, HT(I,J),I=1,NX)
      IF(NPRINT  .EQ.  0) GO TO 490
      PRINT 418
      PRINT 10, ((HTEP(I,J),J=1,NY),I=1,NX)
      PRINT 419
      PRINT 10, ((HIHTEP(I,J),J=1,NY),I=1,NX)
C
7     FORMAT(8(X,I2,X,E13.6))
10    FORMAT(X,15E9.2)
416   FORMAT(//6X,* DEL*/)
417   FORMAT (//6X,* HI*/)
418   FORMAT(//6X,*HIEP*/)
419   FORMAT(//6X,*HIHTEP*/)
C
490   RETURN
C
      END
      SUBROUTINE ABCR
C
      COMMON BSTAR,X3,C1
      COMMON ALPHA,ALAMDA,GINV
      COMMON NX,NX1,NY,NY1,DI,DX(28), DY(14),DEL(29,15), HTEP(29,15),
     C HIHTEP(29,15), P1(29), H1(29), X(29)
      COMMON A(29,14,14), B(29,14,15), C(29,14,14), R(29,14)
      COMMON PHI(29,14),P1PH1(29,14),HT(29,15),NPRINT,NPRINT2
      COMMON PHIOP(29)
C
      DO 501    I=1,NX
      DO 501 J=1,NY1
      DO 501 K=1,NY1
      A(I,J,K) = 0.
      B(I,J,K) = 0.
      C(I,J,K) = 0.
501   CONTINUE
      DO 502 I=1,NX,NX1
      DO 502 J=1,NY1
      B(I,J,J) = 1.
      R(I,J) = 0.
502   CONTINUE
      DO 503 I=2,NX1
      J = 1
      A(I,J,J) = DY(J)/DX(I-1)*(HTEP(I,J) +HTEP(I-1,J)+ALPHA*HTEP(I-1,J)
     A *(P1(I)-P1(I-1)))
      B(I,J,J) = -DY(J)*((HTEP(I+1,J)+HTEP(I,J))/DX(I)+(HTEP(I,J)+
     B HTEP(I-1,J))/DX(I-1) + ALPHA*HTEP(I,J)*((P1(I+1)-P1(I))/DX(I)-
     B (P1(I)-P1(I-1))/DX(I-1))) - GINV*(DX(I-1)+DX(I))*(HTEP(I,J+1)+
     B HTEP(I,J))/DY(J)
      B(I,J,J+1) = GINV*(DX(I-1)+DX(I))*(HTEP(I,J+1)+HTEP(I,J))/DY(J)
      C(I,J,J) = DY(J)/DX(I)*(HTEP(I+1,J)+HTEP(I,J)-ALPHA*HTEP(I+1,J)*
     C (P1(I+1)-P1(I)))
      R(I,J) = DY(J)*((HIHTEP(I+1,J)+HIHTEP(I,J))*(P1(I+1)-P1(I))/DX(I)-
     R (HIHTEP(I,J)+HIHTEP(I-1,J))*(P1(I)-P1(I-1))/DX(I-1) + ALAMDA*
     R (DEL(I+1,J)-DEL(I-1,J)))
```

```
C
      DDX = (DX(I-1)+DX(I))/2.
      DO 504 J=2,NY1
      DDY = (DY(J-1)+DY(J))/2.
      A(I,J,J) = DDY/DX(I-1)*(HTEP(I,J)+HTEP(I-1,J)+ALPHA*HTEP(I-1,J)*
     A (P1(I)-P1(I-1)))
      B(I,J,J-1) = GINV*DDX/DY(J-1)*(HTEP(I,J)+HTEP(I,J-1))
      B(I,J,J) = -DDY*((HTEP(I+1,J)+HTEP(I,J))/DX(I) +(HTEP(I,J)+
     B HTEP(I-1,J))/DX(I-1) + ALPHA*HTEP(I,J)*((P1(I+1)-P1(I))/DX(I)-
     B (P1(I)-P1(I-1))/DX(I-1))) - GINV*DDX*((HTEP(I,J+1)+HTEP(I,J))/
     B DY(J)+(HTEP(I,J)+HTEP(I,J-1))/DY(J-1))
      B(I,J,J+1) = GINV*DDX/DY(J)*(HTEP(I,J+1)+HTEP(I,J))
      C(I,J,J) = DDY/DX(I)*(HTEP(I+1,J)+HTEP(I,J) - ALPHA*HTEP(I+1,J)*
     C (P1(I+1)-P1(I)))
      R(I,J) = DDY*((H1HTEP(I+1,J)+H1HTEP(I,J))*(P1(I+1)-P1(I))/DX(I) -
     R (H1HTEP(I,J)+H1HTEP(I-1,J))*(P1(I)-P1(I-1))/DX(I-1) + ALAMDA*
     R (DEL(I+1,J)-DEL(I-1,J)))
504   CONTINUE
503   CONTINUE
C
      IF (NPRINT .EQ. 0) GO TO 590
      PRINT 521
      DO 505 I=1,NX
      PRINT 525,I
505   PRINT 11,((A(I,J,K),K=1,NY1),J=1,NY1)
      PRINT 522
      DO 506 I=1,NX
      PRINT 525,I
506   PRINT 11,((B(I,J,K),K=1,NY1),J=1,NY1)
      PRINT 523
      DO 507 I=1,NX
      PRINT 525,I
507   PRINT 11,((C(I,J,K),K=1,NY1),J=1,NY1)
      PRINT 524
      PRINT 11,((R(I,J),J=1,NY1),I=1,NX)
C
11    FORMAT(X,14E9.2)
521   FORMAT(////6X,*A(I,J,K)*/)
522   FORMAT(////6X,*B(I,J,K)*/)
523   FORMAT(////6X,*C(I,J,K)*/)
524   FORMAT(////6X,*R(I,J)*/)
525   FORMAT(/6X,*I=*,I3)
590   RETURN
C
      END
```

```
      SUBROUTINE TEPPHI
C
      COMMON BSTAR,X3,C1
      COMMON ALPHA,ALAMDA,GINV
      COMMON NX,NX1,NY,NY1,DI,DX(28), DY(14),DEL(29,15), HTEP(29,15),
     C HIHTEP(29,15), P1(29), H1(29), X(29)
      COMMON A(29,14,14), B(29,14,15), C(29,14,14), R(29,14)
      COMMON PHI(29,14),P1PHI(29,14),HT(29,15),NPRINT,NPRINT2
C
      DIMENSION T(29,14,14), E(30,14,14), F(30,14), RAF(14)
      DIMENSION TT(14,14), TI(14,14), IR(14), EE(14)
C
      DO 601 I=1,NX,NX1
      DO 602 J=1,NY1
      DO 603 K=1,NY1
      T(I,J,K) = 0.
      E(I+1,J,K) = 0.
603   CONTINUE
      T(I,J,J) = 1.
      F(I+1,J) = 0.
602   CONTINUE
601   CONTINUE
C
      DO 604 I=2,NX1
      DO 605 J=1,NY1
      DO 605 K=1,NY1
      TT(J,K) = B(I,J,K)
      DO 607 L=1,NY1
607   TT(J,K) = TT(J,K) + A(I,J,L)*E(I,L,K)
605   CONTINUE
C
C     CALL LIBRARY SUBROUTINE FOR MATRIX INVERSION
      CALL MI(TT,NY1,NY1,DET,IDET,TI,IR,IER,EE)
      DO 608 J=1,NY1
      DO 608 K=1,NY1
608   T(I,J,K) = TI(J,K)
      DO 609 J=1,NY1
      RAF(J) = R(I,J)
      DO 609 L=1,NY1
609   RAF(J) = RAF(J) - A(I,J,L)*F(I,L)
      DO 610 J=1,NY1
      F(I+1,J) = 0.
      DO 610 L=1,NY1
610   F(I+1,J) = F(I+1,J) + T(I,J,L)*RAF(L)
      DO 611 J=1,NY1
      DO 611 K=1,NY1
      E(I+1,J,K) = 0.
      DO 612 L=1,NY1
612   E(I+1,J,K) = E(I+1,J,K) - T(I,J,L)*C(I,L,K)
611   CONTINUE
604   CONTINUE
```

```
C
      NX2 = NX +1
      IF (NPRINT  .EQ.  0) GO TC 690
      PRINT 661
      DO 631 I=1,NX
      PRINT 666,I
631   PRINT 11,((T(I,J,K),K=1,NY1),J=1,NY1)
      PRINT 662
      DO 632 I=2,NX2
      PRINT 666,I
632   PRINT 11,((E(I,J,K),K=1,NY1),J=1,NY1)
      PRINT 663
      DO 633 I=2,NX2
633   PRINT 11,(F(I,J),J=1,NY1)
C
690   CONTINUE
      I = NX
      DO 621 J=1,NY1
      PHI(I,J) = F(I+1,J)
621   P1PHI(I,J) = P1(I) + PHI(I,J)
      DO 622 II=1,NX1
      I = NX-II
      DO 623 J=1,NY1
      PHI(I,J) = F(I+1,J)
      DO 624 K=1,NY1
624   PHI(I,J) = PHI(I,J) + E(I+1,J,K)*PHI(I+1,K)
623   P1PHI(I,J) = P1(I) + PHI(I,J)
622   CONTINUE
      IF (NPRINT2 .EQ. 0) GO TC 691
      PRINT 664
      DO 625 I=1,NX
      PRINT 666,I
625   PRINT 7,(J,PHI(I,J),J=1,NY1)
      PRINT 665
      DO 626 I=1,NX
      PRINT 666,I
626   PRINT 7,(J,P1PHI(I,J),J=1,NY1)
691   CONTINUE
C
7     FORMAT(8(X,I2,X,E13.6))
11    FORMAT(X,14E9.2)
661   FORMAT(////6X,*T(I,J,K)*/)
662   FORMAT(////6X,*E(I,J,K)*/)
663   FORMAT(////6X,*F(I,J)*/)
664   FORMAT(////6X,*PHI(I,J)*/)
665   FORMAT(////6X,*P1PHI(I,J)*/)
666   FORMAT(6X,*I=*,I3)
C
      RETURN
C
      END
```

```
0000000000000000000000000  END OF RECORD
   1     1    2     1     1     0
 0.03125    -0.25      -5.
 1.         10.
 0.3
   7.543660E-13    0.
 0.003      100.
 0.000001
   61    69    29    29    15     2
 0.5       0.5        0.5        0.5        0.25        0.25        0.25      0.25
 0.25      0.25       0.125      0.125      0.0625      0.0625      0.03125   0.03125
0.015625  0.015625   0.00781250.0078125 0.0078125  0.0078125  0.0078125  0.0078125
 0.0078125 0.0078125 0.015625  0.015625  0.03125   0.03125   0.0625    0.0625
 0.03125   0.03125   0.03125   0.03125   0.03125   0.03125   0.015625  0.015625
 0.0078125 0.0078125 0.0078125 0.0078125 0.0078125 0.0078125 0.0078125 0.0078125
 0.015625  0.015625  0.03125   0.03125   0.03125   0.03125   0.03125   0.03125
 0.0625    0.0625    0.0625    0.0625    0.125     0.125     0.125     0.125
 0.125     0.125     0.125     0.125
   0.                 4.721450E-06   1.258592E-05   2.681879E-05   5.580325E-05
   8.104526E-05   1.220191E-04   1.939579E-04   3.351647E-04   6.644889E-04
   1.706840E-03   3.050854E-03   6.887943E-03   1.135745E-02   2.187715E-02
   3.203592E-02   4.993023E-02   6.344260E-02   8.163219E-02   9.284604E-02
   1.056967E-01   1.202896E-01   1.366692E-01   1.547954E-01   1.745317E-01
   1.956441E-01   2.178178E-01   2.626699E-01   3.073501E-01   3.900927E-01
   4.590188E-01   5.679945E-01   6.512894E-01   6.866959E-01   7.187712E-01
   7.480454E-01   7.748653E-01   7.995005E-01   8.221692E-01   8.328140E-01
   8.430270E-01   8.479759E-01   8.528227E-01   8.575694E-01   8.622175E-01
   8.667687E-01   8.712246E-01   8.755866E-01   8.798561E-01   8.881239E-01
   8.960368E-01   9.108461E-01   9.243499E-01   9.366079E-01   9.476705E-01
   9.575759E-01   9.663579E-01   9.807618E-01   9.908762E-01   9.974024E-01
   1.000000E+00
   1.600004E+03   1.265680E+03   9.682892E+02   7.080937E+02   4.854906E+02
   3.884724E+02   3.011240E+02   2.236086E+02   1.561616E+02   9.914780E+01
   5.318671E+01   3.469588E+01   1.954757E+01   1.337918E+01   8.292149E+00
   6.207885E+00   4.472622E+00   3.747008E+00   3.122434E+00   2.848927E+00
   2.601504E+00   2.379973E+00   2.183826E+00   2.012162E+00   1.863708E+00
   1.736796E+00   1.629467E+00   1.464292E+00   1.350633E+00   1.219590E+00
   1.152006E+00   1.095440E+00   1.071396E+00   1.062275E+00   1.055176E+00
   1.049277E+00   1.044282E+00   1.039955E+00   1.036181E+00   1.034440E+00
   1.032793E+00   1.032001E+00   1.031228E+00   1.030474E+00   1.029738E+00
   1.029019E+00   1.028316E+00   1.027628E+00   1.026954E+00   1.025648E+00
   1.024392E+00   1.022034E+00   1.019842E+00   1.017787E+00   1.015850E+00
   1.014002E+00   1.012247E+00   1.009023E+00   1.005711E+00   1.003650E+00
   1.000000E+00
 1.0       1.0        0.5        0.5        0.375       0.375      0.125      0.125
 0.125     0.125      0.125      0.125      0.25        0.25       0.25       0.25
 0.125     0.125      0.125      0.125      0.125       0.125      0.375      0.375
 0.5       0.5        1.0        1.0
 0.25      0.25       0.125      0.125      0.125       0.125      0.125      0.125
 0.375     0.375      0.5        0.5        1.0         1.0
   52   53   54   54   55   55   55   55   56   56   56   56   56   56   57   57
   57   57   57   57   57   57   57   57   58   58   58   59   59
0000000000000000000000000  END OF INFORMATION
```


*U.S. GOVERNMENT PRINTING OFFICE: 1976 _ 635-275/92